CONTENTS

1 INTRODUCTION

The problem of tidal morphodynamics has not been completely solved yet. In the last decades, great advances have been made in understanding morphological phenomena, especially in the fluvial case, even though there are still some open questions waiting for a solution. Empirical relationships have been explained in a conceptual framework and the underlying dynamics have been clarified. One of the most successful examples (as pointed out by S. Ikeda in the preface of the proceedings of the 2nd IAHR Symposium on River, Coastal and Estuarine Morphodynamics, 2001, which collect the state of the art in the field of morphodynamics) is given by the comprehension of the basic mechanisms of meandering in rivers: starting from the first explanations in terms of several factors, now we are able to understand the most relevant aspects and to predict the behaviour of such systems fairly well. On the other hand, empirical relationships in tidal environments (e.g. between tidal prism and cross section area, see O'Brien, 1969 and Jarrett, 1976) are still matter of investigation.

This work does not claim to give an explanation of the questions related to the problems of tidal morphodynamics. It aims to provide a set of *parameters* (i.e. combinations of variables, like velocity, depth, width etc.) able to identify different morphological situations, exploiting the results obtained so far. This is the first step of a long-term project, which finally should result into an ecological characterisation of an estuary.

The local biology of an estuary or lagoon is affected by the morphology: even though the chemical properties of both water and sediments are favourable, the natural environment can be damaged by physical changes. Moreover, they typically occur on a time scale that is slow if compared with the effect of chemical pollution and probably this can explain why such problems have been tackled only in the last few years.

The purpose of the project is to measure the *morphological quality*, providing graphs or tables, based on easily assessable parameters, where threshold lines separate different morphological features (e.g. presence of intertidal areas, islands, single channels etc.) and the related ecological environments. These quantitative indicators should be a useful support for decisions in the management of estuaries.

Actually, the present study has the intermediate goal to determine the most important state variables involved in the problem, without fixing the threshold lines, whose identification is likely to require a stronger effort, both in data analysis and in model formulation.

The definition of controlling parameters presumes that we can grasp the physical mechanisms that drive the evolution of estuarine systems. Unfortunately, this is not completely true, because tidal environments are very complex and, therefore, the most profitable approach to this kind of problem is probably the analysis of data. Of course, a collection of data is not useful itself, but it should be done in the light of a conceptual model. A model is a simplified description of reality and selects few basic aspects of the natural system; looking at its sensitivity with respect to the range of variation of the variables, it is possible to estimate the role of the different factors. Nowadays, although suitable models are not available (a short review of the most recent models can be found in Chapter 7), we can use partial information to identify a few parameters that certainly play a crucial role in estuarine morphology. In this way it is possible to select the important variables. Data can be compared in space, among different locations, or in time, considering the local evolution of the system.

The present study focuses on the *Western Scheldt estuary*, where radical changes from a situation resembling a river delta to a funnel shaped estuary occurred in the last centuries, strongly affected by human activities; historical comparisons can be made only when considering the last two centuries, after the construction of the major part of the dykes.

2 DEFINITION OF THE PROBLEM

We can observe a physical phenomenon considering different scales. If we are interested in the process of erosion and deposition near the bed, pick-up, rolling, saltation of sediments, we define a field of study that has a length scale whose order of magnitude is the size of the single grain of the sediment. Otherwise, if we look at the effect of small bed forms on the flow, we will consider a region that scales with the flow depth.
What we study in this work is the behaviour of an estuary at a much larger scale. We do not consider the whole system, but only part of it. The typical scale has to be determined, but it is probably related with the width, since on this scale are present all the features we are considering: channels, islands and intertidal areas.
Following de Vriend et al. (2000), we use the classification:

- *micro-scale*: the level of the smallest scale morphological phenomena associated with water and sediment motion (ripple and dune formation);
- *meso-scale*: the level of the main morphological features (channels and shoals);
- *macro-scale*: the level at which the meso-scale features interact;
- *mega-scale*: the level at which the principal elements of the entire system interact (i.e. the estuary considered as a whole water body).

The present analysis focuses on the *macro-scale*; for the Western Scheldt it corresponds to a reach of the estuary in which channels and shoals interact (*estuarine sections*, see Paragraph 3.2).
The definition of a length scale strongly affects the period of time we have to consider to see any change. This means that the time scale of observation is strictly related to the choice of the length scale: the larger the length scale, the longer the time scale. Basically, it is related to the amount of sediment that has to be moved.
Furthermore there are, more or less strong, interrelations among different scales, as pointed out by de Vriend (1998) through the concept of the cascade of scales. The evolution of the smaller scales is parametrically incorporated, while the large-scale variations modify the boundary conditions of the smaller scale subsystems.

2.1 Equilibrium and time scales

This analysis does not intend to deal with the evolution of tidal systems. The objective is to determine which equilibrium configuration the system is driven towards, without considering the transitional periods between an equilibrium configuration and the next one.
It is necessary to give a definition of equilibrium related to the length scale and to the time scale we are considering. Indeed, once we have chosen a length scale, the concepts of equilibrium and time scale are strictly related and we can define the former using the latter or vice versa:

- we can identify the *time scale* as the period of time that the system needs to adapt to a change of the boundary conditions. Abstractly, we maintain constant boundary conditions after a change: the system will take time to reach a new, different, equilibrium configuration of the features that are relevant for the selected length scale.
- we can define *equilibrium* as the absence of changes (always for the selected length scale) during the time scale we have chosen.

From a practical point of view, it is not easy to use the first definition, because the boundary conditions often change during the time scale necessary to obtain equilibrium; when considering the whole estuary, the time scale to be considered could be very long (one century or more), as confirmed also by recent investigations (Hibma et al., 2001; Lanzoni and Seminara, 2002).
It is important to note that all the definitions are related to the length scale, as discussed below. The fact that the system is in equilibrium does not mean that it does not show any change: even if we can reach a situation when large scale features are steady, still we can observe smaller scale fluctuations. For example, sediment transport usually never vanishes, but it may give a tidally averaged effect that is null.
The equilibrium at the shorter scale is always driven, even if slowly, by the changes in the upper scales. In natural systems, usually we are not able to find equilibria by the process of upscaling (for a definition of upscaling and downscaling, see Bloschl and Gutnecht, 1996) because equilibrium at the largest scale often does not exist. Moreover, the human tendency to fix the present situation, e.g. by dredging the channels that are silting up, often conflicts with the natural development of the system. The system can also be driven towards an equilibrium that is not compatible with the system itself (e.g. it may tend to disappear because of sediment deposition).
For these reasons, we will adopt the second definition of "relative" equilibrium, considering the period of time of the information available about the system.

If we consider a macro-scale process, the morphological evolution is mainly driven by two factors:
1. the *net flux* of sediments entering/leaving the macro-scale region;
2. the *internal redistribution* of sediment inside the region (i.e. the adaptation of the system to the changes of the local boundary conditions determined by upper scale variations).

As already noted, the latter process might never reach an equilibrium configuration, even if the boundary conditions are steady. An example is given by the apparently cyclic behaviour of the system of shoals and connecting channels, which seem to migrate, disappear and form again, e.g. for the Middelplaat near Terneuzen in the Western Scheldt (Jeuken, personal communication). However, the macro-scale classification does not change and the multiple-channel system is not affected by these variations, which can be considered meso-scale phenomena.

Referring to a given scale, we can think about the variations of the smaller scales as higher frequency oscillations, like the above-mentioned evolution of the connecting channels for the macro-scale. The sketch on the right is an idealised representation of the temporal evolution of a quantity like the area of a cross section: even if the system is not in equilibrium at the mega-scale, it could be considered steady at the macro-scale, with small variation at the lower scales.

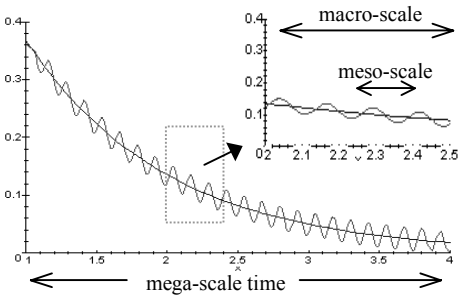

This example is worth to be analysed in further detail. It is known that the area of a cross section of the whole estuary is related to the tidal prism, which can be considered a mega-scale quantity, because its variation occurs on a time scale of tens or hundreds of years. During the macro-scale time scale (few tens of years) it does not show large changes and it is possible to define a momentary state of relative equilibrium. But when we consider shorter time scales, we can see different phenomena: during years the area can vary because of the migration of connecting channels, and during the day there is a rather strong oscillation due to the tidal range.

3 DESCRIPTION OF THE SCHELDT SYSTEM

The river Scheldt can be divided into two parts, from the mouth landwards:
1. *Western Scheldt* (Westerschelde in Dutch), 60 km between Vlissingen, near the mouth, and Doel, close to the boundary between the Netherlands and Belgium (it is possible to denote this reach as the Dutch part of the estuary);
2. *Zeeschelde* (the Belgian part), from the border to Gent.

Upstream of Gent, the Scheldt loses its estuarine character and can be classified as a river (Bovenschelde).
The object of this analysis is the estuarine part of the Scheldt and in particular its Dutch seaward marine part, the Western Scheldt.

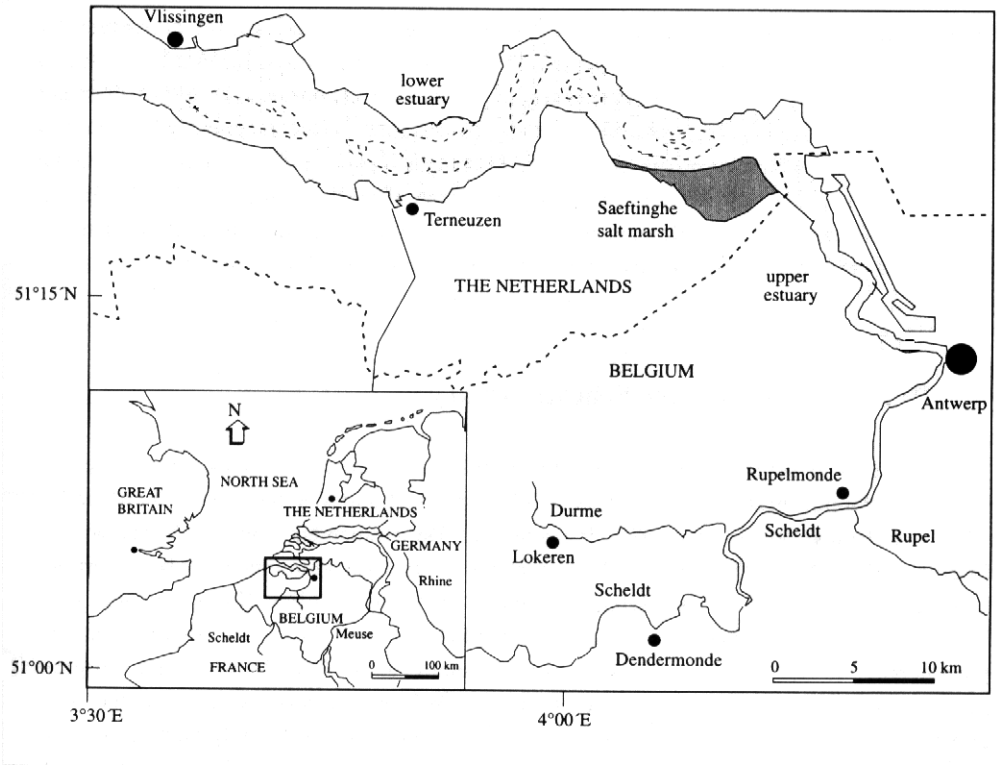

Figure 1. The estuary of the Scheldt.

The Dutch-Belgian border represents an abrupt change between two different morphologies. For this reason, in order to characterise the Western Scheldt and to recognize its peculiarities, we will analyse also the Zeeschelde, from the border only until Schelle-Rupel, where the tidal character of the estuary changes because the mean water level begins to show the slope typical of rivers (see Figure 2); instead, from the mouth to Schelle-Rupel, the mean level is not relevantly different from the Dutch mean sea level (NAP).
It would be possible to consider also the coastal part of the estuary, its outer delta, but that kind of morphological features are not under investigation in the present analysis.

At the same time as the present analysis, another study proposes the identification of three different kinds of morphological features. In this way, the Scheldt estuary can be subdivided into three parts (Crosato, personal communication):
1. the seaward part of the Western Scheldt, from Vlissingen to Hoek van Baarland (estuarine sections 6 and 5 according to Jeuken, 2000, see Figure 3, corresponding to sections 1 and 2 in Figure 4 and Figure 5), can be described as a *multiple-channel system*, where two main channels (ebb- and flood-dominated) are separated by intertidal areas, but with other large or deep longitudinal channels. Several smaller connecting channels cross the intertidal areas;

2. in the region landward of the Western Scheldt, from Hoek van Baarland to the border between the Netherlands and Belgium (close to Prosper in Figure 4), a *two-channel system* is present: the ebb- and flood-dominated channels are separated by one intertidal area, often crossed by secondary channels;
3. in the Belgian part the estuary is a *single-channel system*, where the intertidal areas are present only near the banks, mainly at the inner side of the channel bends.

It is interesting to note that the above subdivision, developed in a different framework, agrees with the results of the present analysis, which will be explained in the following chapters (in particular, see Paragraph 8.2.1).

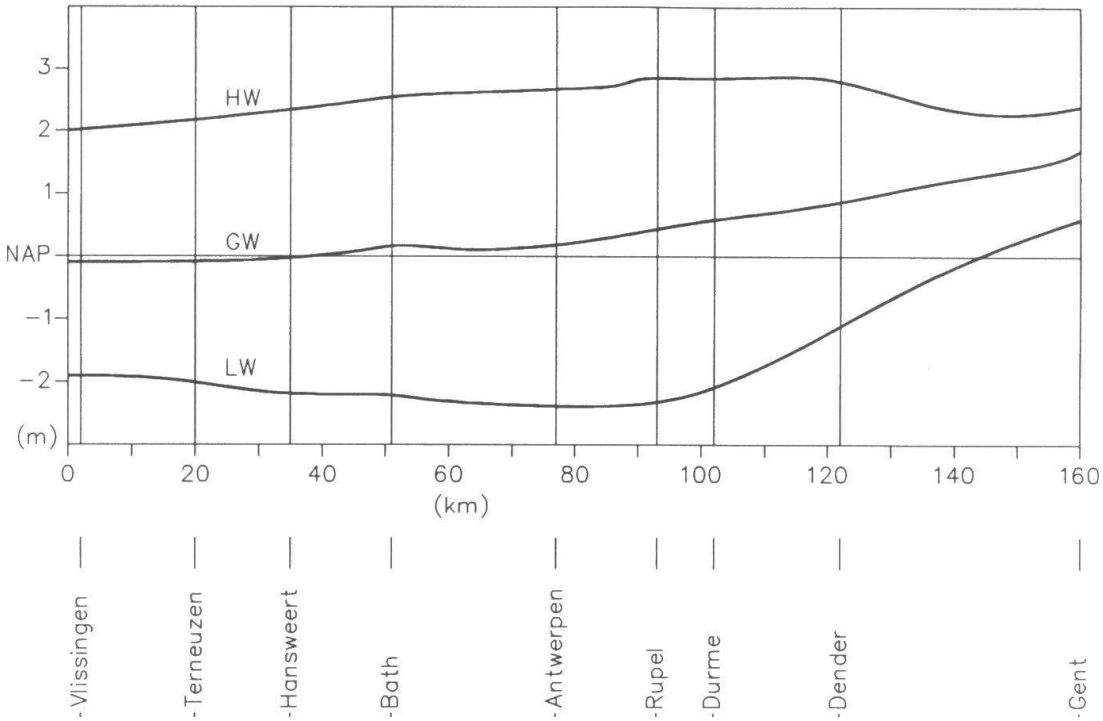

Figure 2. High (HW), mean (GW) and low (LW) water level along the Scheldt estuary (Allersma, 1992).

3.1 Morphological elements

An estuary is composed by several morphological elements; the most important are the channels, the intertidal areas and the islands. The combination of more than one of these components constitutes a macro-scale morphological element.

3.1.1 Intertidal areas

The study of the morphology of the system of channel, shoals and intertidal areas, is the goal of the present part of the project. A definition of intertidal flats and a proposal for a choice of micro-scale parameters affecting local morphology and biotic habitat can be found in Crosato et al. (1999).
The intertidal flats can be subdivided in three zones:

- the *upper* zone, between mean high water level during spring tides (MHWS) and mean high water level during neap tides (MHWN), is completely inundated only during spring events;
- the *middle* zone, between mean high water neap level (MHWN) and mean low water neap level (MLWN), is subjected to a continuous cycle of inundation and drainage;
- the *lower* zone, between mean low water neap level (MLWN) and mean low water spring level (MLWS), is inundated during most of the month and the lower part is exposed only during spring events.

3.1.2 Channels

The channels can be defined from the bathymetry as the deepest parts of the estuary; they convey the major part of the discharge. Typically in every estuarine section there are many channels of different type. It is possible to identify ebb-dominated channels, where the residual currents (i.e. the average of the discharge over the tidal cycle) are directed seaward, and flood-dominated channels, where the residual currents are directed landward.
A conventional value of the bed elevation can be used to bound the channels, but a more precise methodology has been developed by Fagherazzi et al. (1999) and Rinaldo et al. (1999), by means of a remote sensing analysis.

3.1.3 Morphological cells

The complex system of channels and intertidal areas in the Western Scheldt can be described using the concept of *morphological cell*: a zone with an ebb-dominated channel and a flood-dominated channel, usually separated by an island, an intertidal area or even by an always submerged shallow water zone, can be defined between two points (with typical bifurcations where the flood channel separates). They show a cyclic residual pattern of both liquid and sediment transport which can be thought as a *tidal loop*. Please note that the instantaneous velocity during the tidal cycle has the same direction both in the ebb- and in the flood-channel, but the tidally averaged values are opposite.
A qualitative description of the morphological elements of tidal systems has been originally provided by van Veen (1950) in his pioneering contribution. Recently, Winterwerp et al. (2001) have proposed a schematisation of the Western Scheldt in morphological cells.

3.2 The estuarine sections

The identification of the macro-scale zones follows the subdivision proposed by Jeuken (2000) for the seaward part of the estuary (Western Scheldt, see Figure 3), and originates from the concept of morphological cells. The original definition is*: The configuration and morphology of the main channels and the connecting bar channels and cross channels display a repetitive channel pattern that is referred to as the estuarine section.* (Jeuken, 2000, p. 25)

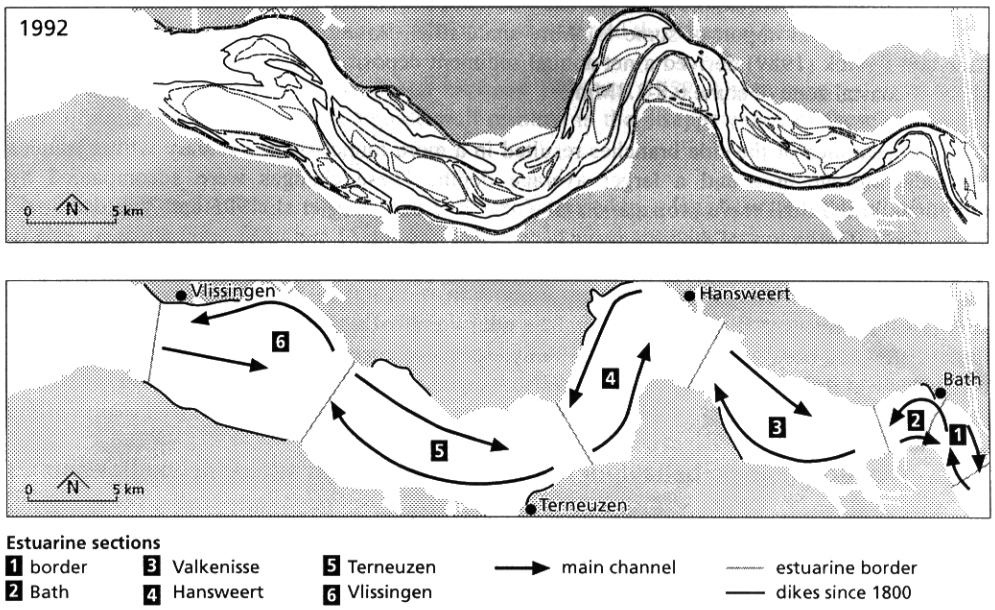

Figure 3. The Western Scheldt bathymetry in 1992 (above) and the six estuarine sections (below) as defined by Jeuken (2000), with the indication of the main ebb- and flood-channels.

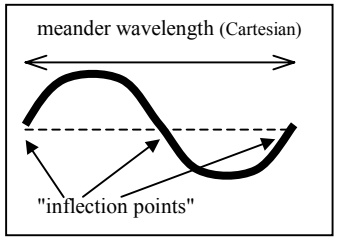

We propose to adopt the width of the "channels-intertidal areas" system as the length scale of the estuarine sections, because it is easy to measure and phisically relevant. Jeuken's criterion does not refer directly to the width, since it is related to the repetitive pattern of ebb- and flood- channels, but the definition seems to be strongly influenced by the curvilinear pattern of the estuary (the Western Scheldt as a whole channel is meandering). The appropriate length scale should be the meander wavelength (precisely half wavelength**,** from an inflection point to another; see the sketch on the right). The relation between the two lengths can be explained by considering that both theoretical results and field observations (Solari et al., 2002) suggest that the meander wavelength typically scales with the channel width, confirming in the tidal case a result found also for rivers.

Another subdivision was proposed by van der Spek (1994), for the whole estuary from Vlissingen to Gentbrugge (see Figure 4). It is clear that the estuarine sections are almost the same from the mouth to Hansweert, while Jeuken (2000) treats in a different way the region including the salt marsh of Saeftinge (Drowned Land of Saeftinge), excluding it from the estuary and subdividing the reach in three sections instead of the two delineated by van der Spek.

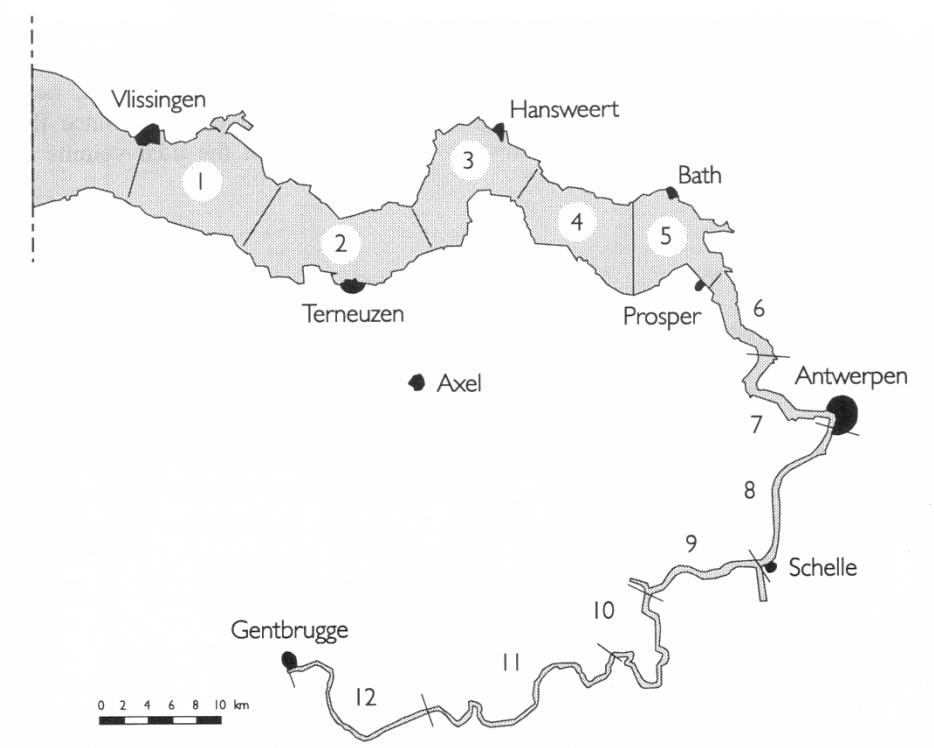

Figure 4. The Scheldt estuary from Vlissingen to Gentbrugge, subdivided into 12 sections (after van der Spek, 1994).

3.2.1 The subdivision of the present analysis

In the present analysis we consider the part of the Scheldt estuary that is mainly influenced by tide, i.e. the reach from Vlissingen to Schelle-Rupel (see Figure 5). Upstream of Schelle-Rupel the water body becomes similar to a river, even if the tidal effect is still relevant until Gent.
The estuary has been subdivided following the indications given by Jeuken and van der Spek as much as possible. The criterion is to select one bend of the meandering channel. The Drowned Land of Saeftinge has not been considered, because its morphology is different and its role in the hydrodynamics of the system can be treated separately.

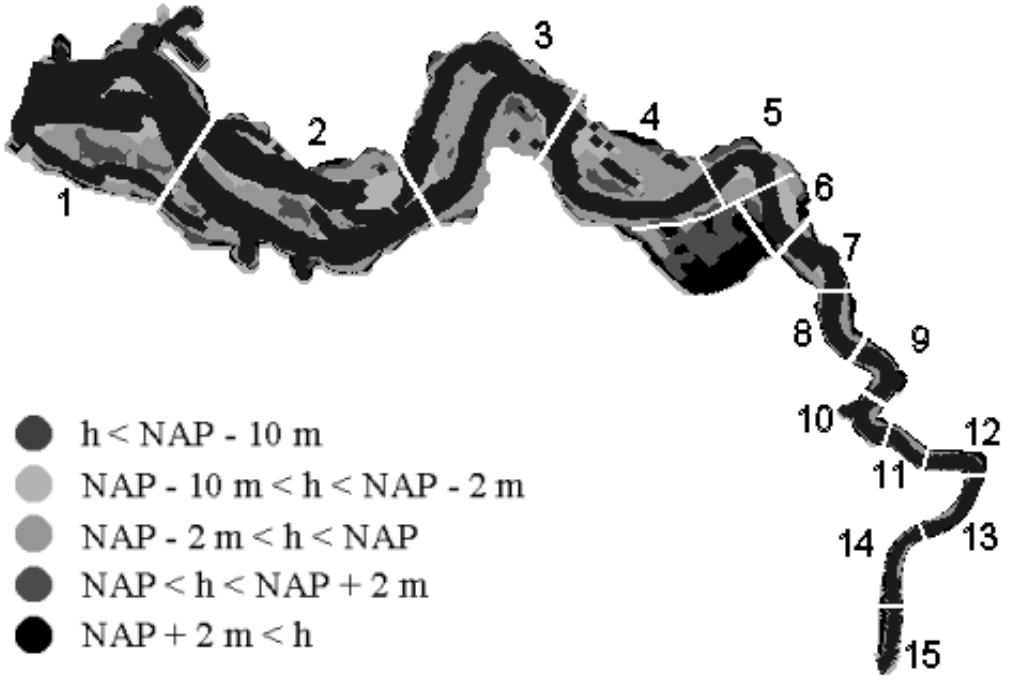

Figure 5. The adopted subdivision in estuarine sections of the Scheldt estuary from Vlissingen to Schelle; in the figure it is possible to distinguish the main channels and shoals (*h* is the bed elevation, NAP is the Dutch mean sea level, see 5.1).

The basic characteristics of the estuarine sections are summarised in the table below; please note that the features of the whole section have been attributed to the centre of the sections, whose position along the estuary is given by the last column. The length is calculated following the curvilinear coordinate (see Figure 6).

n°	*name*	*length [km]*	*x [km]*
1	Vlissingen	12.0	6.0
2	Terneuzen	15.5	19.8
3	Hansweert	10.5	32.8
4	Valkenisse	11.5	43.8
5	Bath	5.0	52.0
6	border NL/B	4.3	56.7
7	Prosper	3.4	60.5
8	Liefkenshoek	3.5	64.0
9		3.9	67.7
10	Kallosluis	3.1	71.2
11		3.0	74.2
12	Antwerp	3.2	77.3
13	Antwerp	4.5	81.2
14	Hemiksem	5.8	86.3
15	Schelle	4.6	91.5

Table 1. Characteristics of the estuarine sections of Figure 5.

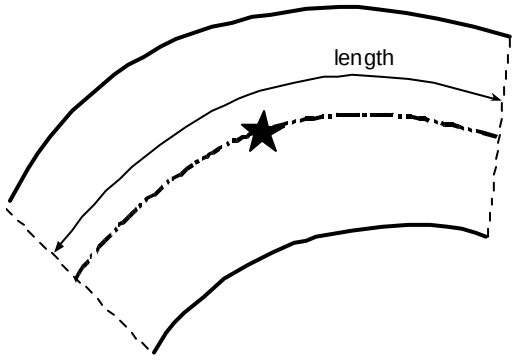

Figure 6. Sketch of an estuarine section with its curvilinear length. The star denotes the centre of the section.

3.3 Brief history of the Western Scheldt and the main human interference

The present situation of the Western Scheldt is the consequence of many driving factors, both natural and anthropogenic. It can be consider a young estuary, whose evolution started only a thousand years ago (van den Berg et al., 1996); the present configuration is strongly affected by the past situation.

It is possible to understand from Figure 7 that the large tidal system has undergone important changes in the last millennium, evolving via a complex tidal network towards an aggregation of islands and finally to the configuration we are examining. A significant variation, for example, is that the original estuary of the Scheldt River was the present-day Oosterschelde (Eastern Scheldt).
Van den Berg et al. (1996) note that the tidal surface decreased strongly from the 17th century until today (-40% for the tidal basin surface), but the tidal prism has not changed or has even increased, due to the higher celerity of propagation of the tidal wave and to the larger tidal amplitude.
The importance of the human interventions in driving the development of such as system cannot be neglected. It is well known that a large amount of land was separated from the sea through the construction of dykes and polders. Nowadays the estuary is almost completely bounded by dykes and the planimetric evolution is stopped. Besides, an important activity of dredging occurred inside the estuary.
However, the strong interest in the modification of this system suggested to collect data about the estuary during the last centuries, and this information is very useful to understand the process of its long-term evolution.

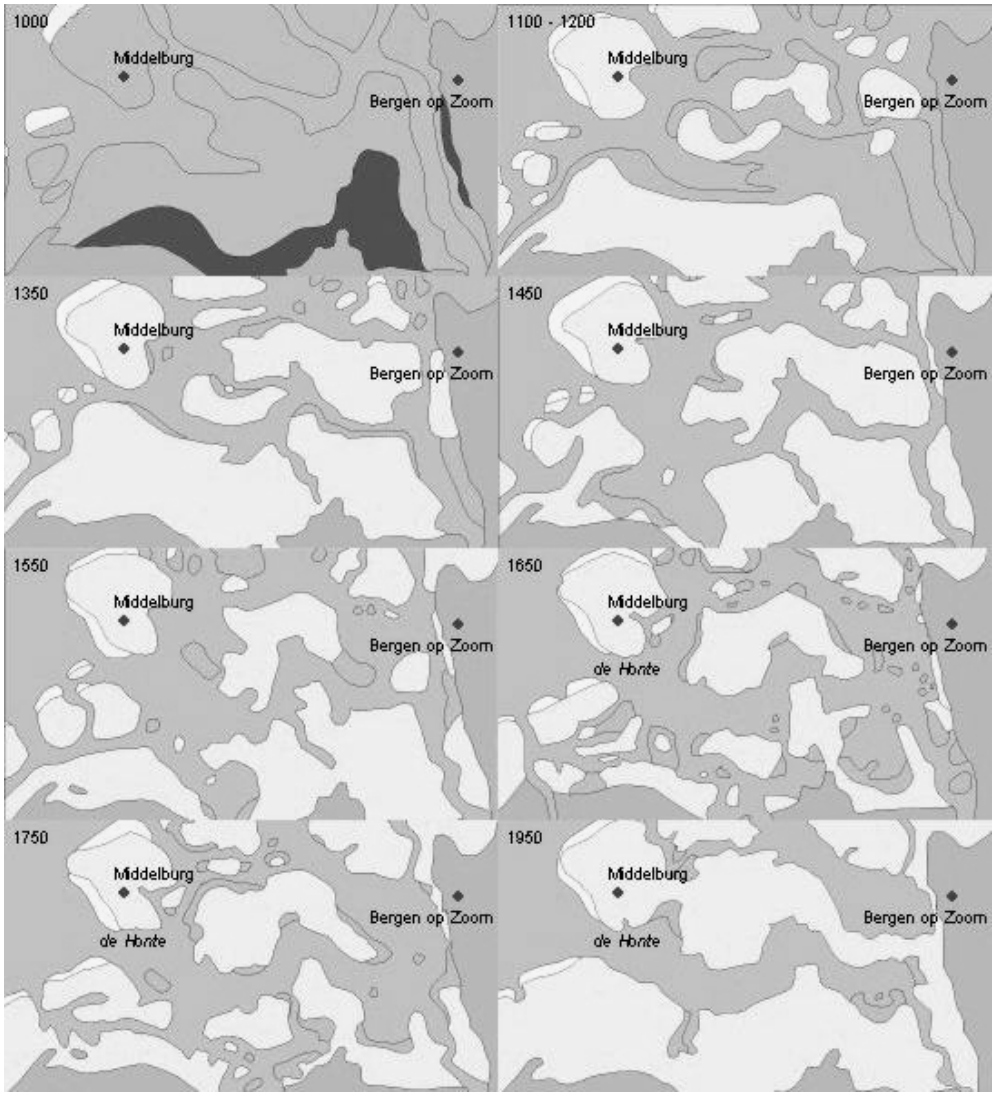

Figure 7. The evolution of the Scheldt estuary since 1000 (source: http://www.waterland.net/sic/animat.htm).

The first hydrographical surveys date back to the 19th century, but the main bathymetric surveys were made after 1931. Important measuring campaigns were carried out in 1955 and in 1968.
Two main dredging phases took place in the estuary, the first in the period 1970-'74, which took approximately 15 years to reach a new local equilibrium (Jeuken, personal communication), and the second in 1998.

3.4 Available data

The data available for the present analysis come from several different sources. Most of the publications give aggregated data for the estuarine sections, such as lengths, volumes, tidal ranges and sediment characteristics (e.g. Jeuken, 2000). There are also maps that can provide qualitative indications about the evolution (1931, 1955, 1963, 1972, 1982, 1986, 1994, 1998, courtesy of Jeuken).

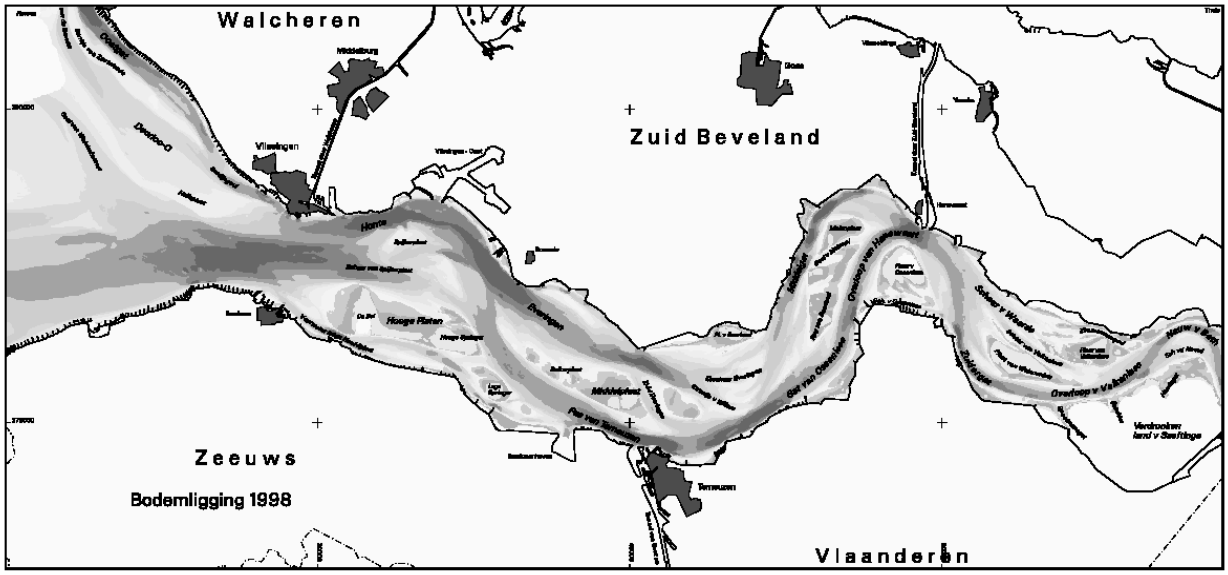

Figure 8. Map of the Western Scheldt in 1998 (courtesy of Jeuken).

The bathymetries of the Scheldt estuary, used for runs of numerical models, were the main sources of quantitative data, as will be explained in Chapter 8.
However, a rigorous analysis of data would require the knowledge of a lot of information, regarding the different aspects of the tidal environment which will be listed in Chapter 5. Moreover it would be important to know the source of such data, which should always be the same, and the kind of measurements that were carried out, to avoid gross mistakes due to different methodologies or to inaccurate elaborations.
It is not easy to get the data for the whole Scheldt estuary from the same source, also because it flows in two separated countries, Belgium and the Netherlands. In fact, the quest for data was a big problem encountered by the author during this analysis and was not completely fulfilled.

4 METHODOLOGICAL APPROACH

The methodological approach can be divided into the following steps:
1. definition of the *variables* involved in the problem (Chapter 5), with remarks about the dimensional units, the scale of observation, the ease of measurement and the significance for the purpose of the present analysis;
2. identification of the relevant *parameters* (Chapter 6), on the basis of theoretical considerations, the use in conceptual models and a brief analysis of data of the Scheldt estuary;
3. description of the available theoretical *models* (Chapter 7), trying to determine the range of sensitivity of the chosen parameters;
4. analysis of the available *data* (Chapter 8), from different sections of the Scheldt showing different morphological features and, if possible, from historical data, in order to assess the real influence of the parameters;
5. verification with data from other estuaries (e.g. Humber, but also Ord, Delaware, Severn, St. Lawrence, Nooghly, Thames, Gironde, Elbe).

Unfortunately, the last point has not been considered, due to the lack of suitable data.
The main point of the present study is the second, i.e. the definition of the groups of relevant factors. We use the terms variable and parameter to refer, respectively, to the measure of an entity and to the combination of several variables into an aggregated information.
The procedure adopted for the identification of the parameters can be divided in two conceptual steps:
- the first step is to select the parameters which are to be included in the analysis;
- the second step is to assess their relevance for the characterisation of the macro-scale features of the estuary.

The following paragraphs explain in detail the two aspects.

4.1 Pre-selection of parameters

A sketch of the method of selection of the relevant parameters is drawn in Figure 9. Different aspects of the problem can be grouped in *factors*, regarding the tidal features, the discharge, the property of sediments, the geometrical characteristics of the water body etc. Every aspect is represented by a *variable*, which has to be a quantitative measurement in order to allow a mathematical analysis. The composition of the variables gives rise to *parameters*, which include the influence of different aspects and their reciprocal interaction. Each parameter mainly affects certain scales: in this way, it is possible to choose those parameters that are important for the scale we are studying.
In the example, where only few elements are considered, for the macro-scale we can take into account the *Shields number* and the *width to depth ratio*, but probably we do not need the *Froude number*, which acts mainly on a smaller scale. Indeed, if we calculate the value of the Froude number for the whole estuarine section we find that it is usually small, but when we are interested in a local analysis, e.g. the formation of ripples and their influence on choice of the habitat by animals and plants, this parameter is supposed to play an important role. Another example is the energy dissipation rate (see Paragraph 6.2.1) that has been shown to be crucial for all biotic parameters (Crosato et al., 1999), when it is defined using local velocities and taking into account the energy arising from the breaking of waves, which is a typical micro-scale phenomenon.
Of course, if we are interested in all the parameters affecting life in a tidal environment, we should include every other parameter whose influence ends on the box *biology*. For example, one of the most important parameters for the local biology is the inundation time, which represents the length of time of flooding for a given area and is related to the distribution of surfaces at different water levels.

There is a problem when we try to give a strict definition of the influence of a parameter on the macro-scale morphological features. In fact, it is obvious that the mega-scale character of the tidal embayment affects strongly the lower scale: for example the estuarine sections of the Western Scheldt are very different from the system of tidal flats and draining channels typical of a lagoon.
To avoid the need to take into account also mega-scale parameters, we restrict our analysis to a single type of tidal environment, namely the macro-tidal estuary, of which the Western Scheldt is an example.

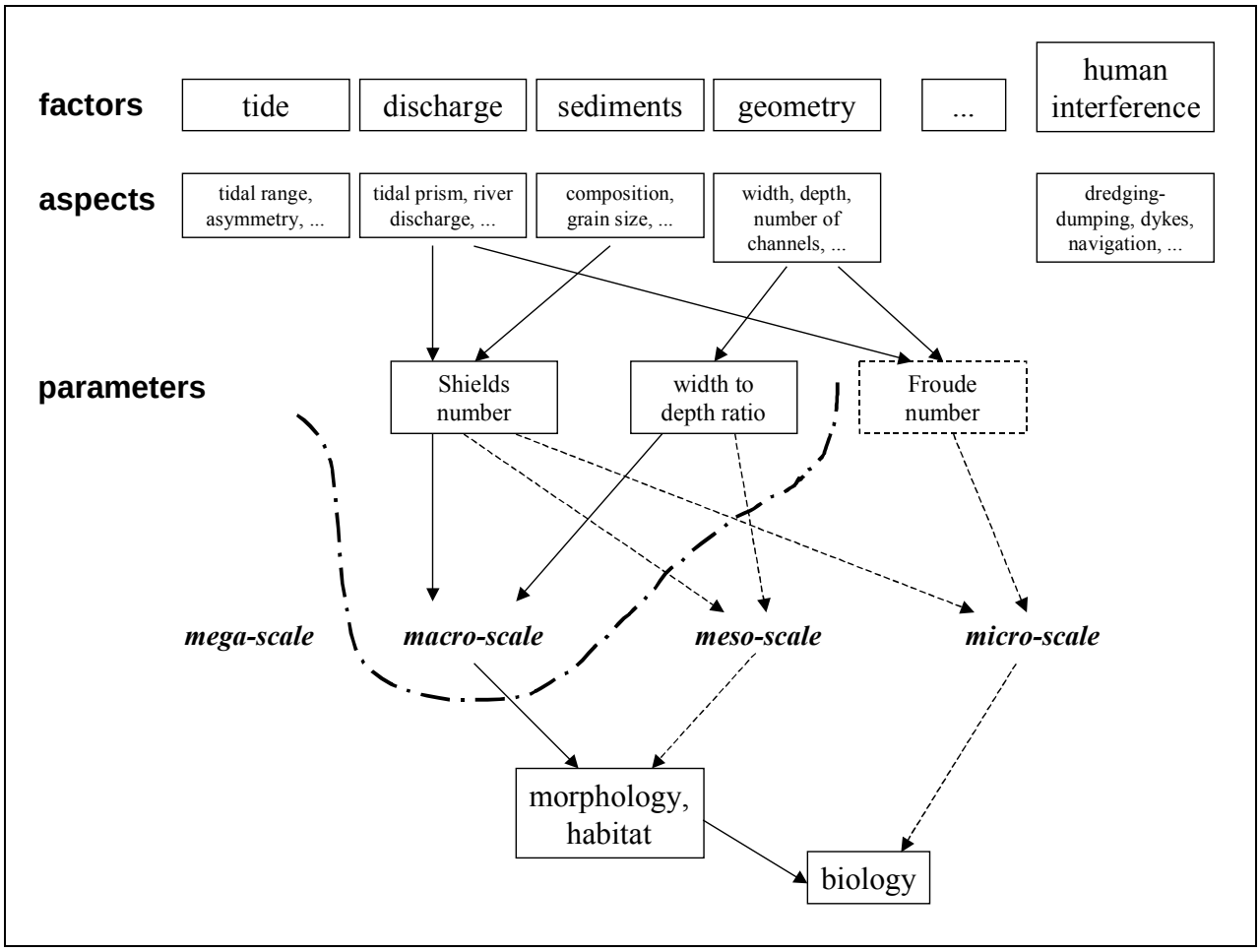

Figure 9. Sketch of the method of selection of parameters affecting the macro-scale. Only few aspects and parameters are drawn. The thick dotted line circumscribes the parameters affecting the macro-scale and the dashed boxes and arrows represent, respectively, parameters and relationships, which do not show significant influences on the scale under investigation.

Please note that this procedure is affected by a selection *a priori*. Indeed, the former identification of the main factors and their basic aspects is related to the knowledge of the author. A list of the variables taken into account is given in Chapter 5.
Furthermore, the composition of variables into parameters is even more subjective. The number of variables is so high that it does not make any sense to try all the possible combinations. Then it is necessary to find some hints to select a smaller number of parameters: this has been done looking at those used in the theories developed so far. A list of such parameters, along with a brief review of the theories, can be found in Chapters 6 and 7.

4.2 Selection criteria

The aim of this study is to provide a short list of parameters able to characterise the morphological features of an estuary. Following the approach suggested in the previous paragraph, we obtain a large number of parameters, which might not be very meaningful or practical to manage.
We need few criteria for a further selection. Parameters should be:

- *dimensionless* (they must not depend on the adopted units and should be valid for different systems);
- *independent* (it is necessary to restrict the number of parameters by avoiding repetitions of the same information in related parameters);
- *distinctive* (e.g. Coriolis force does not vary in the zone of analysis: although it could be important if considering large length scales, it acts in the same manner at a given latitude);
- *applicable* (i.e. easy to measure or to collect data).

The last requirement will be the guideline for the present analysis. Indeed, we are looking for parameters, which should be simple and comprehensible also to researchers that are not morphologists.
The first two points are mainly related to dimensional analysis, a tool widely used in hydraulics. It is based on the so-called Buckingham (or Π) theorem (for a classical text on this subject, see Barenblatt, 1987), which allows to identify how many independent parameters control the system. Moreover, the number of these dimensionless groups is smaller than the number of the variables involved in the problem. If we are considering mass, time and length as the three basic units of measurement, we expect to obtain N-3 independent dimensionless parameters, where N is the number of variables involved into the problem. Unfortunately, in this analysis the procedure is not able to provide a definitive contribution to this point. In fact, the system is so complex that a lot of variables are involved, in particular geometrical, and the reduction in the number of dimensionless quantities is not substantial. For example, if we consider the cross-sectional area, we might define the area of the whole section (at different water levels, namely: mean, high and low tide, for spring and neap tides) or the area of the main channel (total or divided in ebb-dominated and flood-dominated channel) and so on. It is clear that in this case dimensional analysis is important only in the determination of the independence of the selected parameters.

4.3 Note on the use of theoretical models for the morphodynamics

Morphodynamic theories are able to give valuable suggestions about the role played by the different entities because models simplify the real behaviour of the system by taking into account only a restricted number of basic factors.
Hence, even if the models available at the moment are not suitable to describe all the macro-scale features we are interested in, they can lead the analysis to choose the elements that are supposed to drive the evolution of the system. In this context also the use of meso-scale models (like those which will be presented in Paragraph 7.3) can provide an aid towards the solution of the problem, even if they typically deal with compact channels without intertidal areas.
For example, the relation between tidal prism and cross-sectional area is typically mega-scale. If the mega-scale features are steady during the macro-scale characteristic time, we can assume that the cross-sectional area does not vary dramatically if the tidal prism is roughly constant. In this way a complex cross-section can be seen as the evolution of a single channel, and the gross features of the former can be inferred by a meso-scale analysis of the latter. Of course the approximation is strong and maybe incorrect, but in some cases it is the only possibility to obtain theoretical results. An application, which will be discussed below, is the inference of the number of channels in an estuarine section, starting from a model of the bed forms in a simplified geometry.

5 MORPHOLOGICAL VARIABLES

As pointed out in the preceding paragraphs, a comprehensive list of all physical variables playing a role in estuarine systems is neither possible nor desirable. The following tables summarise the most relevant variables, grouped on a conceptual basis.

5.1 Notation

Notation is not always considered as important as it actually is, in particular when it is necessary to exchange information among different groups of researchers. In the following paragraphs we adopt the notation used in morphological literature, even if a standard notation has never been proposed. We feel that some of the difficulties in communication among different disciplines are emphasized by terminological problems.
In the following tables we include also some quantities that can be assumed to be constant in natural systems (e.g. acceleration due to gravity), in order to collect the basic notation in the same section.
A further definition is necessary: *NAP* is the Dutch Ordnance Level (mean sea level in the Netherlands), which is different from other reference levels, like the Belgian mean sea level (NAP = Belgian reference level – 2.33 m).

5.2 Measurable quantities

In this section we present the quantities that can be measured, at least conceptually (an operational definition of how these variables can be measured is not always simple to give and also the basic quantities are often measured in an indirect way).
In the following tables we identify the dimensional units of the variables (column *dim*) with the usual S.I. (International System of Units) notation: L for length, T for time and M for mass.

5.2.1 Geometrical quantities

Geometrical variables are supposed to play a basic role in the problem. Moreover they are often easier to measure with respect to the other types of variable, because only the bathymetry and the water level are needed.

Table 2 clearly shows that there are several possible definitions of the same geometrical quantity, e.g. width, depending on the scale of observation:

- meso-scale, referring to single channels, shoals or intertidal areas;
- macro-scale, considering the estuarine section or, generally, the features of more complex morphological elements;
- mega-scale, when the averaged values, along the whole estuary, are taken into account.

The choice of the most significant definition for macro-scale characterisation is not straightforward, because it may happen that, for example, the local (meso-scale) maximum depth is more relevant than the macro-scale width-averaged value.
Another problem is the choice of the most relevant water level. Three levels are usually taken into account, namely *high water*, *low water* and *mean water*. It is possible to define high and low water for *spring tide* (maximum tidal amplitude in the monthly lunar cycle), for *neap tide* (minimum tidal amplitude) and for monthly averaged tide. De Jong and Gerritsen (1984) suggest that the process of bed formation is mainly related with the flow conditions during spring tides.

In Table 2 we include also the *inundation time* because this aspect is strictly related to the hypsometric description of the bed level.
Please note that, in this context, the term *area* indicates the cross-sectional area, whereas *surface* refers to planimetric surfaces.

geometry		dim	notes
B	*width*	L	
	at low-mean-high water		
	(for spring, average and neap tide)		
	individual channels		meso-scale
	individual tidal flats		meso-scale
	whole cross-section		macro-scale
	average along estuary		mega-scale
D	*depth*	L	
	at low-mean-high water		
	(for spring, average and neap tide)		
	at ebb-flood peak velocity		
	local maximum		meso-scale
	width averaged		macro-scale
	average along estuary		mega-scale
V	*volume*	L^3	
	at low-mean-high water		
	(for spring, average and neap tide)		
	estuarine section		macro-scale
	whole estuary		mega-scale
A	*cross section area*	L^2	
	at low-mean-high water		
	(for spring, average and neap tide)		
	when the maximum discharge occurs		
	only main channels		meso-scale
	whole cross section, including tidal flats		macro-scale
S	*wet planimetric surface*	L^2	
	at low-mean-high water		
	(for spring, average and neap tide)		
	single channels		meso-scale
	estuarine section		macro-scale
	whole estuary		mega-scale
R	*curvature*	L	
	minimum radius of curvature		
	single channels bend		meso-scale
	whole estuarine bend		macro-scale
	presence of intertidal areas		
	planimetric surface	L^2	
	salt marshes		
	tidal flats		
	vegetated area		
	inundation time	T	
	other elements		
	presence of salt wedge		

Table 2. List of geometrical quantities.

5.2.2 Mass balance

In this section we summarise the main volumes and discharges that play a role in the water and sediment balances.

in-out		dim	notes
	water		
Q_r	river inflow (fresh water)	L^3/T	
Q_e	ebb discharge	L^3/T	
Q_f	flood discharge	L^3/T	
P	tidal prism	L^3	
V_e	ebb volume	L^3	
V_f	flood volume	L^3	
	sediments		
	input-output from the sea	L^3/T	
	input-output from the land (river)	L^3/T	
	dredging-dumping	L^3	
	sand mining	L^3	

Table 3. List of quantities involved in the mass balance.

The *tidal volumes* are calculated by integration of the absolute value of the discharge over the ebb period and the flood period (respectively, T_e and T_f):

$$V_{e,f} = \int_{T_{e,f}} \left| Q_{e,f}(t) \right| dt$$

The *tidal prism* is half the sum of the ebb and the flood volumes:

$$P = \left(V_e + V_f \right) / 2 ,$$

or, approximately for short basins, $P = R \cdot S - V_{flats}$, where R is the tidal range (see Paragraph 5.2.5), S the planimetric surface of the basin landward of the selected cross section and V_{flats} the volume of the flats above low tide.

The tidal prism can be used to define a tidally averaged reference discharge $\overline{Q} = P/(T/2)$, where T is the whole tidal period.

With the assumption of sinusoidal tide, we can evaluate a sinusoidal maximum discharge $\hat{Q} = \frac{\pi}{2} \overline{Q}$, which can be used to obtain a reference value of the discharge ($\pi/2 \cong 1.57$), even if the basic assumption is sometimes inaccurate.

The sediment balance is not easy to assess. It is possible to use empirical relationships to evaluate the sediment transport, but the range of error is wide. Important sources of data are the measurements of the sediments extracted from the system (mainly sand mining) and moved inside it (dredging to deepen the channels and dumping of the sediment in other locations).

5.2.3 Kinematic quantities

In this paragraph we include the quantities related to the velocity of water and to the duration of different periods (the most important are ebb and flood durations). However, the discharges are calculated using velocities locally measured and then integrated over the cross section. In this way the discharges are secondary variables like, from this point of view, a lot of the others variables listed in these pages.

The tidal average of the absolute value of the velocity can be taken as a reference value; it is calculated as

$$\overline{U} = \frac{1}{T} \int_T \frac{|Q(t)|}{A(t)} dt ,$$

or, using the tidal volumes, as

$$\overline{U} = \frac{V_e + V_f}{AT} = \frac{\overline{Q}}{A},$$

where A is the cross-sectional area below mean sea level and T is the tidal period.
In analogy with the last definition, we can consider also the maximum discharge during the tidal cycle, in combination with the instantaneous value of the cross-sectional area, in order to estimate the bed-forming flow conditions (maximum velocity).

kinematics		dim	notes
U	velocity	$L\,T^{-1}$	
U	average over depth		meso-scale
u	velocity profile along depth		meso- to micro-scale
	average over width (or cross section)		macro-scale
$\bar{U}$	average over tidal cycle (absolute value)		
U_{max}	peak during the tidal cycle		
	velocity at maximum/minimum ebb water level		
	velocity at maximum/minimum flood water level		
	residual currents (average over tidal cycle)		
	duration	T	
	of ebb		
	of flood		
	of slack water		
	of an assigned velocity		
	sediment transport		
q_s	sediment load per unit width	$L^2\,T^{-1}$	

Table 4. List of kinematic quantities and related aspects.

Residual currents are defined as the tidally averaged value of velocity or discharge. They play a crucial role in the evolution of the estuary because they represent the net effect of the water motion. For example, the residual velocity can be defined as follows:

$$U_{res} = \frac{1}{T}\int_T U dt$$

Please note that also the instantaneous values of the velocity are important since the sediment transport usually depends on velocity through a power law with an exponent larger than one:

$$q_s \propto U^{\alpha},$$

where α ranges between 3 and 5. Consequently, small differences in velocity reflect in possibly large net effect in sediment transport. It might even happen that the directions of residual currents and residual transport are opposite.

5.2.4 Dynamical quantities

Dynamical entities are quantities related to forces or stresses.

The shear stress close to the bed is crucial to assess the sediment transport and the flow resistance. Instead of the bottom shear stress, sometimes it is useful to refer to the *friction velocity*

$$u_f = \sqrt{\frac{\tau}{\rho}}$$

which is practically equivalent, because the range of variation of the water density in natural environments is usually negligible to this end.

dynamics		dim notes
τ	bottom shear stress	$M L^{-1} T^{-2}$
	maximum local value width averaged	
τ_w	wind shear stress	
	specific density	$M L^{-3}$
ρ	water	
ρ_s	sediments	
g	acceleration due to gravity	$L T^{-2}$
	viscosity, diffusivity	$L^2 T^{-1}$
	kinematic eddy	
	Coriolis force	$M L T^{-2}$

Table 5. List of dynamical entities and related aspects.

The effect of *wind* on the morphology of tidal inlets is not easily assessable. It generates waves, with short wavelength, which mainly act on shallower areas, where the sediments are resuspended and eroded. Their deposition usually occurs into deep channels and the whole system tends to flatten (examples of this tendency are given by the Oosterschelde in the Netherlands and some regions of the lagoon of Venice in Italy). This behaviour is counteracted by the higher stream velocity, and consequently higher bottom erosion, inside the channels with respect to the shoals.
In the present analysis we will not consider the role of the wind because suitable theories for macro-scale estuarine evolution are not available in our knowledge. Moreover, the deep and large channels of the Western Scheldt are probably the elements that drive its morphology, differently from the case of lagoons, where the major part of the surface show depths of the order of one metre or even less.

The friction coefficient

The role of friction can be represented by the *Chézy coefficient*

$$C_h = \frac{U}{u_f}$$

which represents the closure often used to calculate the cross-sectional averaged velocity of the uniform flow

$$U = C_h \sqrt{g R_h s}$$

where s is the slope in the fluvial case and R_h is the hydraulic radius $R_h = A/B_w$ (B_w is the wet boundary, i.e. the sum of the widths of bottom and banks). Using the definition of friction velocity, the bottom shear stress is determined as follows, when the velocity is known (or both the discharge and the area of the cross section):

$$\tau = \rho\left(U/C_h\right)^2$$

Alternatively the drag coefficient is used:

$$C_D = \frac{1}{C_h^2}, \qquad \tau = C_D \rho U^2$$

In the following chapters it will be clear that a correct estimation of the frictional term is definitely necessary for a proper description of the sediment transport, which mainly depends on the bottom shear stress.
The above definition of the Chézy coefficient is dimensionless, but, for historical reasons, the dimensional form

$$C_* = C_h \sqrt{g} = k_s R_h^{1/6} = \frac{1}{n} R_h^{1/6}$$

is often used, where k_s is the Gauckler-Strickler coefficient (units of measurement $m^{1/3}/s$) and n is the Manning coefficient ($n=1/k_s$).
It is not easy to estimate the friction term; several relationships have been proposed in addition to the one above (Manning, Gauckler-Strickler), which can also take into account the effect of the roughness due to the presence of bed forms like the dunes. A widely used formulation has been proposed by Einstein (1950) and extended to the case of dunes by Engelund and Hansen (1967):

$$C_h = \sqrt{\frac{\theta_e}{\theta}}\left[6 + 2.5\ln\left(0.4\frac{D}{ds}\frac{\theta_e}{\theta}\right)\right]$$

where $\theta_e = 0.06 + 0.3\theta^{3/2}$ if $\theta_e < \theta$, and $\theta_e = \theta$ otherwise. Here θ_e represents the effective part of the Shields parameter (for the definition, see Paragraph 6.1.5), which is directly acting on the grains of sediment on the bottom (and hence cannot be larger than the total Shields stress).
If the sediment is coarse, dunes do not form and the relationship is valid with $\theta_e = \theta$.

5.2.5 Tide

Tide is obviously the most noticeable feature of estuarine and coastal environments. Its description is not the same everywhere, because the tidal wave changes while it propagates along the estuary.

tide		dim	notes
	tidal wave		
R	tidal range	L	
a	semi-diurnal (M_2) amplitude	L	
Φ	semi-diurnal (M_2) phase	rad	
	higher harmonics characteristics (M_4...)		
	asymmetry (flood - ebb dominated)		
	resonant behaviour (due to convergence, depth)		
	seaward boundary condition		
	transversal phase lag of tide		

Table 6. Tide description.

The *tidal range* is defined as the difference between the water level at high (*hw*) and low (*lw*) tide:

$$R = H_{hw} - H_{lw},$$

where H is the water level with respect to a given coordinate system (e.g. NAP in the Netherlands).
The tidal range can refer to different tidal conditions, namely spring, neap and mean (monthly averaged) tide. For these definitions see the next paragraph.
The *tidal amplitude* is usually defined as

$$a = R/2$$

The tidal wave spectrum shows several components, and the most important is the semi-diurnal astronomical tide (M_2), related with the revolution of the moon around Earth. Another important component is the first overtide M_4, whose frequency is twice the frequency of the M_2; higher harmonics usually play a negligible role in the morphological evolution of the estuary (even if they are important for water motion). Overtides are present at the mouth of the estuary when the offshore shelf is wide and flat (Dongeren and de Vriend, 1994).

When the estuary is short with respect to the tidal wavelength, water level and velocity (or discharge) are out of phase of approximately π/2 rad; for example, H~sin(t) and Q~cos(t). In real cases, even if the tidal forcing is purely sinusoidal (M_2), frictional and topographic effects give rise to overtides that change also the phases along the propagation of the tidal wave (Friedrichs and Armbrust, 1998).
For the Western Scheldt, Figure 10 shows the behaviour of the free surface level and the water discharge at the mouth of the estuary and at the Dutch-Belgian border.

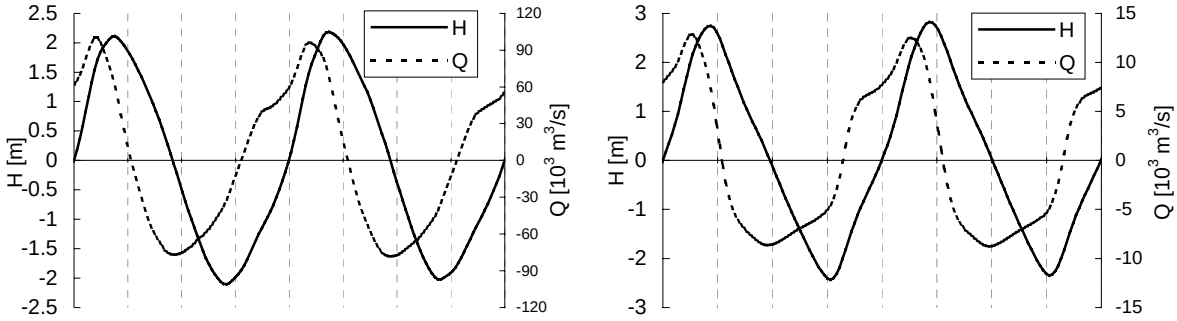

Figure 10. Water level and discharge during two tidal cycles, at the mouth of the estuary (Vlissingen, left) and at the border between Netherlands and Belgium (right). Data are taken from computations of SOBEK numerical model.

Spring and neap tides

The tidal range is not constant during the monthly cycle of the Moon around the Earth, because when the gravitational effect of the Sun is added the water level variation is larger (*spring tides*), while when it is subtracted the tidal range is smaller (*neap tides*). The former situation occurs when both the Sun and the Moon are aligned, the latter when the line Moon-Earth is perpendicular to the line Sun-Earth. Both the situations occur twice a month.
The result is shown in Figure 11, where it is clear that the tidal range during spring tide is much larger than during neap tide.

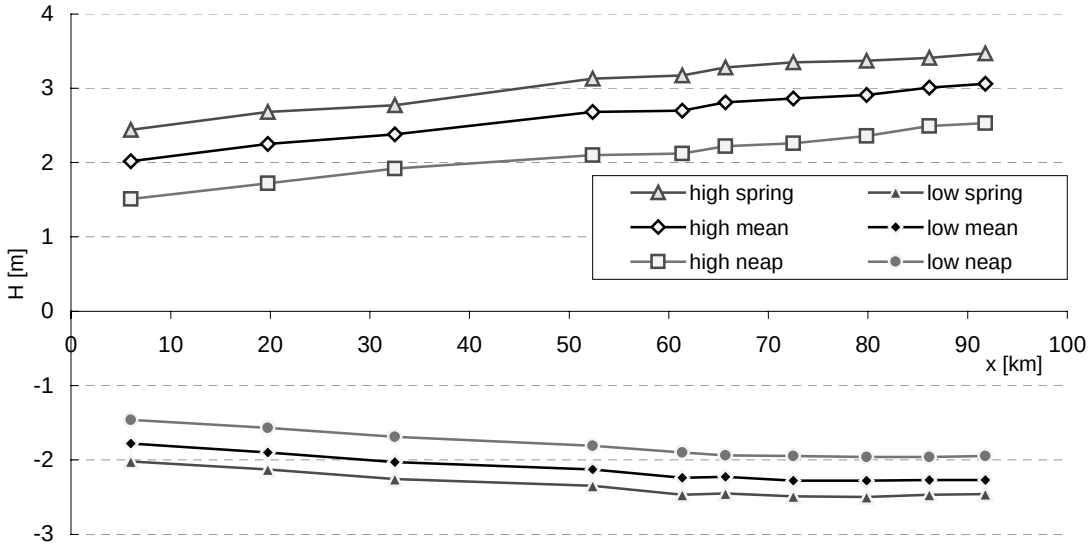

Figure 11. Measured free surface levels at high and low water along the Scheldt estuary, during spring, mean and neap tides.

5.2.6 Bed, water and vegetation

This paragraph includes several aspects of sediments, water and few indication about the type of vegetation that grows on the bed and the banks.

The *sediment* characterisation can be quantitatively made considering the average size and the distribution of different sizes.
The grain size, and consequently the type of sediment, is relevant for the process of erosion and sedimentation. A relatively small fraction of organic matter is sufficient to change a prevalently sandy mixture from a non-cohesive towards a cohesive behaviour.

The geometrical average d_{50} is usually considered to determine the type of sediments, while the coarser d_{90} gives information about the frictional flow resistance.

bed composition, water		dim	notes
	sediments		
d	reference grain size (d_{50}, d_{90}, ...)	L	
	grain size distribution	L	
	standard deviation	L	
w_s	deposition velocity	$L T^{-1}$	
	cohesive – non-cohesive	%	
	sand - silt - clay	%	
c	concentration in water	$M L^{-3}$	
	water		
	salinity	$M L^{-3}$	
	temperature	°C	
	vegetation		
	type		*descriptive*

Table 7. Bed, water and vegetation.

Water *salinity* plays a crucial role in all the situations where a salt wedge is present, because stratification affects the hydrodynamics and hence the morphology of the estuary. However, the Scheldt estuary is quite well mixed and the effect of stratification is negligible. Salinity can be very important for biology at the micro-scale because the content of salt in the soil is one of the main parameters for the existence of vegetation.

The *temperature* of water is another important parameter for biology, but it acts on the morphology only by means of the stratification of the liquid phase. Please note that if we use the temperature as a variable, from a dimensional point of view we introduce a new basic unit. However, we are not going to take into account the effect of temperature, for three main reasons: the stratification in well-mixed systems, due to small influx of water at higher temperature, is usually negligible; it primarily acts on a micro- or meso-scale; data about that are not available.

The effect of *vegetation* on the morphological features is one of the newer fields of the present-day research and would require a much deeper discussion. In the present contribution we are not going to analyse its importance and it is left to further research. It is important to note that there is a strong feedback between morphology and vegetation: the former creates the habitat where the latter can develop and, on the other hand, the presence of vegetation influences the sediment erosion and deposition. In this context, we can only summarise the main effects:

- land formation: vegetation creates new organic soil;
- bank stabilisation: the roots of the plants keep the sediments together and the formation of organic soil gives cohesion to it;
- sediment trap: several kinds of plants act as a trap for sediments.

All the above effects play a stabilising role on the morphological elements, but the continuous accretion of land can hinder the system to reach an equilibrium point.

5.2.7 Outer forcing

Table 8 summarises several completely different aspects related to the forcing factors that are not internal, in the sense that they are external with respect to the natural development of the estuarine system.

Some of the factors listed above are not easy to be included in morphological theories, because of their occasional or unpredictable character.

outer forcing	dim	notes
human interference		
construction of dykes		
deepening and mining		
navigation		
waves due to ships		
number of ships	T^{-1}	
tonnes of weight travelling per day	$M\,T^{-1}$	
extreme events		
storm (e.g. in the North Sea)		
sea surge		
breaking of dikes		
sea level rise	$L\,T^{-1}$	long term evolution

Table 8. Forcing effects from outside of the natural system.

The **construction of dykes** has two major effects on morphological evolution:

- it stops the lateral migration of the estuary, if occurring, and fixes the present day situation. In this way, the natural evolution of the system towards a different equilibrium (e.g. adaptation to new mega-scale boundary conditions) can be opposed by the fixed boundaries along the estuary;
- it seems that the presence of artificial banks leads to a deeper scour in the outer bend.

The second effect has been observed in a meandering river by Friedkin (1945, cit. in de Vries et al., 2001) and afterward by others. In his pioneering work, Van Veen (1950) noted that the turbulence created by banks attracts the channels towards them. Recently, Fredsøe et al. (2001) and Gíslason and Fredsøe (2001) found analogous effects, both in straight and curved channels, due to secondary circulations created by the difference of roughness and by the presence of a sharp corner between the bed and the artificial banks.

The effect of **navigation** on the morphology has not been adequately investigated yet. In the Scheldt, the influence of the continuous passage of big ships and cargos could be relevant. Besides, dredging (and consequently dumping) activities have the aim to increase the depth of the channels that go to the *Port of Antwerp* (picture on the right), which is one of the most important in the world.

Port of Antwerp - Number of ships and Gross Tonnage

Year	Number	Gross tons	Average GT
1975	17,376	83,772,000	4,821
1980	17,151	102,696,382	5,988
1985	16,420	119,631,146	7,286
1990	16,764	140,830,679	8,401
1995	15,223	167,858,597	11,027
1996	15,417	177,692,412	11,526
1997	15,861	182,340,352	11,496
1998	16,122	198,874,328	12,336
1999	15,493	197,345,696	12,738
2000	16,105	203,064,400	12,609

Source: Antwerp Port Authority (www.portofantwerp.be)

During 2000, an average of more than 44 ships have passed every day, carrying over 600 000 tons per day to Antwerp.

The morphological evolution can be affected by this passage in different ways:

- the ships induce waves that break when they reach the shoals, determining their erosion;
- the propellers act directly on the sediments on the bottom, destabilising it, mainly by means of resuspension mechanisms.

A separate comment should be made on the importance of **extreme events** in driving the evolution of the system. In fact these events (big storm, sea surge, breaking of dykes etc) are so strong that they are able to remodel the landscape even if they are singular and unpredictable. In this analysis we will not investigate this kind of factors.

5.3 Dimensional scales

In this paragraph we list the main spatial and temporal scales that can be defined in a tidal embayment.

scales		dim	typical value
L	length scale	L	
	estuary length		160 km
	convergence length		
	depth variation length		
	tidal excursion		7 km
	settling lag		
L_m	meander wavelength		
L_g	frictionless tidal wavelength		440 km
L_f	frictional length scale		
T	time scale	T	
T	tidal period		44700 s
	morphological (at different length scales)		
	time scale of consolidation of cohesive sediments		
ω	tidal frequency	T^{-1}	1.41E-4 Hz

Table 9. Spatial and temporal scales.

The definition of these scales can vary according to different authors. Here we report the most important ones.
The period of the semi-diurnal M_2 tidal component is usually taken as 12.41 h.

The **tidal frequency** is defined in the straightforward manner

$$\omega = \frac{2\pi}{T}$$

such as we can use a dimensionless time coordinate that is defined between 0 and 1 during one tidal period.

Depending on the schematisation adopted, we can define different **convergence lengths**. The most common is the exponential decay of width from the mouth landward,

$$B(x) = B_0 \exp(-x/L_w)$$

where L_w is the distance where the width is decrease of a factor e^{-1}. However, it is also possible to use the linear variation law

$$B(x) = B_0 (1 - x/L_w)$$

where L_w is the distance where the width conventionally vanishes.
Related with the convergence length of the width, we can introduce also the length of depth variation, which is less significant and not very easy to define.

The **tidal excursion** is the distance travelled by water particles, on the average, during one tidal cycle:

$$\ell = \overline{U} T$$

where $\bar{U}$ is the average velocity and T is the tidal period.

Hence $\ell = \frac{\overline{Q}}{A} T = \frac{2P}{A}$, where P is the tidal prism and A the area of the cross section (see also Paragraph 5.2.3).

The **frictionless tidal wavelength** is the theoretical length of the tidal wave without friction:

$$L_g = T\sqrt{gD}$$

where D is a reference value of the depth.
The **frictional length** scale can be evaluated, following Schuttelaars and de Swart (2000), as

$$L_f = \frac{2\pi\sqrt{gD_{\max}}}{\omega}\sqrt{2\Big/\left[-1+\sqrt{1+\left(\frac{8C_D aL}{3\pi\mu D_f D}\right)^2}\right]}$$

where D_f is a frictional depth, such as $\frac{1}{D_f} = \frac{1}{L}\int_0^L \frac{dx}{D}$, and μ is a constant between 0 and 1 related to the effective depth in the friction term of the momentum equation.

The **settling lag** is the distance of sedimentation of the grains transported as suspended load. It is not a real length scale, because it depends on several quantities and especially on the velocity, but it can be worth to be evaluated to assess whether the adaptation of the suspended transport can be considered immediate or not. It is also related to the distance travelled, on the average, by a particle of sediment.

The **meander wavelength** can be defined as the length between two corresponding points along the bends of two consecutive meanders. We can consider an intrinsic definition, following the axis of the channel, or a Cartesian one, as the right line distance (which is of course shorter than the former).

Several length scales have a corresponding time scale. Among the other scales we can indicate the **morphological time scale**, which is defined as the reference time when significant changes occurs in the morphology, at the scale under examination. Since its evaluation is not simple, researchers normally use the sediment continuity equation to define it, because this equation controls the evolution of the bottom elevation.

5.3.1 Tidal range and mega-scale classification of estuaries

The tidal range can hardly be considered a length scale, but it is a dimensional parameter so widely used that it requires a separate treatment.
Tidal range, defined as the dimensional tidal amplitude at the mouth, is often used in the mega-scale classification of estuaries (for a introductory review, see Seminara et al., 2001): *micro-tidal* (tidal range <2 m); *meso-tidal* (2-4 m); *macro-tidal* (>4 m).
Other types of classification rely on parameters that are different, but often show strong correlations with the tidal range (Seminara et al., 2001), namely:

- the ratio between tidal prism and the volume of fresh water discharged by the river during the tidal cycle, where macro-, meso- and micro- refer to the order of magnitude of this ratio;
- the mixing between fresh and salt water (salt wedge estuaries - micro-tidal; partially mixed estuaries - meso-tidal; well mixed estuaries - macro-tidal).

Following this classification, the Western Scheldt results to be a well-mixed, macro-tidal estuary, because the tidal range is around 4 m at the mouth, the contribution of fresh water is negligible and there is no salt wedge.

6 RELEVANT PARAMETERS

The following list of parameters does not claim to be exhaustive. The chapter aims to show which parameters conceptual models have considered, which might have a role in the problem and which are good candidates to be the controlling factors. Referring to the methodological approach introduced in Chapter 4, this list is somehow before the pre-selection, because it includes also mega-scale parameters. The reason of their inclusion lies in the fact that they have been considered in morphodynamic theories. Besides, it is not easy to separate mega-scale influence from macro-scale effects.

The parameters are introduced with some theoretical comments and some basic analyses of data from the Scheldt estuary, with the aim to get some suggestions for the selection procedure, especially considering the length scales. A deeper investigations of data, together with the final selection, follows in Chapter 8.

6.1 Dimensionless parameters

In this section the dimensionless parameters are presented. As pointed out above, all parameters should be dimensionless, but some dimensional parameters are introduced in Paragraph 6.2 because of their wide use.
Dimensionless parameters usually are ratios of different aspects of the problem, which do not necessarily balance when the value of the parameter is 1. Considerations about the importance of such parameters are often made hereafter and the terminology *large* or *small* should refer to their order of magnitude (>>1 or <<1) or to comparisons among different situations.

6.1.1 Mass balance

Tidal prism / fresh water volume

As pointed out above (see Paragraph 5.3.1), the ratio between tidal prism and the fresh water inflow

$$tr = \frac{2P}{Q_r T}$$

is a parameter used in the mega-scale classification of estuaries to estimate sea/river dominant effect and it is often related to the tidal range.
In the case of the Western Scheldt, the importance of the river discharge can be considered negligible. Tidal prism varies from $860 \cdot 10^6$ m^3 at Vlissingen to $150 \cdot 10^6$ m^3 at the border between the Netherlands and Belgium.
Average river discharge is about 120 m^3/s, with a maximum value of 400 m^3/s (Allersma, 1994), which correspond to a volume of $5.4 \cdot 10^6$ m^3 and $17.9 \cdot 10^6$ m^3 during the tidal cycle, respectively.
Therefore, the value of this parameter varies from 320 for average discharge (96 when Q_r is maximum) at Vlissingen, to 56 (17) at the border.
In the upstream part, where the tidal prism decreases and the estuary can be considered a tidal river, the influence of fresh water discharge increases and this parameter might be important for the characterisation of single reaches of the estuary.

Suspended load / bed load

Most of the tidal environments are characterised by sediment with a grain size less than 0.2 mm. For this type of sands and for the common velocities, the sediments are transported mainly in suspension during the major part of the tidal cycle. In this way the ratio between suspended load and bed load is usually large. However, as pointed out by Fredsøe (1978), and recently by Schramkowski et al. (2001), bed load cannot be completely neglected, because it has a fundamental stabilising effect on the formation of bars with high transversal modes (see Paragraph 7.1). Basically, the bed load tends to flatten the sharp peaks since the gravitational force gives rise to a transport of sediments close to the bottom towards the lower locations, where the transversal slope increases.

6.1.2 Geometrical ratios

Ratios between geometrical variables are widely adopted in theories because of their simplicity and their significance.
Since the attention is focused on the macro-scale, the definitions of the geometrical entities are assumed to be different with respect to the usual meso-scale framework. Instead of measuring depth, area and width of the cross sections, the most suitable choice is to use volumes, planimetric surfaces and reference length of the reach of estuary under consideration.

For a single estuarine section, the operational definition of **average depth** adopted in this study refers to the volume of water below the water level and the corresponding planimetric wet surface:

$$D_{av} = \frac{V}{S}$$

while, if we consider a particular cross section, the exact definition is the ratio between the cross sectional area and the width at the free surface.

A macro-scale averaged **cross-sectional area** can be valued as

$$A_{av} = \frac{V}{L}$$

where L is the reference length of the estuarine section (see Figure 6). Its definition is not straightforward and needs a gross evaluation.

The corresponding definition of macro-scale **width** is

$$B_{av} = \frac{S}{L}$$

with the same notation of the above formulas.

High water depth / low water depth

This parameter and the following one are proposed by Dronkers (1998) as the two controlling parameters of the equilibrium configuration of tidal basins:

$$r_{D*} = \frac{D^*_{hw}}{D_{lw}}$$

At low water level during tides, the average depth

$$D_{lw} = V_{lw} / S_{lw}$$

is defined as the ratio between the volume and the planimetric wet surface. At high water level, the original Dronkers' definition

$$D^*_{hw} = D_{lw} + R$$

is the sum of low water depth and the tidal range. Please note that this depth can be considerably different from the average depth at high tide

$$D_{hw} = V_{hw} / S_{hw}$$

when the typical cross section is compound. This fact implies that the ratio

$$r_D = \frac{D_{hw}}{D_{lw}}$$

can be different from r_{D*} and therefore expresses different meanings. Indeed, r_{D*} stresses the effect of the tidal range, while r_D is based mainly on the geometrical features of the cross-section at the two water level (high and low water).

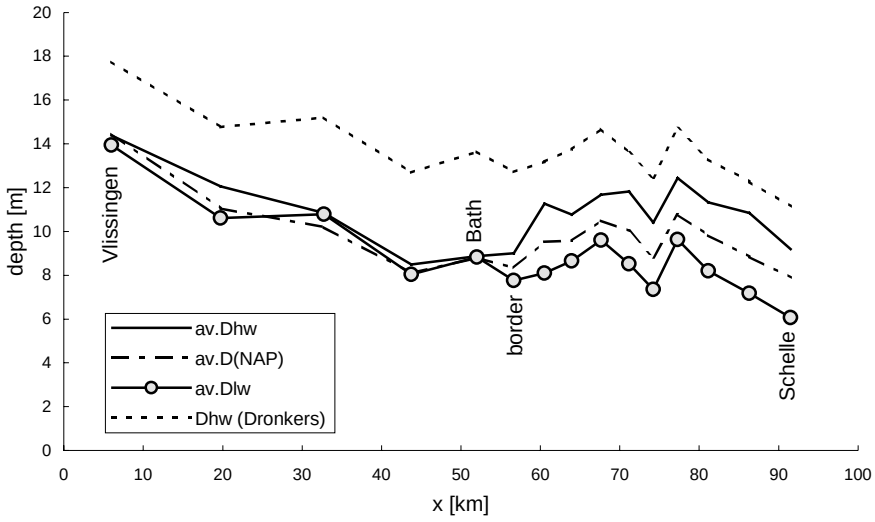

Figure 12. Different definitions of reference depths, along the sections of the Scheldt estuary (from Vlissingen to Schelle).

Figure 12 shows the variation of the average depths along the estuary. There is a clear distinction between two zones:

- from Vlissingen to the border, the value of depth at high tide D^*_{hw} suggested by Dronkers is quite different from the average high water depth D_{hw}. On the contrary, the average depth does not vary significantly at low (D_{lw}) and at high tide (D_{hw}), because the cross-sectional width is much larger in the latter case;
- upstream of the border, the morphological features changes and the difference of the averaged depths at different levels increases, because the cross-section is more compact.

The influence of the shape of the section is explained in detail in the following paragraphs.

Planimetric wet surface: high water / low water

The other parameter used by Dronkers is the ratio between the wet surface at high tide and at low tide:

$$r_S = \frac{S_{hw}}{S_{lw}}$$

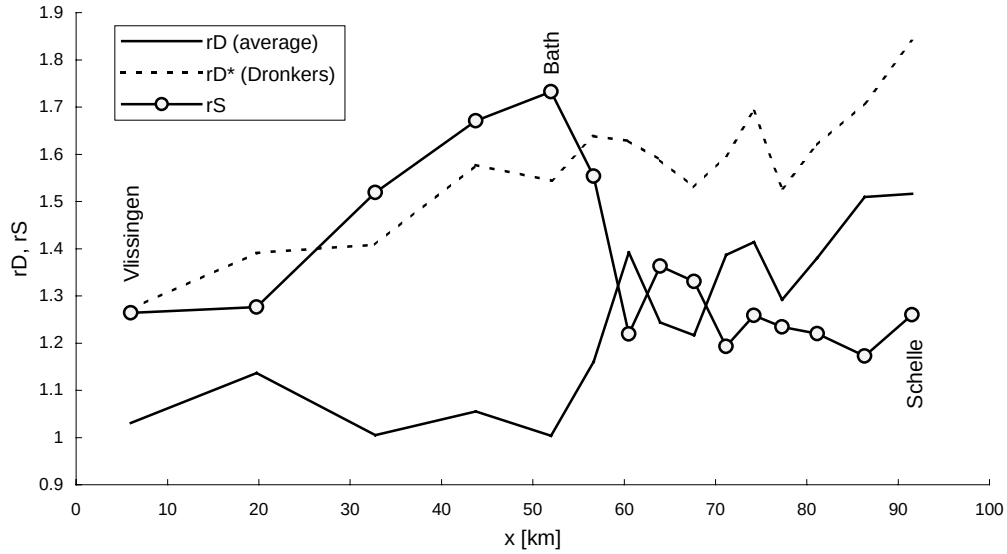

Figure 13. Ratios between depths and between surfaces at high and low water, for the estuarine sections of the Scheldt estuary (from Vlissingen to Schelle).

This parameter gives valuable information about the presence of intertidal areas. In fact, the difference between surfaces at high tide and at low tide is just the definition of the planimetric surface of the intertidal areas.
The advantage of this parameter is that it is very easily measurable, but it shows the limitation that it is not able to distinguish among different types of intertidal areas (i.e. whether they are similar to islands in the middle of the channel or close to the banks).
From Figure 13 we can detect the transition from the seaward part of the estuary to the Belgian part if we observe the abrupt decrease in the surface ratio and the increase in the average depth ratio (as already noted above in Figure 12).
The validity of the theory by Dronkers will be discussed in Paragraph 8.2.1.

Volumes: high water / low water

In analogy with the previous parameters, it is possible to introduce also the ratio between volumes of water below an assigned level

$$r_V = \frac{V_{hw}}{V_{lw}}$$

This parameter is strongly related with the following one (see Figure 15).

Tidal range / depth

The ratio between the tidal range and a characteristic depth (to be chosen among the several definitions of average depths)

$$r_R = \frac{R}{D}$$

is intuitively a basic parameter for a tidal embayment. If we consider the average depth at low water, the difference between this parameter and the previous one (r_V, see Figure 15) is related to the volume of water above the intertidal areas.
Indeed

$$r_V = \frac{V_{lw} + \left(V_{hw} - V_{lw}\right)}{V_{lw}} = 1 + \frac{S_{lw}R + \Delta V_{it}}{V_{lw}} = 1 + \frac{R}{D_{lw}} + \frac{\Delta V_{it}}{V_{lw}} = r_{D^*} + \frac{\Delta V_{it}}{V_{lw}}$$

$$r_R = \frac{R}{D_{lw}} = r_{D^*} - 1$$

where ΔV_{it} is the volume of water, at high tide, above the intertidal areas (see Figure 14).

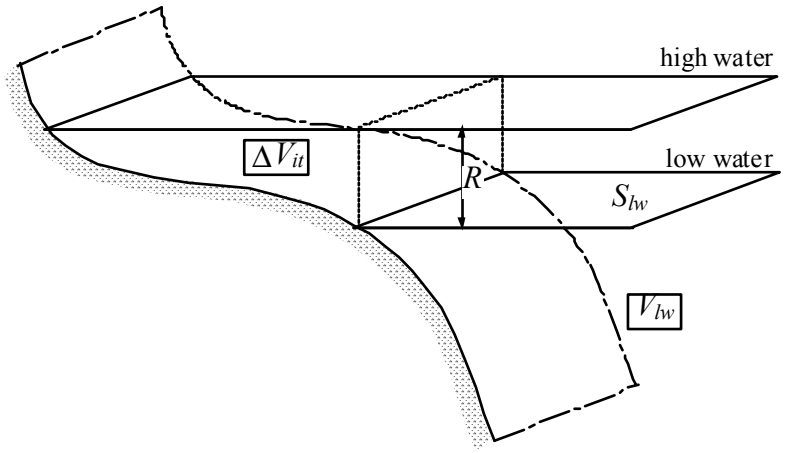

Figure 14. Sketch of the volumes at high and low tide.

In this way we can also define the averaged water depth above the intertidal areas

$$D_{it} = \frac{\Delta V_{it}}{S_{hw} - S_{lw}}$$

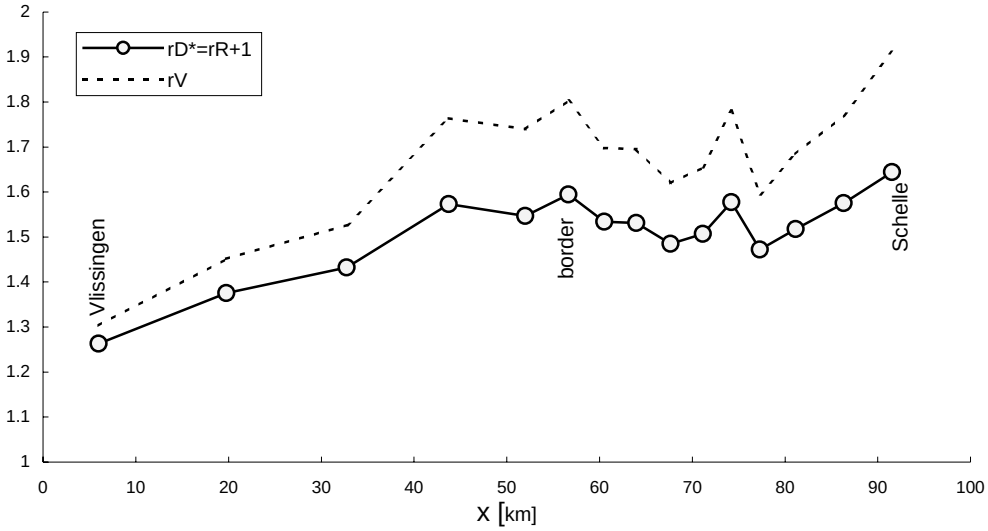

Figure 15. Ratio between tidal range and average depth at low water r_R (for sake of comparison, the related ratio r_{D^*} is plotted in continuous line with circles), and ratio between volumes at high water and low water r_V (dashed line), along the sections of the Scheldt estuary (from Vlissingen to Schelle).

Width to depth ratio (aspect ratio)

The ratio between the width and a characteristic depth of the cross section, usually called *aspect ratio*,

$$\beta = \frac{B}{D}$$

has been proved to represent the major controlling factor for the fluvial case, both in theories (Seminara and Tubino, 1989; note that the actual definition of β given by the authors makes use of half width instead of width) and in field observations (for the river Rhine in the Netherlands, see Schoor et al., 1999). In the tidal case it seems to play a crucial role as well (Seminara and Tubino, 2001).

The definition of β in the models refers to a single channel (meso-scale) and the extension to the macro-scale (channels and tidal flats) does not seem to be straightforward. Furthermore, in a tidal embayment, the definition of width and depth is not univocal because it depends on the water level. We use three values of β using the average depth defined above at high, mean and low water level:

$$\beta_{hw} = \frac{B_{hw}}{D_{hw}}, \quad \beta_{mw} = \frac{B_{mw}}{D_{mw}}, \quad \beta_{lw} = \frac{B_{lw}}{D_{lw}}$$

From Figure 17 we can observe the distinction between the two parts of the Scheldt estuary:

- in the Dutch part β increases with the water level (i.e. β at high tide is larger than β at low tide), because the cross sections typically show a significant increase of width in the higher part;
- in the Belgian part the trend is the opposite (i.e. β decreases when the tide increase), because the cross section is more compact.

This behaviour can be easily explained if we consider three schematised types of sections. If we define a section as

$$width = (maximum\ depth)^{\ n}$$

we have that[1]

$$\beta = (n+1)\ (maximum\ depth)^{\ (n-1)}$$

[1] The schematised section in the *y*-*z* plane (see Figure 16) is described as $y = z^n$. We can integrate to obtain the cross-sectional area $A = \int_0^D y dz = \int_0^D z^n dz = \frac{D^{n+1}}{n+1}$, where D is the maximum local depth. Hence we can evaluate the average depth as $D_{av} = \frac{A}{B} = \frac{D^{n+1}}{n+1}\frac{1}{D^n} = \frac{D}{n+1}$ and finally $\beta = \frac{B}{D_{av}} = D^n \frac{(n+1)}{D} = (n+1)D^{n-1}$.

According to different values of n, we can have:

a) *U-shaped* section (n<1, limit case n=0 for rectangular section), β decreases when the water level increases;
b) *V-shaped* section (n=1, triangular section), β remains constant;
c) *Y-shaped* section (n>1), β increases with the water level.

The first case is typical of the Belgian part, while the third case can describe approximately the Dutch part. A more detailed analysis of data from the real case is done in Paragraph 8.1.2.

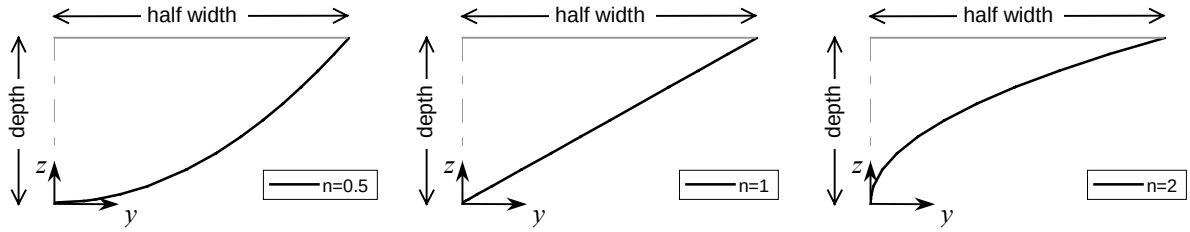

Figure 16. Examples of schematised sections: U-shaped (n=0.5), V-shaped (n=1) and Y-shaped (n=2).

The U-shaped section can also be defined as *compact* section, while an Y-shaped section corresponds to a cross-section characterized by a deep narrow channel (or channels) and a widening width at higher water levels.

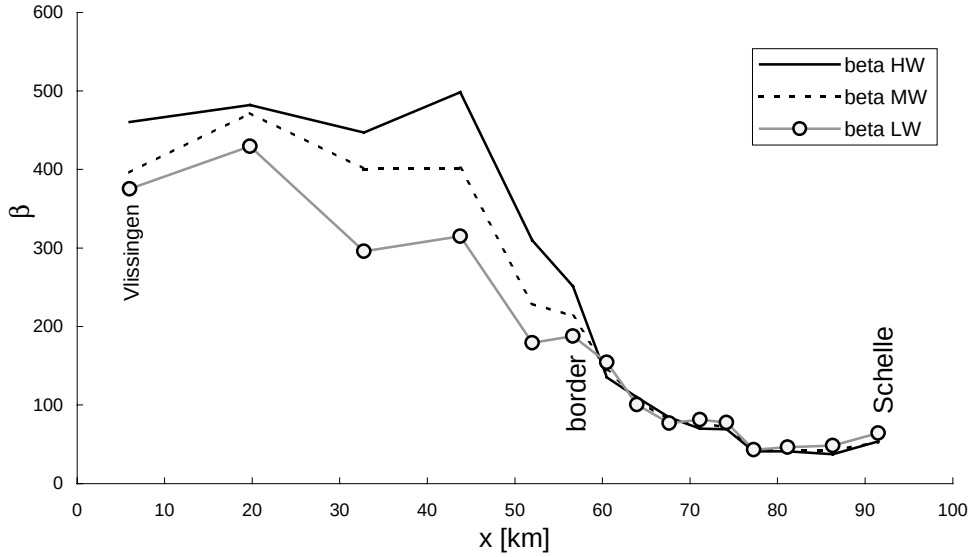

Figure 17. Width to depth ratio for high water level (HW), mean water (MW) and low water (LW), along the estuarine sections of the Scheldt estuary (from Vlissingen to Schelle).

However, the role of the parameter β is not only descriptive. Indeed, it has been related to the development of the instabilities of the bed topography, which arise from the coupling of hydrodynamics and bottom erosion/deposition processes. Such perturbations of the bottom of the channel are called bars and have been analytically studied during the past twenty years in the fluvial case (see for instance Colombini et al., 1987; Seminara, 1998).

The *alternate bars* are the basic type: a longitudinal repetitive pattern of scour and deposition; for a specific cross-section, they show a transversal structure of scour near one bank and deposition in the other. Higher transversal modes can be considered, which can give rise to a more complicated topography (e.g. a bar in the middle of the channel). A more detailed description of the types of bars is given in Paragraph 7.1.

It has been shown that a threshold exists for β in rivers, above which alternate bars can freely develop in straight channels; a further increase admits also the growth of higher transversal modes. Seminara and Tubino (2001) extended such considerations to tidal channels and found that β play an important role as well.

This general result of the theory is confirmed by the analysis of different estuaries shown in Figure 18 (Allersma, 1994): an increase in the aspect ratio results in a higher number of channels.

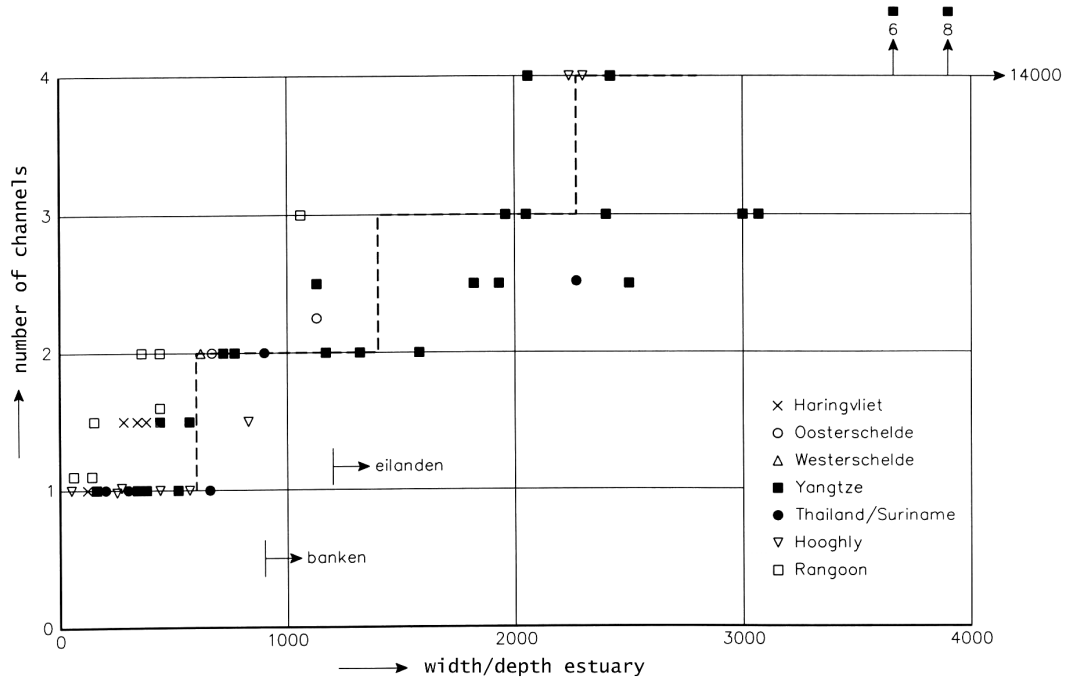

Figure 18. Number of channels vs. ratio width/depth, for different estuaries (Allersma, 1994; the titles of the axes have been translated from Dutch into English).

Geometrical features of the main channels

The presence of well-developed channels suggests to consider the width to depth ratio for each main channel (thus excluding the intertidal areas in the middle of the estuarine sections), following the meso-scale approach for which the local theories (e.g. Seminara and Tubino, 1989, for rivers and Seminara and Tubino, 2001, for tidal channels; see also Paragraph 7.3.1) are valid. Hence we can obtain some indications about the trend in bottom evolution by studying the formation of bars.

The estuary, considered as a whole channel, shows very high values of β (average) in the seaward part, as can be noticed in Figure 17, but the main channels are deeper and narrower. If we apply the theories to the former case, we find that high transversal modes can grow and islands can potentially form; on the other hand, the lower values of β in the latter case suggest that only the lower modes (e.g. alternate bars) are excited.

Curvature ratio

The curvature of the channel axis has a strong influence on the altimetric and planimetric evolution of the channels because it induces a secondary circulation and consequently the development of point bars (forced bars, see Paragraph 7.1). These bars are typically stationary since they are driven by geometrical, slowly changing forcing (or constant where the banks are fixed by dikes). Indeed, we can assume that the time scale of planimetric evolution is much longer than that of altimetric deformation of the bed. This is even more justifiable if we notice that the planimetric boundaries of the Scheldt have been fixed by the construction of the dykes along almost all the estuary.

If we adopt the width of the channel as the length scale for planimetric quantities, we can define the dimensionless curvature as

$$\nu = \frac{B}{R}$$

where R is the minimum radius of curvature of the bend, usually referring to the channel axis.

This parameter is usually small, as recently confirmed by field observations (Solari et al., 2002). For this reason, using perturbation methods, if it is taken as the order of magnitude of the perturbations with respect to the basic state, a linear stability analysis can be successful. However, a larger value of the curvature ratio should result in a faster initial growth of bars from an hypothetical plane bed and maybe in a larger final amplitude.

Dimensionless wavenumber

All deviations from a straight line can be decomposed, by using Fourier analysis, into different components and it is often possible to find that some harmonics are much more important that the others. This is typically the case of the curvature in meandering rivers.
Bed forms are often periodic. If we consider a single harmonic of wavelength L_b, we can define the dimensionless wavenumber as follow (using the channel width as the length scale, as suggested by Seminara and Tubino, 2001; Solari et al., 2002, show that field observations confirm this scaling also for meanders):

$$\lambda = 2\pi \frac{B}{L_b}$$

Typical values of λ for tidal meanders fall in the range 0.2÷0.4 (Solari et al, 2002).

Strouhal number

The Strouhal number is a mega-scale parameter (Schuttelaars and de Swart, 1999):

$$S_t = \frac{\overline{U}}{\omega L} = \frac{1}{2\pi}\frac{\ell}{L} = \frac{\hat{a}}{D}$$

which can be related to a local definition through a reference tidal amplitude $\hat{a}$ (for the definition of the variables, see Chapter 5). If we consider the continuity equation

$$\frac{\partial A}{\partial t} + \frac{\partial Q}{\partial x} = 0\,,$$

using the scaling $\partial A/\partial t \sim O(B\hat{a}\omega)$ and $\partial Q/\partial x \sim O(BDU/L)$, where L is a suitable length scale, the two terms must balance:

$$U \sim \hat{a}\omega L/D$$

The Strouhal number can be used to measure the importance of the non-linear hydrodynamic terms in the shallow water equations. It is often a small parameter.
This ratio, such as the two following parameters, describes mega-scale characteristics of the estuary. However, the ratio between tidal excursion and a reference length can be used to get information about the macro-scale zones; please note that, for the Western Scheldt, tidal excursion can be of the same order of the length of the estuarine section.

Length / frictionless tidal wavelength

The ratio between the embayment length and the frictionless tidal wavelength gives a measure of the type of tidal embayment (Schuttelaars and de Swart, 2000):

$$l_g = \frac{\omega L}{\sqrt{gD}} = 2\pi \frac{L}{L_g}$$

The behaviour of an estuary strongly varies depending upon it is short (lower values of l_g) or long. In the former case, the tidal wave is reflected at the end of the estuary and can be assumed to be stationary (i.e. the free surface level rises and falls almost at the same time in the whole estuary).
This parameter, like the following one, is intrinsically related to the mega-scale description of the estuary, since it involves global length scales. For the Scheldt estuary (160 km from Vlissingen to Gent) this parameter is certainly not small and the estuary cannot be considered short.
Even if it is mainly important for the mega-scale, obviously the type of tidal embayment has striking consequence also on the macro-scale development.

Frictional length / frictionless tidal wavelength

The ratio between the frictional length and the frictionless tidal wavelength is

$$l_f = \frac{L_f}{L_g}$$

This mega-scale parameter has been included in the analysis of Schuttelaars and de Swart (2000) to study the resonant behaviour of the tide propagation in long estuaries.
We are not able to consider the influence of all these mega-scale parameters on the macro-scale features of the estuarine sections because such analysis should require the knowledge of data from a lot of different estuaries, which are not available at the moment.

Length / convergence length

The convergence length, suitably made dimensionless using the length of the estuary

$$l_w = \frac{L}{L_w}$$

gives rise to a parameter that can be very relevant for the mega-scale description of the estuary, both for the hydrodynamics (Lanzoni and Seminara, 1998; recently Toffolon et al., 2002, considered its influence on the amplification of the tidal wave during the propagation in convergent channels) and the morphology.
However, since only one estuary is studied in the present analysis, we cannot assess the relevance of this factor on the macro-scale morphology.

6.1.3 Tidal wave

Some aspects related to the tidal wave have already been taken into account above (see Paragraph 5.2.5), while others are analysed in further detail in this section.
A reasonable description of the vertical oscillation, due to the tidal wave, can be expressed as

$$H = H_0 + a_{M2}\cos(\omega t - \phi_{M2}) + a_{M4}\cos(2\omega t - \phi_{M4})$$

where H_0 is the mean level, which can vary on a time scale slower than the tidal period.

Tidal asymmetry

The tidal asymmetry can be defined in different ways according to the variables taken into account. Basically there are two definitions (Jeuken, 2000):

$$asymmetry = \log(\Pi_{ebb} / \Pi_{flood}) \quad \text{or} \quad asymmetry = \Pi_{ebb} - \Pi_{flood}$$

where Π is the variable under consideration, for instance the duration of the ebb and flood phases.

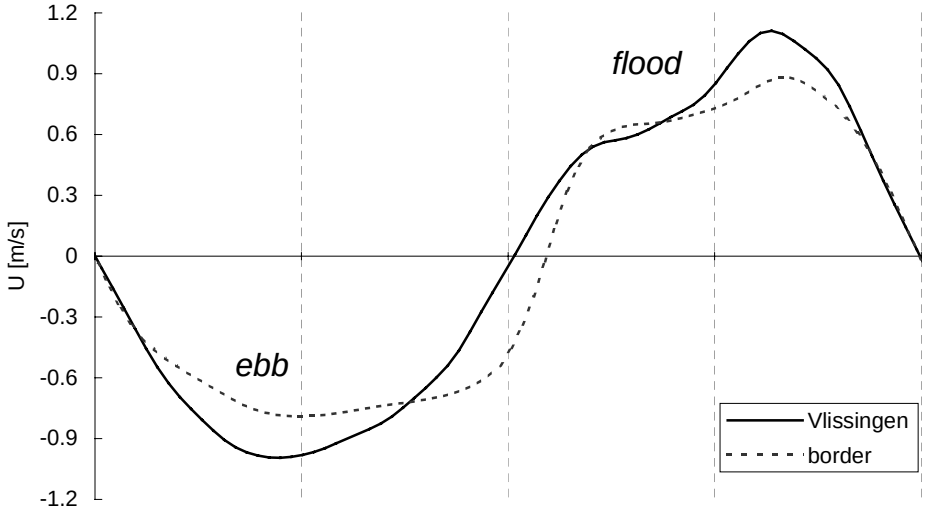

Figure 19. Cross-sectional averaged velocity during the tidal cycle, at the mouth of the estuary (Vlissingen) and at the border between Netherlands and Belgium (computations of the SOBEK numerical model).
The two curves are translated to align the time of the beginning of the ebb phase (U=0, dU/dt<0) for sake of simplicity in the comparison between the durations of the ebb and flood phases.

Tidal asymmetry is important in mega-scale models because it gives the tidally averaged residual currents. Indeed, since the sediment transport typically depends on the velocity by means of an exponent larger than 1, the differences between the ebb and the flood peaks are increased. For this reason, several models assume that a symmetrical behaviour during the tidal cycle is necessary in order to reach an equilibrium configuration of the estuary (e.g. see Dronkers, 1998).
Figure 19 shows the trend of the cross-sectionally averaged velocity in two locations of the Western Scheldt. Note that the behaviour during the flood phase (positive velocity) is different from the ebb phase (negative velocity). In the Scheldt estuary the flood peak is higher than the ebb peak, but the duration of the flood phase is shorter. If we relate the flood phase (velocity directed landward) with the rising phase (increasing water level) and the ebb phase with the descending phase, we can see from Figure 20 that the ebb phase is longer than the flood phase along the whole estuary.

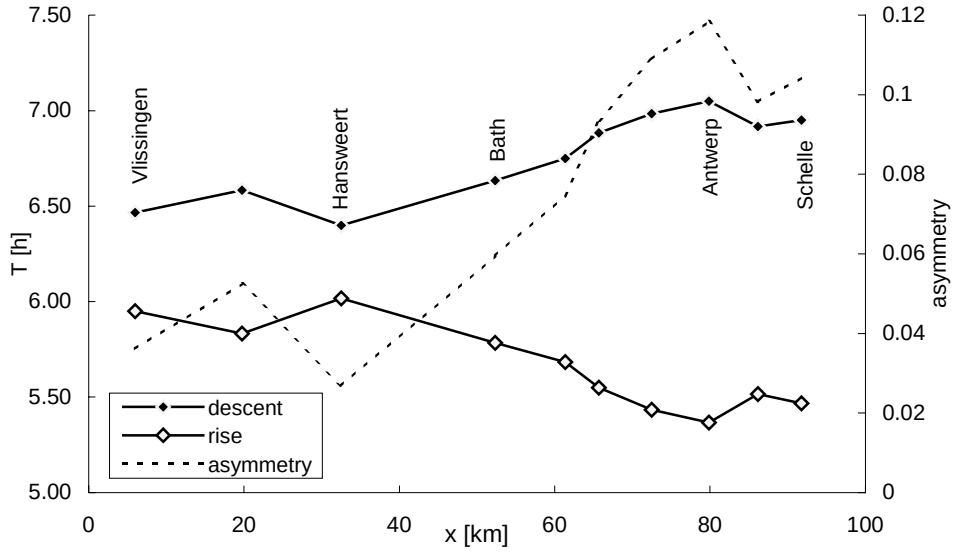

Figure 20. Durations (in hours) of the rising (flood) phase and the descending (ebb) phase; asymmetry between durations with the logarithmic definition: *asymmetry* = log (T_{ebb}/T_{flood}).

Characteristics of M_4 and M_2 tidal components

The ratio between the amplitudes of the M_4 and M_2 components of the tidal wave

$$m_4 = \frac{a_{M4}}{a_{M2}}$$

is proposed by Schuttelaars and de Swart as a relevant parameter for a mega-scale description of the tidal embayment, along with their phase difference

$$\varphi_4 = \phi_{M4} - 2\phi_{M2}$$

The former parameter gives an evaluation of relative importance of the higher component with respect to the basic semi-diurnal tidal amplitude, while the latter is important in the assessment of the residual terms.
A negative value of the phase difference φ_4 results in a longer ebb than flood duration (as in the case of the Western Scheldt), hence producing more intense flood currents. As already noted (see Paragraph 5.2.3), sediment transport is a non-linear function of the velocity and the consequence is a net sediment transport into the embayment.

Phase lag between discharge and water level

Another parameter to be considered is the phase lag between the maximum water levels and the peak of the discharge. For sake of simplicity, the simple laws

$$Q = Q_{\max}\cos(\omega t) \qquad H = a\cos(\omega t - \alpha)$$

can be used to represent, with the angle α, the phase lag between the time when the maximum discharge and the high water level occur. In the Western Scheldt and in many other estuaries, α is approximately $\pi/2$ (as can be inferred also from Figure 10): the peaks of both ebb and flood discharge occur around the mean water level. This is

important because, as already noted, the bed-forming conditions are related to the largest values of the bottom shear stress, and hence to velocity.

6.1.4 Sediments

Particle Reynolds number

The Reynolds number of the grain of sediment is defined in the following way:

$$R_p = \frac{\sqrt{g\Delta d_s^3}}{\nu_k}$$

Since the gravity g, the relative density of sediments Δ and the kinematic viscosity ν_k can be considered constant, R_p is a dimensionless version of the sediment grain size d_s. In fact, the relative density of sediments

$$\Delta = \frac{\rho_s - \rho}{\rho}$$

is almost always constant for sands ($\rho_s \cong 2650$ Kg m^{-3}, $\rho \cong 1000$ Kg m^{-3}, $\Delta \cong 1.65$).

Dimensionless grain size

The proper length to scale the sediment grain size is the water depth:

$$d_a = \frac{d_s}{D}$$

even if there are several possibilities for the choice of the grain size and the reference depth D. The reference grain size can vary according to the utilisation; the geometrical mean d_{50} is probably the most used, but also d_{90} is considered in order to evaluate the friction coefficient.
The dimensionless diameter is important for the determination of flow resistance. For instance, Einstein's relation (1950) for the Chézy coefficient

$$C_h = \frac{1}{\sqrt{C_D}} = 6 + 2.5\ln\left(0.4\frac{D}{d_s}\right) = 6 + 2.5\ln\left(\frac{0.4}{d_a}\right)$$

depends only on the dimensionless grain size (if no dunes are present, see also Paragraph 5.2.4).

Sediment composition

The sediment composition varies along the estuary: in the seaward part it is mainly sand (although the grain size is coarser in the channels and finer in the shoals), while upstream the percentage of clay and silt increases. Data for the Scheldt estuary are shown in Figure 35.
A small percentage of silt or clay can give cohesion to the mixture of sediments, changing its properties, especially for erosion and deposition processes. The major part of the models deals only with non-cohesive sediments. For a review about cohesive sediments see van Ledden (2000).

6.1.5 Dynamical ratios

In this section we define those parameters that arise from the ratios between forces.

Shields parameter

The ratio between the bottom shear stress τ and the submerged weight of sediment per unit of surface is usually called Shields parameter or Shields number:

$$\theta = \frac{|\tau|}{(\rho_s - \rho) g d_s} = \frac{C_D U^2}{g\Delta d_s}$$

It is related to the capability of the stream to pick up sediments.

Middelkoop (2001) and Schoor et al. (1999) included the Shields parameter among the most relevant parameters for rivers, and Seminara and Tubino (2001) showed that it can be considered one of the factors controlling meso-scale morphological evolution. Schuttelaars and de Swart make use of a related parameter (see next section).
If a critical value θ_c of the Shields number can be defined, i.e. no sediment transport occurs below this threshold, its evaluation might play a crucial role in the models if the velocities are low. Note that, once that the critical shear stress is given, it is possible to determine the period when bed is steady during the tidal cycle requiring that $\theta(t)<\theta_c$.

Bottom friction parameter

Schuttelaars and de Swart define a tidally averaged dimensional friction parameter as

$$\chi_{\dim} = \frac{8}{3\pi} C_D U_{\max}$$

where $U_{\max}$ is the maximum cross-sectional velocity during the tidal cycle.
It can be used to linearize the bottom shear stress τ (an underscore represents a vector)

$$\underline{\tau}(t) = \rho \chi_{\dim} \underline{U}(t)$$

according to the procedure originally proposed by Lorentz (1922). It is easy to demonstrate that, if we take a sinusoidal velocity $U = U_{\max}\cos(\omega t)$, the bottom shear stress can be expressed, using a Fourier expansion, in the following form:

$$\frac{\tau}{\rho} = C_D |U| U \cong C_D U_{\max}\left[\frac{8}{3\pi} U_{\max}\cos(\omega t) + \frac{8}{15\pi} U_{\max}\cos(3\omega t) + \ldots\right]$$

where the first term of the series is $\tau(t) \cong \rho C_D \frac{8}{3\pi} U_{\max} U(t)$.
The dimensionless form proposed by the authors is

$$\chi = \frac{\chi_{\dim}}{\omega D} = \frac{8}{3\pi} C_D \frac{U_{\max}}{\omega D}$$

or, introducing a reference tidal amplitude $\hat{a}$ (see Paragraph 6.1.2 and Schuttelaars and de Swart, 1999),

$$\chi = \frac{8}{3\pi} \frac{C_D \hat{a} L}{D^2}.$$

Ratio of inertia and advection

The ratio between inertia and advection can be expressed, using the width B as the length scale of the phenomenon, as follows:

$$\upsilon = \frac{\omega B}{U} = 2\pi \frac{B}{\ell}$$

Its value is relevant for the range of applicability of theoretical models. Seminara and Tubino's models (see Paragraph 7.3.1) are valid under the assumption that this value is small, so that it is possible to neglect the inertial term with respect to the advective and frictional terms in the momentum equation. If the chosen length scale is comparable to the tidal excursion, like in the large estuarine section of the Western Scheldt, the above assumption is not directly justifiable.

Rouse number

The Rouse parameter arises from the ratio between depositional and frictional effects:

$$R_o = \frac{w_s}{u_f}$$

where w_s is the sediment deposition velocity, which can be evaluated for uniform sediments, following Parker (1978), as

$$w_s = \sqrt{g\Delta d_s}\, 10^{-1.181\cdot x + 0.966 - 0.1804\cdot x^2 + 0.003746\cdot x^3 + 0.0008782\cdot x^4} \qquad \text{where} \quad x = \log_{10}(R_p).$$

The Rouse number can be used to assess whether the suspended load is present (usually the threshold is R_o<~1) and its relevance.

Froude number

The Froude number is the ratio between advection and gravitational forces

$$F_r = \frac{U}{\sqrt{gD}}$$

It is a widely used parameter, whose importance is broadly recognized. In tidal environments it is usually small, since depths are quite large. However it can be relevant in shallow water areas to study micro-scale bed forms, such as ripples, and to assess the adaptation of the biology to the morphological habitat (Crosato et al., 1999).

Richardson number

The Richardson number is the parameter commonly used to obtain indications about the water stratification. Its local definition is the following

$$R_i = -g\frac{\partial\rho}{\partial z}\Big/\rho\left(\frac{\partial u}{\partial z}\right)^2,$$

where z is the vertical coordinate starting from the bottom. A more usable definition (bulk Richardson number) assumes a linear variation of density and velocity with depth:

$$R_{i(b)} = -gD\frac{\Delta\rho}{\rho_D(\Delta u)^2}$$

where ρ_D is the depth-averaged density, $\Delta\rho$ and Δu the differences of density and velocity between the upper and lower level of the layer considered.
The Richardson number can be important in those situations where the mixing of salt water and fresh water is difficult (e.g. salt wedge) or where hot water discharge is present. Since the Western Scheldt is well mixed, this parameter does not play a crucial role in its description.

6.1.6 Time scale ratios

Tidal period / morphological time scale

The ratio between the morphological time scale and the tidal period is crucial in the definition of the approach to the theoretical description of the system.
This parameter strongly depends on the definition chosen for the morphological time scale. It can be generically defined, using the width as the length scale (Seminara and Tubino, 2001), as

$$\sigma = \frac{Q_s}{\omega(1-p)BD}$$

where Q_s is the sediment transport scale (volumetric, per unit width) and p is the porosity of the sediments composing the bed of the channel.
According to the case under consideration, whether only bed load is present or the suspended load is dominant, the value of σ can vary; a discussion about the importance of this parameter can be found in Solari and Toffolon (2001). However, its value is usually small in tidal environments. Hence a tidally averaged sediment continuity equation can be accepted to describe the evolution of the bed suitably, because the process of erosion-deposition is much slower than the variation of the flow field during the tidal period.
Schuttelaars and de Swart propose a slightly different version of the same parameter:

$$\sigma = \frac{\alpha U^2}{\rho_s(1-p)D\omega}$$

which considers only the suspended load (choosing an explicit dependence of the sediment transport with respect to velocity) and α is the sediment pickup constant; Schuttelaars and de Swart (2000) suggest a value $\alpha \sim 3\ 10^{-2}$ Kg s m^{-4} for sands with d_s=2 10^{-4} m.

Deposition time / tidal period

The ratio between the time scale of the deposition process and the tidal period can be expressed, following Schuttelaars and de Swart (2000), as:

$$\hat{\gamma} = \frac{\omega}{\gamma}$$

The authors propose that $\gamma = w_s^2 / k_v \sim 4\ 10^{-3}\ s^{-1}$ for fine sands, where k_v is the diffusion coefficient that describes the mixing of sediments in the vertical.
A different definition is

$$\hat{\gamma} = \frac{\omega D}{w_s}$$

where D/w_s is a measure of the settling time.

Tidal period / diffusion time

The ratio between the tidal period and the diffusive time scale is

$$\mu = \frac{\mu_*}{\omega L^2}$$

where μ_* is a constant diffusion coefficient ($\mu_* \sim 100\ m^2\ s^{-1}$, used in Schuttelaars and de Swart, 2000).

Inundation time

An important parameter, especially for biology, is the duration of the inundation of the area under consideration. It can be easily made dimensionless using the tidal period.
The inundation time of an intertidal area is related to the hypsometric curve, i.e. the description of the planimetric surface versus the water level. Indeed, from the knowledge of such a curve and of the law of tidal variation of the free surface level, the inundation time is easily assessable.

6.2 Dimensional parameters

In this section we briefly analyse some parameters that are dimensional, but are used in the same way as the dimensionless parameters because their reference scale can be assumed constant. A typical example of this kind of variable is the grain size: as pointed out in Paragraph 0 its dimensionless form is the Reynolds particle number, but the relationship does not vary for almost all practical conditions.

6.2.1 Energy dissipation

The concept of energy dissipation has been used originally for rivers but it can be easily extended to tidal channels.
The *stream power*, or energy dissipation rate, is the decrease of potential energy of a river per unit of time and per unit of river length (Middelkoop, 2001):

$$P_S = \frac{\Delta E_{pot}}{\Delta t \Delta x} = \rho g \frac{\Delta V}{\Delta t} \frac{\Delta H}{\Delta x} = \rho g Q s$$

where P_S is the stream power [W/m], E_{pot} is the potential energy ($=\rho V g \Delta z_w$) [J], H is the free surface level and s is water surface gradient.
It is also possible to define the *unit stream power* [W/m^2], which is more appropriate as a local indicator of flow strength:

$$\frac{P_S}{B} = \frac{\rho g U^3}{C_*^2} = \rho u_f^2 U = \tau U$$

where U is the depth averaged velocity [m/s] and C_* is the dimensional [$m^{1/2}/s$] Chézy coefficient for hydraulic roughness (see Paragraph 5.2.4).

In the estuarine case, the energy dissipation rate per unit of surface at the bottom should include the effect of waves, which play a minor role in rivers. Thus the energy dissipation in estuaries is related to three factors: current, orbital flow and wave breaking.
This parameter has been found to be crucial for the local biology (Crosato et al., 1999), but it is mainly a meso-scale (ecotope scale) or even micro-scale (habitat scale) parameter.

7 THEORETICAL MODELS OF ESTUARINE MORPHODYNAMICS

In this chapter we give a short review of the most recent theories regarding estuarine morphodynamics.
A lot of work has been done in the recent years to take into account as many aspects of tidal morphodynamics as possible. We can classify the theories developed so far in **global** theories and **local** theories, respectively for mega-scale and for meso-scale; we are not interested in micro-scale phenomena. The macro-scale classification lies in the midst of global and local description and should make use of the results of both approaches. Schuttelaars, de Swart and Schramkowski (2001) have tried to make a link between local and global theories, but the merging is not achieved yet.
Recently some models have been proposed with the intention of tackling some aspects of tidal morphodynamics. It is possible to classify the models in two big groups, namely conceptual (idealised) models and numerical models. The former models are based on a simplified description of the phenomenon in order to understand few aspects; the latter try to include as many elements as possible to reproduce the evolution of the system in the best way.

Most of the ***idealised models*** developed so far (see Paragraph 7.2 and 7.3) are *linear* models and deal with small amplitude perturbations of the bottom topography and the flow field.
Strictly, such linear models are not suitable to study the case with islands, emerging bars etc, because they can give information only on the process of initial formation of bed forms. When non-linear interactions among different bar modes become relevant, the final configuration can be quite dissimilar: usually higher modes collapse into lower ones (see Mosselman, 1993; for a numerical computation see also Enggrob and Tjerry, 1999).

However, the information given by this kind of models can be useful to understand the "richness" of morphological features (i.e. if the theory foresees no formation of bars, we can rightly expect to have a single channel).
Nevertheless, all the theoretical models require several closure relationships, which are based on empirical observations, laws deriving from interpolations of measurements and sometimes extrapolations.
In this way, it is strongly recommended to check the sensitivity of the model with respect to these kind of closures, which can change the response in a significant way.

Numerical models (e.g. Delft3D) are very powerful tools for the analysis of complex cases. They can deal with large amplitude perturbations, but unfortunately show other restrictions. Basically, when considering a wide range of the parameters, they provide information about the behaviour of the system only at the expense of large computational time, in particular for the long-term morphological evolution of tidal environments. Furthermore they give a description of the evolution of the system, but they do not easily allow to deepen the insight of the significant mechanisms.
In the present analysis we will use some results obtained by numerical simulations; with a proper calibration of the parameters, these models allow to reproduce in a quite good way the real behaviour. For a theoretical setting of numerical modelling in estuaries, see Wang (1989).

7.1 An overview of bed forms

In this section we briefly introduce the main features of the bed forms. A more detailed review on morphodynamics can be found in Seminara (1998). For an introduction, see also de Vries et al. (2001).
Natural channels are rarely plane and straight. We can identify altimetric patterns (perturbations of the bottom elevation), like:

- ripples, dunes, antidunes (which are typically small scale bed forms);
- free bars, forced bars (large scale features);

and planimetric patterns (perturbations of the alignment of the channel axis), like:

- meandering;
- braiding.

Their classification depends on the spatial and temporal scales under investigation. The following paragraphs deal with the large scale (meso-, macro-scale) free and forced altimetric variations of the bottom topography.

Free bars

Free bars are altimetric patterns that freely develop in straight channels when stability thresholds are exceeded. They can be described as a repetitive sequence of scour zones and depositional diagonal fronts, whose planimetric scale is the channel width in the fluvial case (Tubino et al., 1999).
The simplest pattern is that typical of alternate bars (see Figure 21); more complicated transverse characteristics are allowed in wider channels, namely central and multiple row bars.

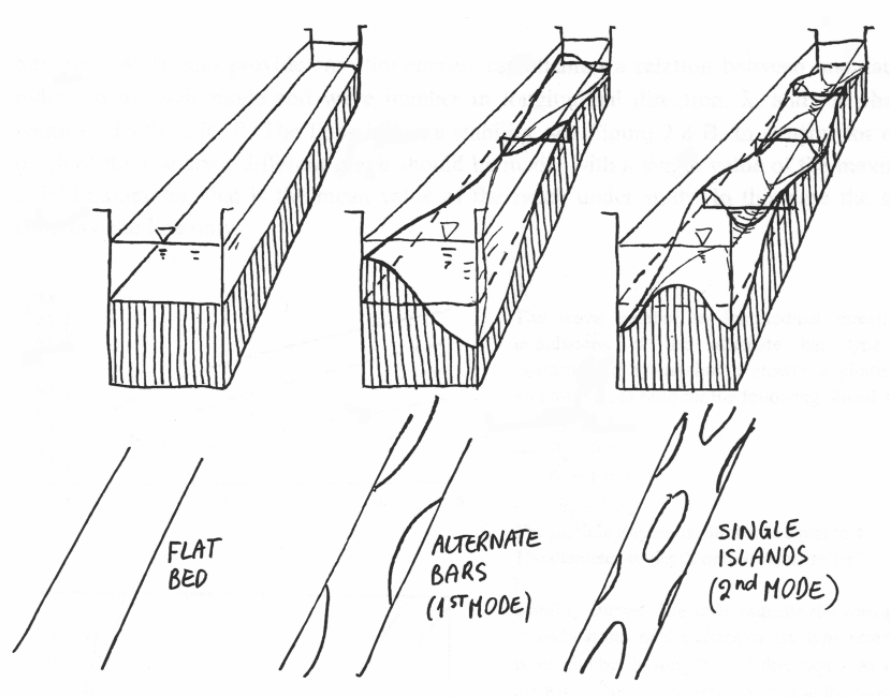

Figure 21. Sketch of the different altimetric patterns (de Vries et al., 2001): plane bed, alternate bars, central bars.

The type of configuration is usually related to the dominant transversal mode of the associated Fourier representation of the bottom elevation.

Forced bars

A different type of bars can develop as the result of forcing effects of curvature, width variations, confluences. They are called forced bars or *point bars* and may also interact with free bars; their non-linear interaction can affect the development of planimetric patterns like meandering (see Seminara and Tubino, 1992, for further details).
The antisymmetric forcing due to the curvature of the meandering channel gives rise typically to an alternate bar pattern, while central bars are characteristic, for instance, of the symmetric forcing of repetitive variations of width.

The formation of forced bars is due to the secondary circulations that arise, for instance, in the curvilinear reaches of rivers, or when the topographic variations are strong (e.g. variations in the width of the channel).
In a *bend*, two forces are out of balance: the transversal pressure gradient, due to the lateral inclination of the free surface, is constant along the vertical; the inertial force, which in a curvilinear coordinate system gives rise to an apparent centrifugal force with a quadratic dependence on velocity, varies following the velocity profile (see the sketch on the right: Falcon, 1984).
The imbalance originates a secondary circulation usually directed towards the inner part of the bend close to the bottom and towards the outer bank at the free surface. The consequence is a transport of sediments in the direction of the inner bank, where the typical point bar is created.
Furthermore, the increased depth at the outer banks induces an increase in the

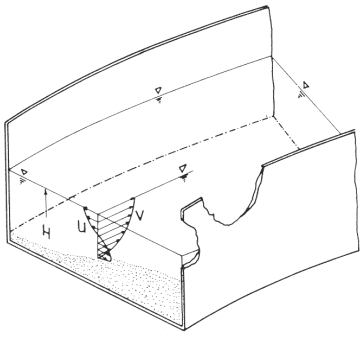

bottom shear stress and, through the erosion of the bank, a modification of the planimetric configuration. This preferential erosion at the outer bank is responsible for the amplification of meanders.
Please note that point bars in meandering rivers are almost always visible at the inner bank of the bends and can be seen also in the Scheldt estuary (see Paragraph 8.2.1).

7.2 Global models

Global theories consider the estuary as a whole (i.e. on the mega-scale), but they can give useful information about the behaviour of the system at the macro-scale. Here we summarise the basic features of some models recently developed.

7.2.1 Hydrodynamic models

The propagation of the tidal wave in estuaries has been studied for a long time. Green (1837) treated this problem in the frictionless case with slowly varying width and depth. After such contribution, based on an energy argument, several 1D (one-dimensional) models have been proposed in the last decades.
Since Green's assumptions are almost always unrealistic, Jay (1991) and Friedrichs and Aubrey (1994) took into account also the effect of friction and the convergence of the width, within the framework of linear models.
Recently, Lanzoni and Seminara (1998) developed a 1D numerical model to include all the non-linear features, which are mainly due to finite tidal amplitude. The authors propose a subdivision of the estuarine systems according to the width convergence (strongly or weakly convergent) and to the relative importance of friction (strongly or weakly dissipative). They also provide simplified analytical solutions for some of the cases under investigation.

7.2.2 Morphological models

The morphological evolution of estuaries has been studied only more recently. In this section we briefly consider some analyses concerning the mega-scale evolution of the bottom profile. A direct application of the following models is not feasible at the macro-scale level, because in most cases the approach is one-dimensional (thus neglecting the transversal characterisation, which is the basic element for the identification of the structure of parallel channels, shoals and islands inside the estuarine sections) or even zero-dimensional, and the assumptions are not always sufficient to describe the estuarine sections suitably.

Several contributions have been proposed by **Schuttelaars and de Swart**, dealing with the morphodynamics of tidal inlets. They adopt a tidally averaged formulation for the sediment continuity equation, assuming that the bottom evolution is much slower than the tidal period (for further details on time-averaging of non-linear equations and on the conceptual framework, see Schuttelaars, 1997).
In Schuttelaars and de Swart (1999) the assumption of short tidal embayment allows to study the case of a constant width channel with a simplified approach within a linear 2D-H (two-dimensional, vertically averaged) formulation. The width is kept constant and the channel is assumed to be short with respect to the tidal wavelength in order to obtain a standing tidal wave.
The assumption of short embayment has been relaxed in following contributions (Schuttelaars and de Swart, 2000 and van Leeuwen, Schuttelaars and de Swart, 2000) within the framework of a 1D model. Such approach is able to determine morphodynamic equilibria and takes into account also non-linear interactions.
The case of a convergent tidal embayment (i.e. with a decreasing cross-sectional width) has been tackled by Schuttelaars and de Swart (2001) with the same 1D model.

Lanzoni and Seminara (2002) extended their hydrodynamic model (Lanzoni and Seminara, 1998) to consider also estuarine morphodynamics. The model is one-dimensional and the equations are solved numerically by using the two-step method of McCormack, which allows to treat the case of large deformation of the longitudinal profile of the bottom. The long-term morphodynamic evolution is tackled and some equilibrium configurations are presented. Recent laboratory observations (Bolla Pittaluga et al., 2001) seem to confirm the numerical results.

A comparison between the equilibrium bottom profiles of the estuary provided by the above models, Schuttelaars and de Swart (2000) and Lanzoni and Seminara (2002), shows that a notable disagreement in the seaward part of the channel is present. Even if the approach is not the same, the different behaviour is probably due mainly to the different boundary conditions adopted at the mouth of the estuary, which will require a deeper analysis.

7.2.3 Semi-empirical models

Examples of semi-empirical models for estuarine morphology are given, for instance, by van Dongeren and de Vriend (1994) and Wang et al. (1998). They are based on the assumption that every morphological element tends towards to an equilibrium state depending upon the hydrodynamic conditions.
The approach of the ESTMORF model (Wang et al., 1998) is one-dimensional; the cross-sectional area is divided into three parts, which are considered separately: channel (under MLW, low water level), low tidal flat (between MLW and MSL, mean sea level) and high tidal flat (between MSL and MHW, high water level). It is assumed that an equilibrium state can be defined and the morphological development tends to restore the equilibrium when it is disturbed. In this way, the model makes use of three variables, for which an equilibrium relationship is given: the cross-sectional area of the channel is related to the tidal volume; the heights of low and high tidal flats are related to the tidal range and to the total area of the basin.

7.2.4 Zero-dimensional models

A special kind of idealised models is the group of models that are known as zero-dimensional, because they involve only equations of balance for the whole system under investigation, introducing some empirical closure for lower scale phenomena. For instance, Di Silvio (2001) has recently proposed such a model for the lagoon of Venice.

A relationship based on the concept of morphological equilibrium in a estuary (i.e. vanishing long-term averaged sediment flux through the sea inlet) has been presented by **Dronkers** (1998). The author finds a simple formulation that involves the ratio between wet planimetric surfaces at high and low tide and the ratio between depths (for notation, please refer to Paragraph 6.1.2):

$$r_{D^*} = \sqrt{r_S}$$

The relationship is valid for the mega-scale description and considers the whole estuary. Even if it might be theoretically extended also to the macro-scale analysis of the estuarine sections, it shows some limitations, which will be discussed in Paragraph 8.2.1.

7.3 Local models

While global models take into account the forcing given by the mega-scale boundary conditions, local models make use of the results of the global models in order to describe the system at the leading order. In this way they can study the smaller scale perturbations of the basic state flow, which are assumed to be only weakly dependent on the global evolution (i.e. they occur on a different time scale). This approach is not always justifiable, especially when the global and local characteristic scales cannot be clearly separated.
Local models available at the moment refer to a single channel and therefore can be classified as meso-scale models.
We can summarise the main limitations that the following models share:

- meso-scale approach;
- linear analysis: they cannot deal with finite amplitude perturbations;
- sediments are assumed to be cohesionless: if it is necessary to take into account the cohesive fraction (silt, clay), models should adopt different relations for erosion and deposition and results might change.

The linear models described below are not able to deal with macro-scale features like the complex system of channels and shoals in the macro-scale estuarine sections. It would be necessary to develop a different kind of model, which could take into account also the presence of the morphological cells in meandering estuaries (presence of an ebb-dominated channel, usually along the outer bank of the bend, and a flood-dominated channel), which is supposed to act strongly on the sediment transport paths.

7.3.1 Seminara, Tubino et al.

In this section we illustrate the assumptions and the results of a local model of bar formation in tidal channels.
It belongs to a family of models that have been proposed by several authors in the last twenty years. The basic approach was developed by Seminara and others (for a review, see Seminara, 1998) in order to study the formation of bars in rivers, and its consequence on the planimetric development (within this topic, one of the first contribution is due to Ikeda et al., 1981; see also Blondeaux and Seminara, 1985). Field and laboratory data seem to confirm this type of theoretical approach (see, for instance, Garcìa and Niño, 1993; Lanzoni, 2000; Knaapen et al., 2001).

The extension to the tidal environments has been provided only recently. Seminara and Tubino (1998, 2001) tackle the problem of free instability in *straight* channels, i.e. the spontaneous response of the bottom topography coupled with the hydrodynamics. It has been demonstrated that free bars can develop if the controlling parameters exceed a threshold value. The case of *meandering* channels has been studied as well: a description of the models developed so far is given below.

The linear analysis of free bars provides their growth rate and their migration rate. The former separates the region of amplification, where free bars are excited, from the region of suppression and gives valuable information on the fastest growing wavenumber, which is supposed to be the selected one in a linear schematisation; the latter provides the velocity and the direction of the migration of such bed forms.

While the amplitude of the deformation of the bed is small, i.e. in the linear range (as confirmed also by the results of non-linear numerical models), its exponential amplification is given by the growth rate. Figure 22 shows a typical behaviour of the growth rate of free bars: the contour plot allows to assess the amplification factor as a function of the width to depth ratio β and the dimensionless wavenumber λ, for a given set of the other dimensionless parameter involved in the analysis (Shields parameter θ, dimensionless grain size d_s, particle Reynolds number R_p). The marginal stability curve is given by the values of β and λ for which the growth rate vanishes and the perturbations do not grown nor tend to disappear. In this way it is possible to define two regions in the β–λ plane:

1. where the perturbation are suppressed the bed remains flat;
2. where the perturbations are amplified, bars are supposed to form.

A threshold value β_{cr} can be estimated from the figure: the lower value of β on the marginal stability curve. Below this critical point no bars can develop, while above it there is at least one value of the wavenumber λ that is supposed to be freely excited. In this way, when the width to depth ratio of the channel is known, along with the other parameters, we can predict its meso-scale configuration.

The plot describes the behaviour of the first transversal mode, but similar considerations can be made also for higher modes.

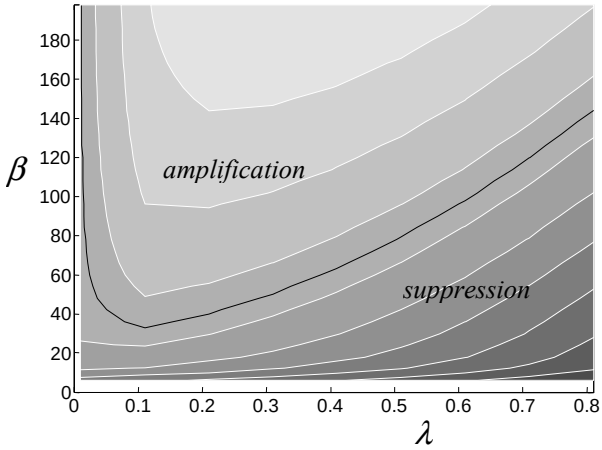

Figure 22. An example of a contour plot of the growth rate of free bars in a straight channel, as a function of the width to depth ratio β and the dimensionless wavenumber λ (see Paragraph 6.1.2).
The black line is the marginal stability curve, which separates the region of suppression of free bars (below the line) and the region of amplification (above). A threshold value for the aspect ratio can be defined as the lower point of the curve.

The model is based on the use of perturbation techniques: if a basic state is given, a linear stability analysis of the small amplitude perturbations is able to provide useful information about the behaviour of the system, even if it is valid strictly only in the first stage of incipient deformation of the bottom. For a terminological introduction please refer to de Vries et al. (2001).

The model is three-dimensional and hence allows to describe in a proper way the influence of the suspended sediment transport, which is typically the main component of the sediment transport during most of the tidal cycle.

The assumption of shallow water is made and the effect of the banks is neglected, since the width of the channel is typically much larger than the depth. Due to the former hypothesis, the pressure can be assumed to be hydrostatically distributed. The equations considered are:

- two momentum equations: the Reynolds equations for the longitudinal and transversal directions (the vertical equation gives the hydrostatic distribution of pressure);

- the continuity equation for the liquid phase;
- the advection-diffusion equation for the concentration of the suspended sediment;
- the sediment continuity equation, which controls the evolution of the bottom elevation; it is the 2D version of the Exner equation.

The boundary conditions are:

- at the free surface, the definition of solid boundary (kinematic condition, which gives the evolution of the free surface elevation) and the vanishing sediment flux;
- at the bottom, the no-slip condition (velocities vanish at a reference value) and one boundary condition either for the sediment concentration or for the sediment flux;
- at the banks, the vanishing transversal flux of both water and sediments.

The unknown variables are the three components of the velocity vector, the suspended sediment concentration, the bottom elevation and the free surface level.
On the basis of an analysis of the characteristic scales of the problem, the inertial terms (time derivatives of the velocity vector) are neglected in comparison with the advective and frictional ones.
The model can be easily extended to consider other factors, like the effect of the Coriolis force.

The solution of this kind of model is quasi-analytical for the perturbations and the results are simple to obtain. The integration of the equations over depth requires a numerical calculation, which can be carried out with usual numerical techniques, such as the Runge-Kutta 4^{th} order method.
All these characteristics allow to explore a wide region of the parameters in a short time. For this reason this models can be easily used to understand their relevance.
However, this theory makes several assumptions that are not always easily justifiable. The main limitation, common to other meso-scale models, is that it considers only one single channels, without intertidal areas. The other critical points are:

1. the longitudinal perturbation is assumed to be periodic, i.e. a wavelength of the perturbation pattern repeats itself infinitely (hence the domain is assumed to be infinite);
2. within the description of the basic state, the water level is kept constant during the tidal period (i.e. the tidal range is assumed to be small compared with the depth); the time-dependent longitudinal gradient of the free surface is assigned (global description of the basic flow).

Both the assumptions are not strictly true in an estuary like the Western Scheldt, but they can be justified in other tidal environments, like the lagoon of Venice, for which the model was originally developed.
In particular the first point is critical if the wavelength of the perturbations is comparable with the length scale of the embayment and if it is necessary to take into account the effects of the finite length of the domain.
The second assumption is undoubtedly wrong in the Scheldt estuary, where the tidal range is approximately 5 m and the averaged depth is around 10÷15 m. However, the theoretical results can be qualitatively valid also in such a case.
The authors are currently working to relax the second assumption, while the first is harder to be tackled in the present scheme of solution.

The role of tidal asymmetry

Tidal asymmetry seems not to play a crucial role in the selection of the growing modes. Figure 23 shows the contour plot of the growth rate for the first two odd modes, respectively tidally averaged in the case of a sinusoidal tide (left column) and for an unidirectional flow with a constant velocity equal to the peak value of the former case (fluvial case, right column). Is appears clearly that the results are qualitatively the same, even if the contour plots have two different legends, since in the tidal case the growth rate is obviously smaller than in the fluvial case.

This kind of behaviour can be explained if we consider that the bed-forming conditions occur when the velocity is large and that in the scheme of the model it is not relevant the direction of the flow (whether seaward or landward).
The presence of overtides does not affect the growth rate in a significant way.

On the other hand, the asymmetry of the tidal wave might play a role on the *migration* of free bars. In fact, when the tide is symmetric the net result is that these bars are steady, but if residual currents are present, bed forms can move on a time scale that is dependent on the order of magnitude of the net sediment transport and on the wavelength of the bed forms. However, the criteria of bar formation are related to the growth rate and not to the migration rate.

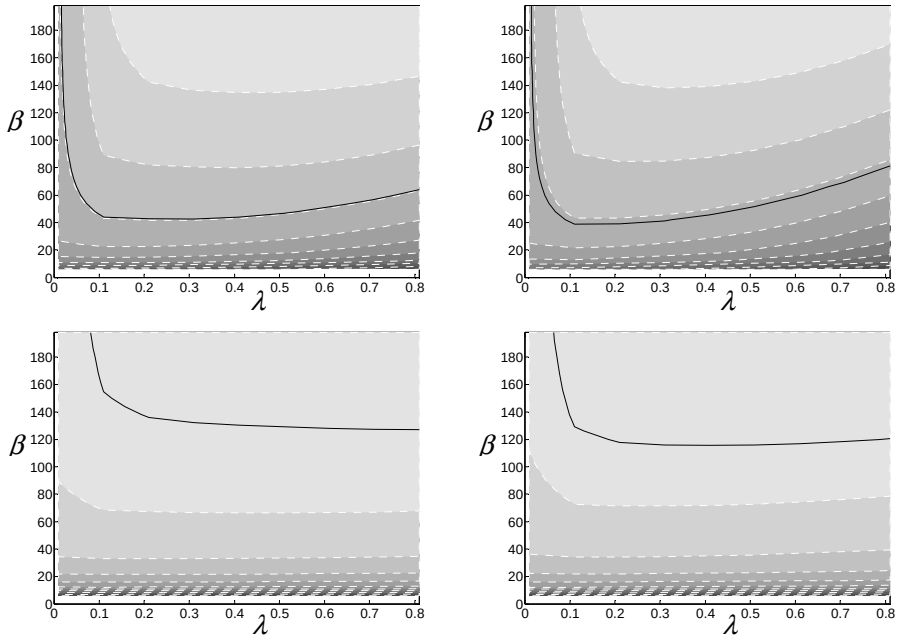

Figure 23. Comparison between results for the growth rate of free bars, for tidally varying velocity (left column) and constant unidirectional velocity (right column). Above: first mode; below: second odd mode. Parameters are taken from realistic values of the Belgian part of the Scheldt estuary.

Meandering channels

The evolution of the system can also be driven by the forcing effects of curvature or width variation. Notably, the case of meandering channels is widespread everywhere in both fluvial and tidal environments. The forced response in tidal channels, with the formation of forced point bars, has been investigated by Solari (2001) and Solari et al. (2002). An improvement of the model has been given recently by Solari and Toffolon (2001), in order to relax the assumption previously made about the relative order of magnitude of the temporal scales involved in the problem.

In a meandering channel, there can be a phase displacement between the curvature and the hydrodynamics due to inertial effects; hence the forced bars can be localised upstream or downstream the bend apex. That is the reason why meanders migrate. According to the meander wavenumber, the phase lag is different and the meander can grow or disappear: in this way we can determine a set of possible meander wavenumbers, while the rectilinear configuration is stable for the other wavenumbers.
The same behaviour occurs in tidal channels, but the direction and the intensity of the velocity changes during the tidal cycle. If the tide is symmetric, the forced bar can only form either at the outer or at the inner bend apex, bringing respectively to an amplification of the meander or to its rectification, because the point bar move during the tidal cycle without showing any net migration. Solari et al. (2002) assumed the instantaneous adaptation of the bottom topography to the hydrodynamic conditions, but a more accurate analysis of the relative importance of the time scales (tidal period and morphological time scale) suggested to relax that assumption, retaining the time derivative in the sediment continuity equation (Solari and Toffolon, 2001).

7.3.2 Schuttelaars, de Swart et al.

A local model, analogous to the previous one (Seminara and Tubino, 2001), has been developed by Schramkowski, Schuttelaars and de Swart (2001) with a 2D formulation, averaged over the vertical. The parameters chosen are slightly different, but the qualitative behaviour seems to be similar. The main differences are:

- Seminara and Tubino use a 3D description of the concentration and the flow field, which allows to treat carefully the effect of the perturbed topography on the vertical profiles, which are assigned in the 2D-H formulation; this feature can be important in the evaluation of the longitudinal phase lag of the maximum shear stress and sediment transport with respect to the structure of the bottom perturbation;
- the 2D-H formulation requires suitable parameterisations of the averaged coefficients (e.g. sediment diffusion);

- Schramkowski et al. use a tidally-averaged formulation of the equation of the bed evolution, while Seminara and Tubino obtain the net effect by integrating the instantaneous results over the tidal cycle;
- Schramkowski et al. retain the local acceleration terms, while Seminara and Tubino neglect them assuming that the ratio between inertia and advection is small.

The results of both models significantly depend on the closure relationships that are involved and a quantitative comparison is not easily assessable. Moreover, the lack of field or laboratory data in the tidal case does not allow to have clear indications about the correspondence of the model with respect to reality.

Global-local model

Schuttelaars, de Swart and Schramkowski (2001) have recently proposed another interesting idealised model, which tries to consider both the global and the local perturbations of the bottom topography. The approach is two-dimensional and the results are obtain by using a linear stability analysis. Published results of the model are shown in Figure 24.

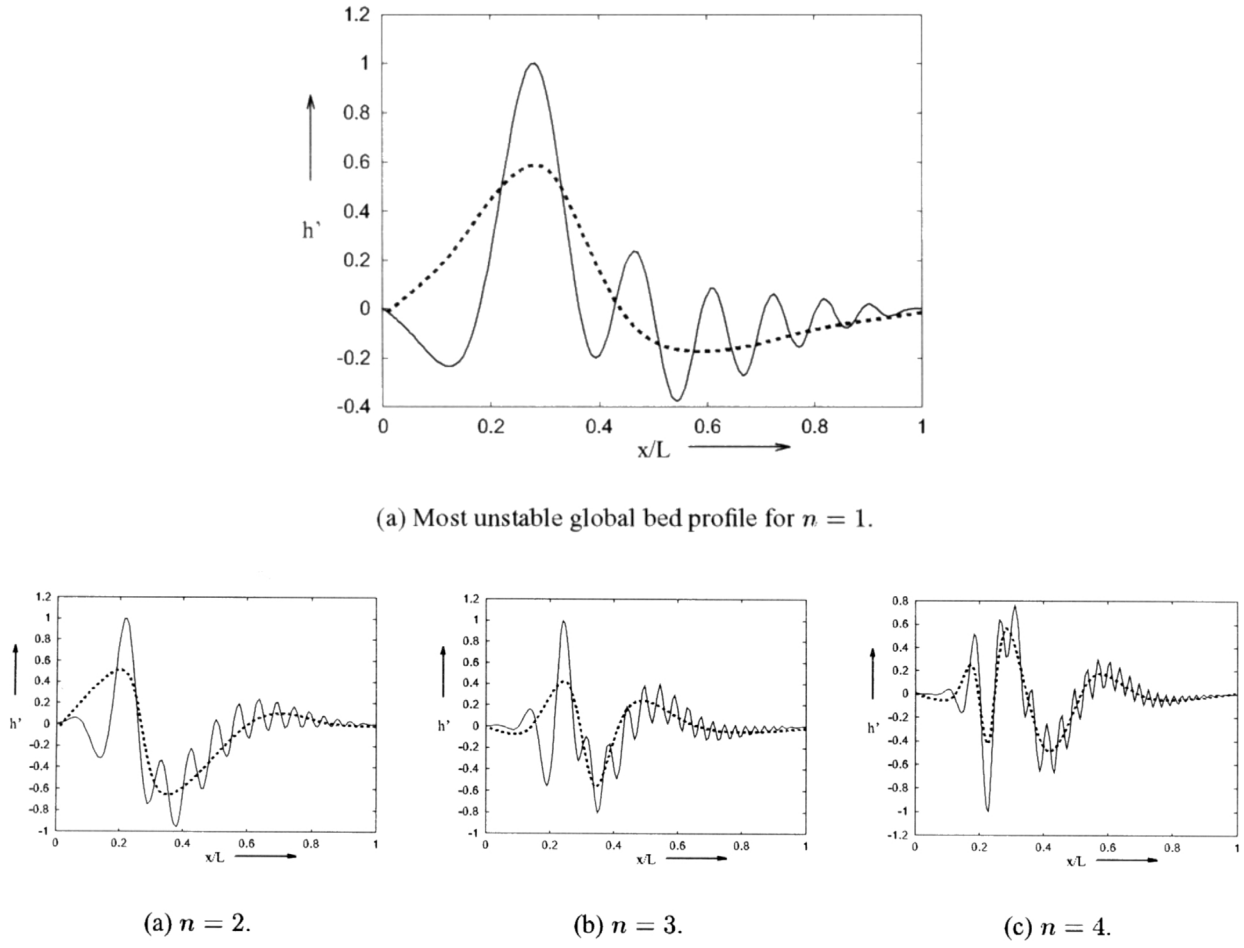

Figure 24. Bottom structure for the most unstable modes with n=1, 2, 3 and 4 (Schuttelaars, de Swart and Schramkowski, 2001). The dotted line shows the global bed perturbation (without local structures). The maximum amplitude of the bed perturbation is scaled to one. [χ_{dim}=0.0004 m/s]

If compared with the models by Seminara and Tubino (2001) and Schramkowski et al. (2001), this model has the main advantage that it deals with the finite length domain of the tidal embayment. The local modes are superimposed on a slower global mode, whose length scale decreases with the increase of the transversal mode *n* considered.

The authors suggest that the model shows a strong dependence on the friction parameter χ_{dim} (see Paragraph 6.1.5), which is expected to be the main controlling parameter.

However, the value of this parameter adopted to obtain the results shown in Figure 24 is quite small: χ_{dim} =0.0004 m/s corresponds, for a typical velocity of 1 m/s, to a dimensionless Chézy coefficient $C_h \cong 46$. The dimensional value

is $C_* \cong 144$ m$^{1/2}$/s (see Paragraph 5.2.4), while commonly adopted values are around $C_* \cong 55 \div 65$ m$^{1/2}$/s, or even smaller if the dunes are present (an increase in the flow resistance corresponds to a decrease in C_*).
As pointed out by the authors, for realistic values of the friction factor it is very difficult to make a clear distinction between global and local modes, and this is one of the points presently investigated.
Furthermore, the numerical solution of the eigenvalue problem is neither easy nor quick to obtain (Schuttelaars, personal communication). This fact might be a rather strong limitation for the use of this model to investigate the role of the different parameters involved in the problem, which is the aim of the present analysis, since the evaluation of a wide set of different combinations of parameters should require a long time.
From this point of view, the quasi-analytical solution obtained by Seminara and Tubino (2001) or Schramkowski et al. (2001) is favourable.

7.3.3 The equilibrium section of a channel

Most of the estuarine sections of the Western Scheldt are constituted by channels and intertidal areas.
An aspect that primarily concerns the single channels is the *equilibrium form of the section* (for the fluvial case, see Parker, 1978), i.e. the transversal profile of the bottom elevation, which is basically related to the lateral redistribution of stresses.
The estimation of the equilibrium section, or simply of the ratio between depth and width, can be very important when considering the effects of the deepening of a channel (e.g. because of dredging). We can consider different possibilities:

- an higher depth can result in a larger cross-sectional area of the channel, with a net erosion and a transfer of the sediments towards other locations;
- the new situation can be stable;
- the preceding situation can be restored.

This kind of meso-scale development is influenced also by larger scale behaviour. Besides, another interesting question is whether the new local equilibrium, which will be reached after the initial perturbation, affects the mega-scale quasi-equilibrium, for example with a variation of the tidal prism passing through the section.
We are currently investigating this problem, looking for a suitable description when the complex geometry of the morphological cells is considered.

7.3.4 Competition between channels

Another interesting phenomenon to study is the competition between two parallel channels, e.g. ebb- and flood-dominated channels in the morphological cells of the Western Scheldt. Wang and Winterwerp (2001) tackled this problem investigating the stability of the bifurcation point with respect to dredging and dumping activities; Winterwerp et al. (2001) have tried to examine the consequences on the whole estuarine system.

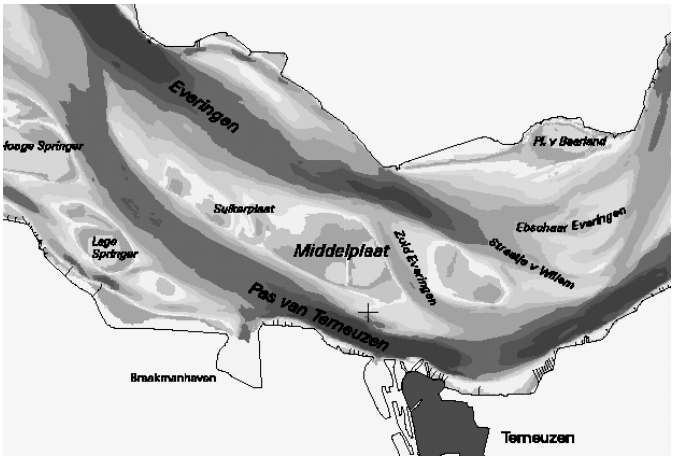

Figure 25. The estuarine section of Terneuzen: on the left the bifurcation point between the flood channel (close to the inner bank) and the ebb channel (close to the outer bank) is evident; on the right the flood channel is not directly connected to the ebb channel.

The stability of the bifurcations has been studied in rivers (see, for instance, Wang et al., 1995); in particular, it is the basic mechanism that rules the evolution of braided rivers.
Several models for fluvial bifurcations have been proposed, one-dimensional or two-dimensional or with an mixed approach (see for instance Bolla Pittaluga et al., 2002, with a 2D description of the nodal point in the framework of a 1D model for the channels).
In tidal systems, the alternate direction of the flow during the tidal cycle sometimes determines the development of two different nodal points. In Figure 25 it is visible the difference between the nodal point during flood (where a clear bifurcation is present) and ebb (where a bifurcation is not fully developed since the flood channel stops before arriving to the nodal point).
A qualitative description of the features has been provided also by van Veen (1950).

A suitable description of the bifurcation points is one of the main aspects in the description of the morphological cells of the Western Scheldt. Due to the presence of large intertidal areas between the two (or more) parallel channels, a special schematisation is required to reproduce their effect, which is usually not present in rivers.

8 DATA ANALYSIS

Due to lack of suitable data, the quantitative analysis has been restricted to the present-day situation. The available data were mainly geometrical and have been extracted from two different bathymetries:

- 1992: data on a mixed rectangular-curvilinear grid (typical size around 100 m) from the outer delta to Gent (project Scaldis, courtesy of van Ledden);
- 1996: data on a curvilinear grid (typical size around 50 m) from the outer delta to Antwerp (courtesy of Hibma).

The latter bathymetry has been used to study the estuarine sections of the Western Scheldt (Dutch part), while the former for the Belgian part, from the border to Schelle.

Other recent analyses of data of the Western Scheldt estuary can be found, for instance, in Jeuken (2000), Neessen (2000) and Grass (2001).

8.1 General observations

In this section some significant results of the analysis of data are presented. The aim is to find correlations between the presence of the intertidal areas and the other parameters.

8.1.1 Numerical evaluation of the intertidal areas

The ratio between planimetric surfaces at high and low water level r_S (see Paragraph 6.1.2) is probably the best parameter for a quantitative description of the presence of intertidal areas. Indeed,

$$r_S = \frac{S_{hw}}{S_{lw}} = 1 + \frac{S_{it}}{S_{lw}}$$

where S_{it} is the surface occupied by the intertidal areas. So, if we accept this parameter as a meaningful indication, the target of the analysis can be translated in finding a functional relation as

$$r_S = f(\pi_1, \pi_2, \pi_3, ...)$$

where r_S is assumed to depend mainly from a restricted number of parameters π_i. In this way, we can look for the controlling parameters.

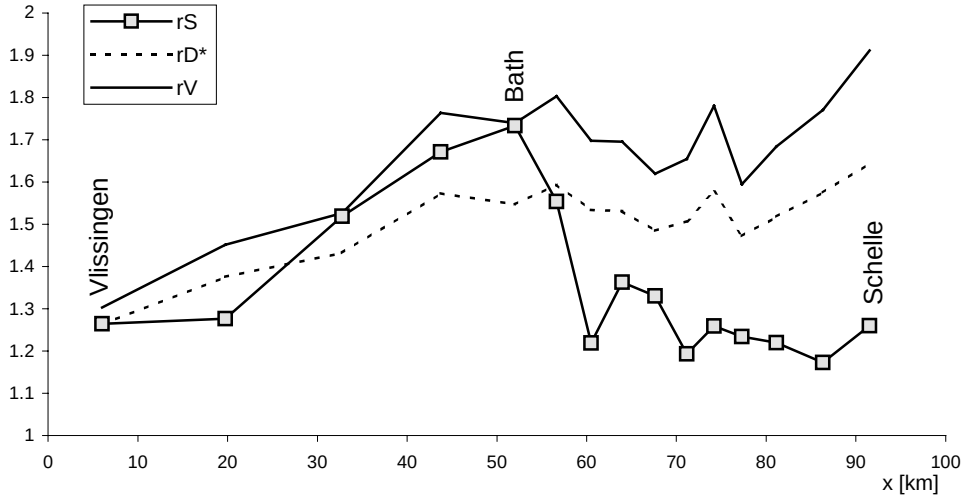

Figure 26. Comparison of the ratios between depths, surfaces and volumes at high and low water, from Vlissingen to Schelle. Please note that $r_{D^*} = r_R + 1$.

The most evident relationship is that the surface of the intertidal areas increases with the increase of the tidal range. This fact is confirmed in the seaward part of the estuary, as can be seen in Figure 26, where the parameter r_S is

compared with r_V (ratio between water volumes at high and low tide) and $r_{D*} = r_R + 1$ (r_R is the ratio between tidal range and average water depth). From Vlissingen to Bath all these parameters show the same increasing trend, whereas an abrupt fall in r_S occurs upstream of Bath; the other two parameters seem not to change in the same way.

This characteristic behaviour can be explained considering the passage from the single-channel system of the Belgian part of the estuary to the multiple-channel system of the Dutch part, with the change of the type of macro-scale section. The different shape of the sections is investigated in detail in the next paragraph.

8.1.2 Geometrical features

A bathymetry provides a lot of information about the characteristics of the estuarine sections. As pointed out in Paragraph 6.1.2, geometrical entities are very useful to distinguish different morphological situations.

Shape of the section

The threshold between the Dutch and the Belgian part of the Scheldt estuary can be seen from several indicators; the most important is the ratio between width and depth (Paragraph 6.1.2).
Figure 27 shows the trends of the reference areas and the widths of the macro-scale estuarine sections along the estuary. The trend of the area is smooth, while the width displays a transition between two different behaviours, which can explain the abrupt change in the morphological features of the estuary.

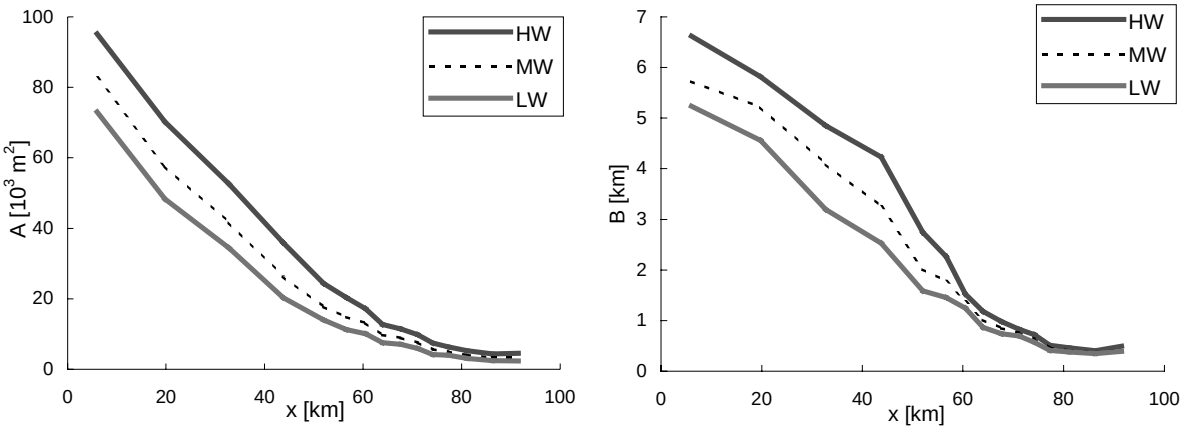

Figure 27. The macro-scale averaged cross section area A and width B, for high water (HW), mean water (MW) and low water (LW), from Vlissingen to Schelle.

Figure 28 shows the threshold between two zones inside the estuary: multiple channels in the Dutch part and a single channel in the Belgian part. Besides, the first two estuarine sections seaward show a different behaviour regarding the ratio between surfaces: another threshold will be defined in Paragraph 8.2.1.

It is interesting to consider two examples of the different kinds of section:
1) a single-channel section from the Belgian part;
2) a multiple-channel section from the Dutch part.

The attention is focused on the macro-scale characteristics of the estuarine section; the following plots do not describe the real cross section, but an averaged behaviour of all the cross sections within the reach of estuary (please refer to the definitions in Paragraph 6.1.2).

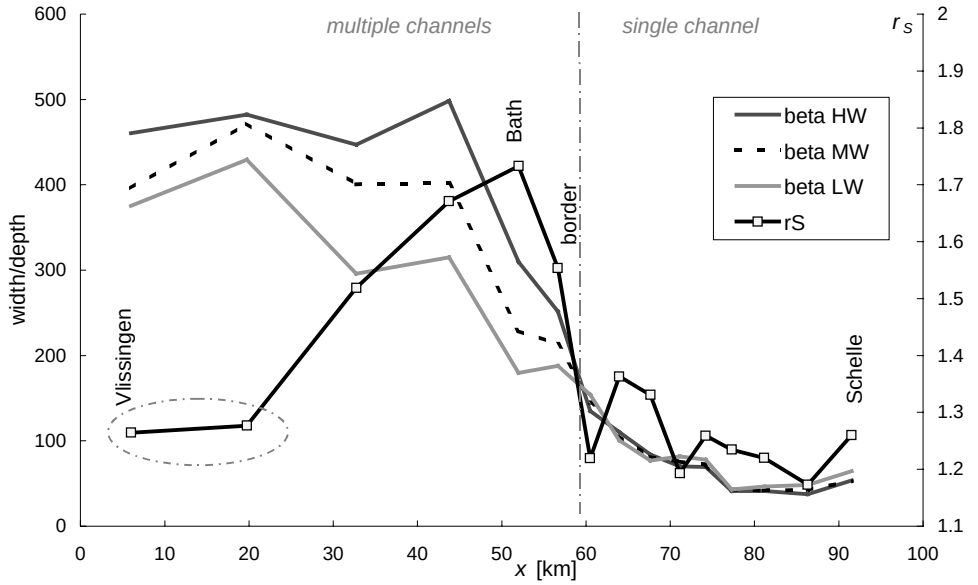

Figure 28. The ratio r_S between surfaces compared with the width to depth ratio β. A threshold can be identified near the Dutch-Belgian border (upstream of Bath, dash-dot vertical line). Another threshold can be identified referring to the first two estuarine sections (dash-dot ellipse, see Paragraph 8.2.1).

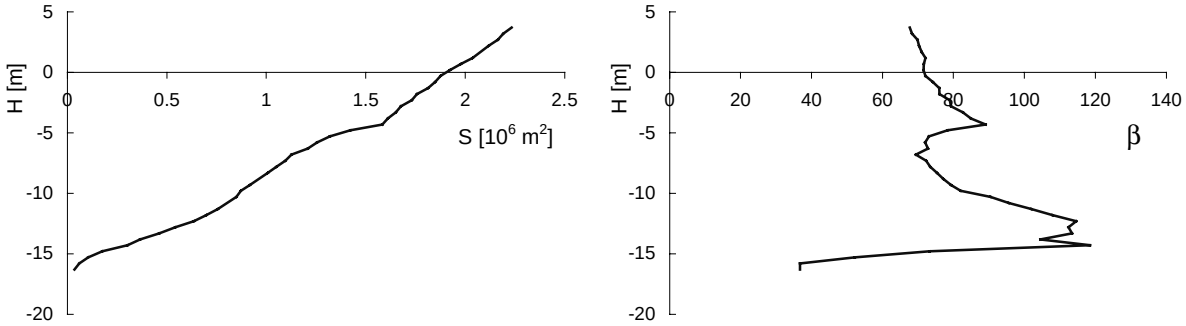

Figure 29. The hypsometric curve (the planimetric surface S as a function of the free surface level H, on the left) and the trend of the width to depth ratio β (on the right), for the estuarine section 11 of the Scheldt estuary, close to Antwerp (see also next figure). For the location of the estuarine sections see Figure 5.

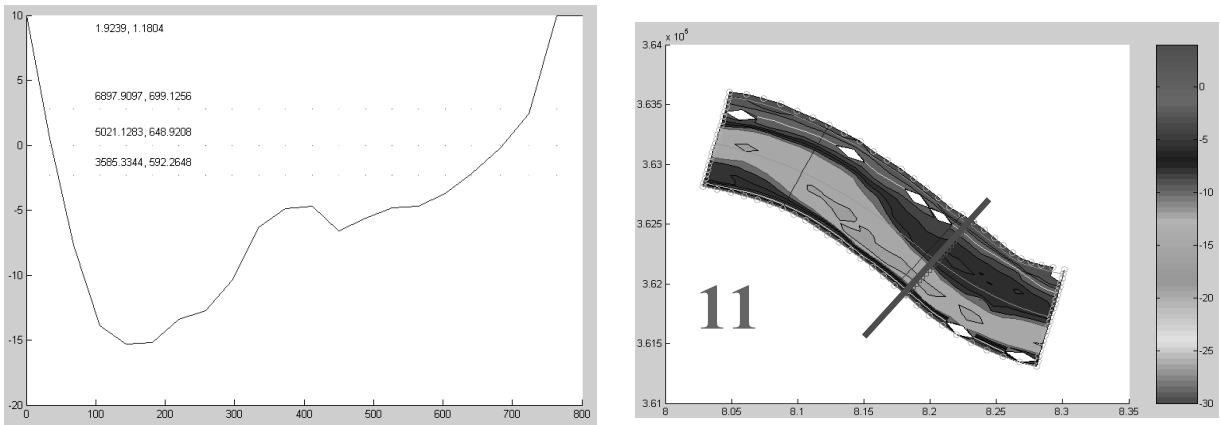

Figure 30. An example (left) of the real cross sections within the estuarine section (right).

It is possible to recognized from Figure 29 a behaviour resembling the hypothetical *U-shaped* section (see Paragraph 6.1.2), with an aspect ratio decreasing with the increase of the water level in the region around the tidally averaged level. This is peculiar of a "concave" cross section, like the one shown in Figure 30, where the increase of width with the water level is limited. It is interesting to note that it is possible to recognize one main channel and a forced alternate bar, typical of meandering channels.

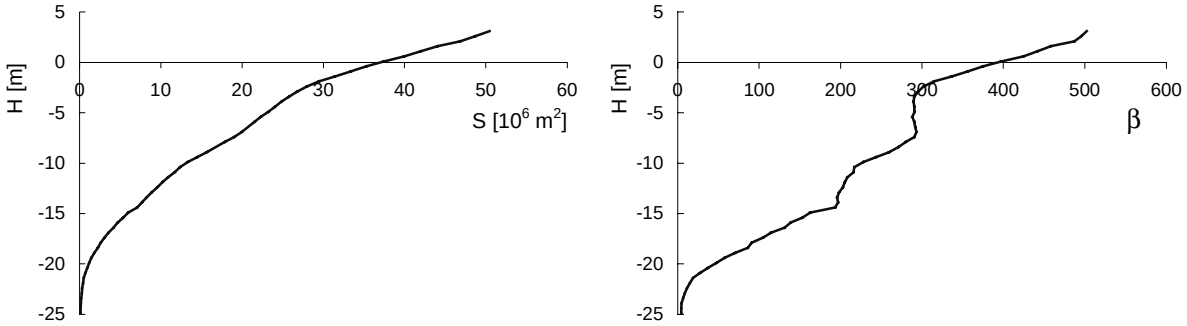

Figure 31. The hypsometric curve (left) and the trend of the width to depth ratio (right), for the estuarine 4 section of the Western Scheldt, near Valkenisse.

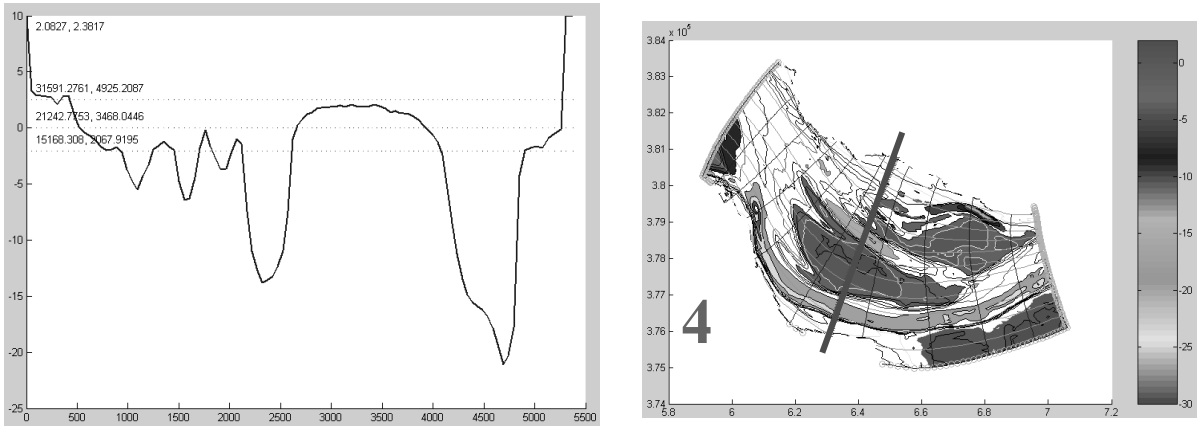

Figure 32. An example (left) of the real cross sections within the estuarine section (right).

On the other hand, Figure 31 shows the hypsometric curve of an estuarine section within the Western Scheldt, close to Valkenisse. It is not difficult to recognize that the general behaviour looks like the theoretical *Y-shaped* section, with an aspect ratio increasing with the water level. This can be easily explained considering Figure 32: even if every single channel is more or less "concave", the global trend of the whole section is "convex", i.e. the width of the free surface grows more rapidly than the cross section area.
In this way we recognize that the presence of more than one channel has important consequences, and it is probably related with the extent of the intertidal areas.

8.1.3 Velocity

Estimation of a reference velocity is not always easy to assess, because we can define several different velocities. We might consider different locations, different times during the tidal cycle or different types of averaging procedures.
A simple macro-scale definition of velocity can be derived by using the tidal volumes, their duration and the relative cross-sectional areas, as pointed out in Paragraph 5.2.3.
Van den Berg et al. (1996) refer to de Jong and Gerritsen (1984) to present a plot (see Figure 33) of the total ebb discharge (volume) versus the cross-sectional area below NAP for different location along the Western Scheldt. Even if they use that graph for a different purpose, the result is quite surprising: the relationship between discharge and area is described by a linear relation in a fairly good way. This would mean that the averaged velocity, defined as above, is almost constant along all the estuary.

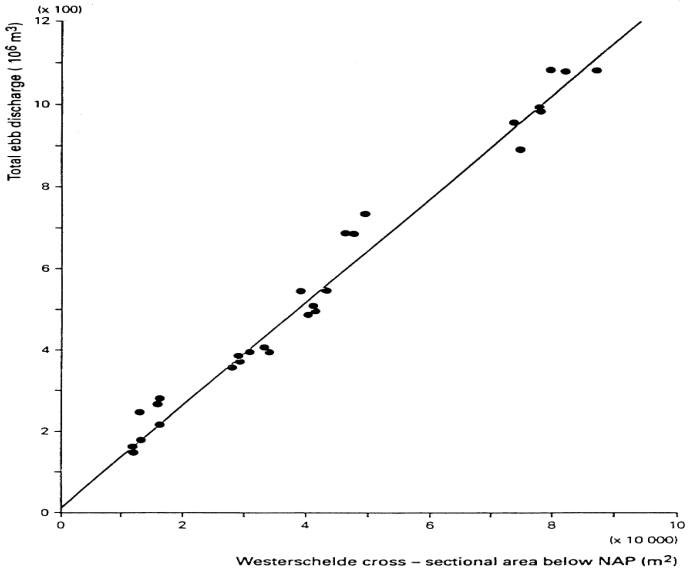

Figure 33. Cross-sectional area as related to ebb tidal volume (Van den Berg et al., 1996).

The above field observation is confirmed by the simulation of the SOBEK model shown in Figure 34, where the velocity of the whole cross section is defined as ratio of the discharge and the flow area: the ebb peak of the velocity is ranging around 0.8÷1.0 m/s and the flood peak around 0.9÷1.2 m/s, but the tidal averaged velocity is around 0.7 m/s, without showing relevant differences along the 60 km of the Western Scheldt.

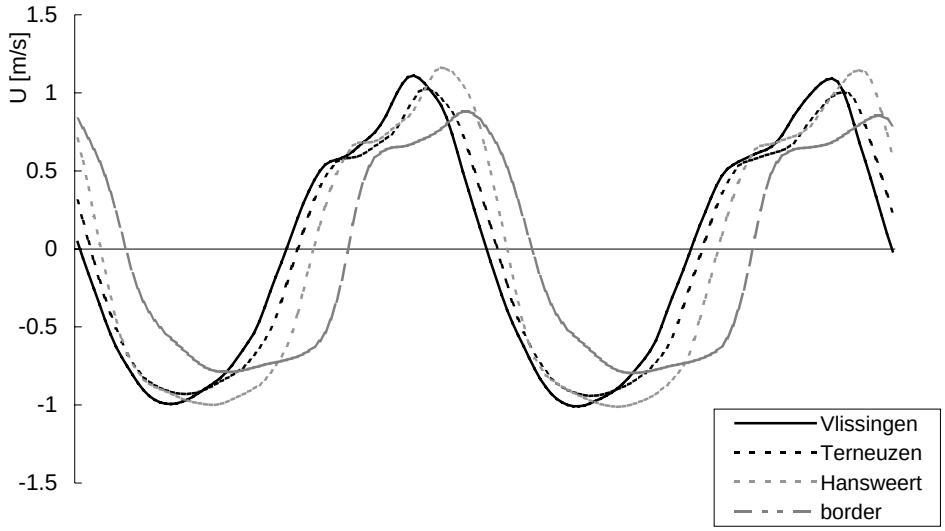

Figure 34. Velocities in four different cross sections of the Western Scheldt, namely Vlissingen, Terneuzen, Hansweert and the border between the Netherlands and Belgium (SOBEK numerical model).

8.1.4 Sediment

The sediment characterisation is essential to assess a reasonable value of the friction coefficient and to evaluate both the bed and the suspended load. Figure 35 shows the type of sediments along the Scheldt estuary and the average grain size of the sand fraction. Normally, coarser sandy sediments are dominant in the seaward part of tidal environments, whereas finer sediments, with a larger fraction of silt and clay, are carried by rivers. This trend can be seen also in the Western Scheldt, where d_{50} of sand decreases going from the mouth to the Dutch-Belgian border (approximately at km 60), with a significant increase of the silty fraction from Bath (approximately at km 50) to a

location slightly downstream of Antwerp (around km 70). Instead, the part of the estuary upstream of Antwerp shows coarser sandy sediments, with a globally diminishing fraction of silt.
A morphological model with sand and mud has been proposed by van Ledden and Wang (2001).

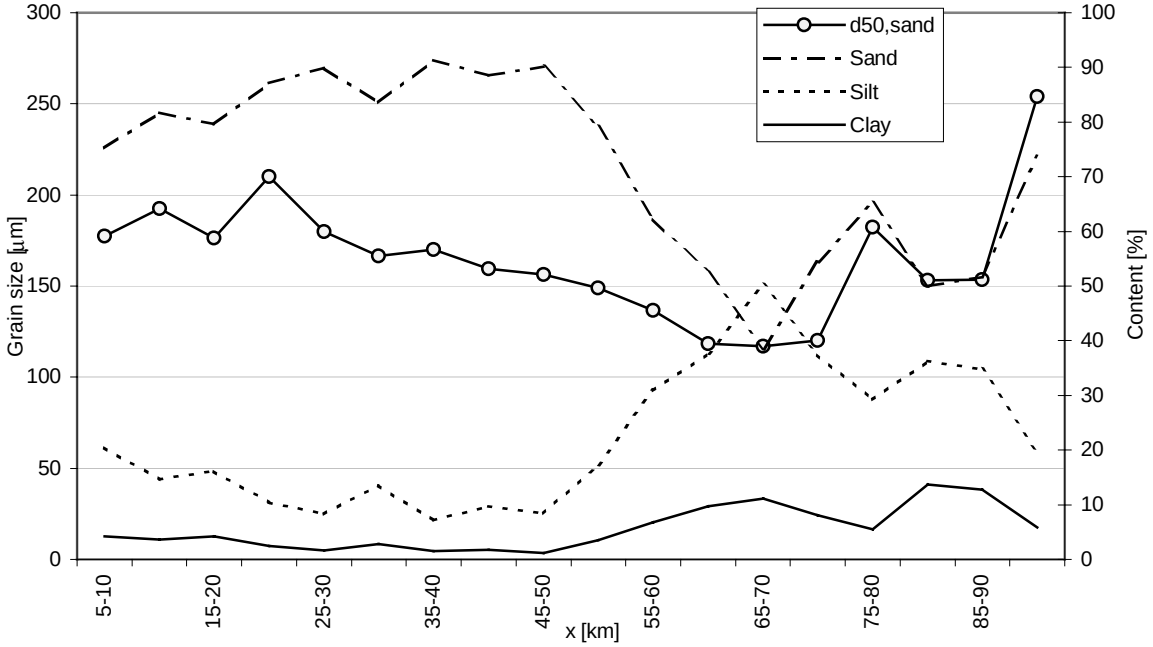

Figure 35. Sediment characteristics of the Scheldt estuary in 1992 (courtesy of van Ledden).

This information about sediment can be included in models through empirical parameterisations (flow resistance, sediment erosion and deposition). All the models presented above do not deal with cohesive sediments (significant fraction of silt and clay) and we reasonably expect that different closure relationships will bring to different results.

8.1.5 Dredging and dumping

During the last century the activities of dredging (deepening of channels by removing sediments) and dumping (redistribution of the dredged sediments in other parts of the estuary) have played a non-negligible role in driving the evolution of the system. As an example, the following figures show the changes occurred in the reach of the estuary near Hansweert, from 1955 until 1998. The Schaar van Waarde flood channel is losing importance to the advantage of the ebb channel. It is still not clear if this kind of evolution is mainly natural or induced by human activities, and the quantification of the latter factor is not easy. However the dredging and damping activities have boosted the system to attach importance to the ebb channel, which was preferred to deepen in order to increase the passage of ships towards the port of Antwerp.

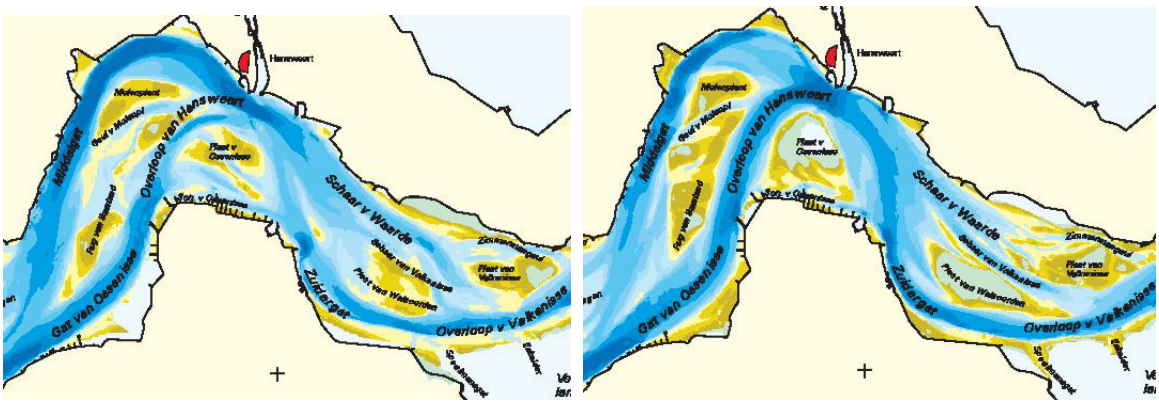

Figure 36. The estuarine section near Hansweert in 1955 (left) and in 1998 (right) (courtesy of Jeuken).

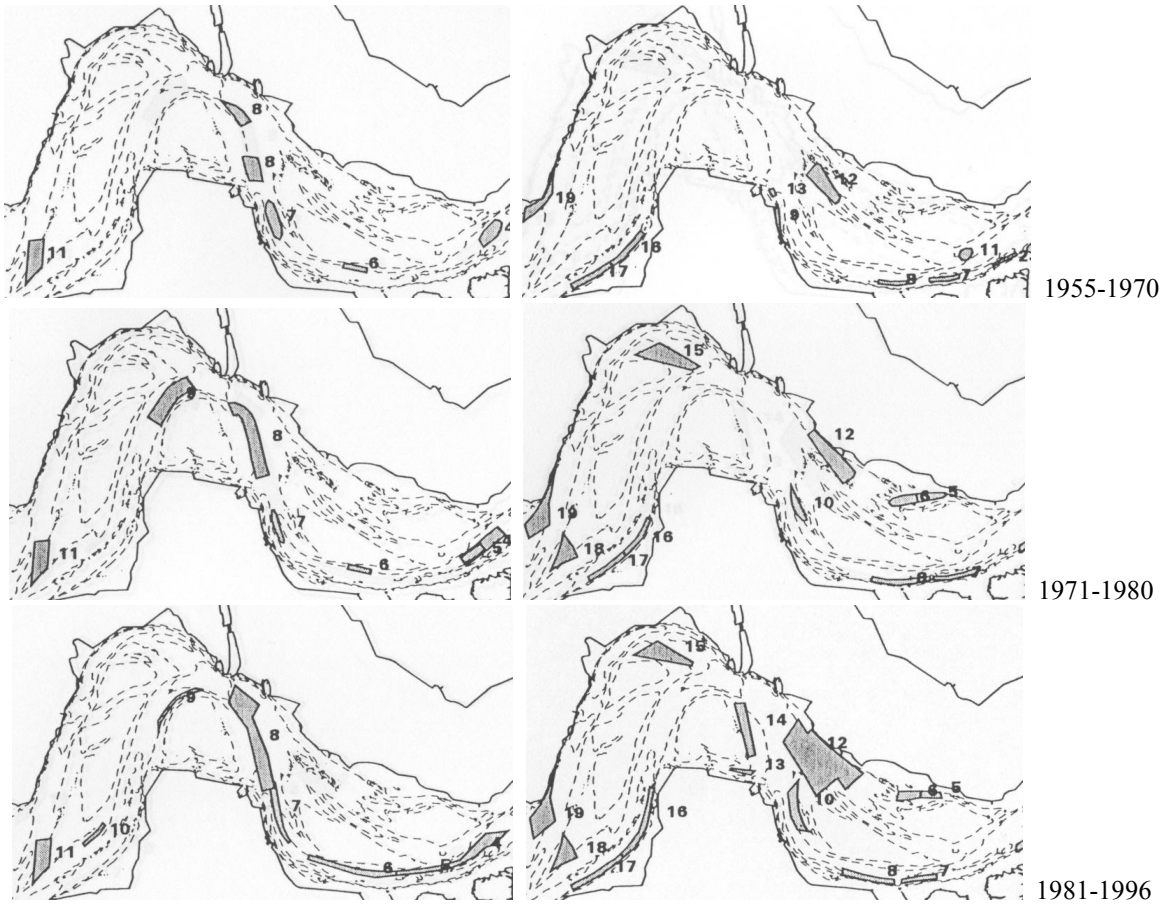

Figure 37. Dredging (left column) and dumping (right column) locations in the estuarine section near Hansweert from 1955 until 1996 (Neessen, 2000).

It is not easy to separate *a priori* the effect of the human activities from the natural development of the system, in particular in such a complex situation as a nodal point of two channels, and this problem would require a deeper investigation.

8.2 Comparison with theories

In this chapter we try to apply some of the theories presented, namely Dronkers' equilibrium approach and Seminara and Tubino's stability analysis. Unfortunately, we cannot compare the results of Schuttelaars and de Swart's global-local theory because of the lack of published results with realistic value of parameters (for a discussion see Paragraph 7.3.2).

8.2.1 Geometrical relationships

It is already clear that the border between the Netherlands and Belgium represents a passage between two different morphologies, from a complex system with several channels to a single channel. This fact can be seen also using the parameters proposed by Dronkers (1998).
Figure 38 shows that the relationship proposed by Dronkers (see Paragraph 7.2.4) is not valid in the macro-scale characterisation of the Scheldt estuary, since the disagreement between theoretical results (continuous line) and field data is not negligible for the aim of the present analysis. On the other hand, the parameters proposed by Dronkers are very useful and allow to obtain other suggestions about the morphology of the estuary, which will be discussed in the next section.

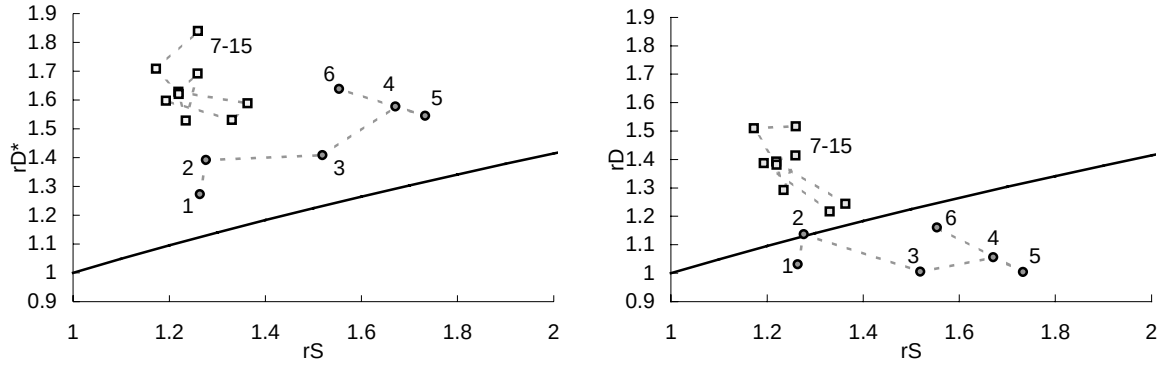

Figure 38. Comparison between theoretical equilibrium (continuous line: Dronkers, 1998, see also Paragraph 7.2.4) and field data of the estuarine sections (numbered circles: Western Scheldt, estuarine sections 1-6; squares: Belgian part of the estuary, estuarine sections 7-15). On the left the ratio between depths at high and low water is computed following Dronkers' definition (r_{D*}), on the right with the definition of average depths (r_D). For the differences between the parameters see Paragraph 6.1.2.

Another threshold?

The graphs in Figure 38 suggest an interesting remark: the points can be grouped in clusters. One group consists of the Belgian part of the Scheldt estuary (squares). The estuarine sections of the Western Scheldt (circles), instead, do not form such a consistent group, but they can subdivided in two parts: one consists of the sections 3, 4, 5 and 6 (from Hansweert to the border), while the other two sections (1 and 2, Vlissingen and Terneuzen) seem to be closer to the former group.
This further threshold between different zones in the Western Scheldt was anticipated by the subdivision proposed at the beginning of Chapter 3: the sections near the mouth show a multiple-channel system, instead of the two-channel system of the other estuarine sections.
The reasons of this difference are not clear yet. Some possible explanations are:

- the first two estuarine sections have a larger aspect ratio β and then a higher number of channels can develop;
- the tidal range is smaller (in particular if we consider the dimensionless ratio tidal range/average depth, see Figure 26) and then the intertidal areas are less wide;
- the sea has a more direct influence on the morphodynamics of the sections near the mouth of the estuary.

In order to evaluate which is the most relevant factor, it is necessary to deepen the analysis, especially for the last point of the list, since it requires a more accurate description of the exchange between the estuary and the sea, taking into account the role of the outer delta and the coastal currents.

8.2.2 Morphological models

In this paragraph, we try to apply one of the morphological models presented in the previous chapter, namely the local, meso-scale model proposed by Seminara, Tubino et al. (see Paragraph 7.3.1, also for the interpretation of the figures). We present these results because we are currently participating to the development of such model, and we were not able to find in literature applications of the other models with a set of parameters suitable to the situations we are investigating.
The use of the model is not straightforward in the Western Scheldt because of its complex geometry and the presence of intertidal areas and more or less deep channels. However, it is suitable to analyse the Belgian part of the Scheldt estuary when the right values of the parameters are considered.
The results presented in this paragraph should be used only as a qualitative suggestion of the behaviour of the morphological system in two different macro-scale zones. At the moment, a quantitative analysis is beyond the capability of these idealized models.

In Figure 39 we try to apply the model to a schematised section of the *Belgian part* of the estuary: on the left side, the marginal stability curves of the first three odd modes are plotted, with a Manning coefficient n=0.022 $m^{-1/3}s$ (this is the value used in the numerical simulations of Delft3D model, corresponding to a dimensionless Chézy coefficient C_h=21). On the right, the growth rates of the first three odd transversal modes are plotted as a function of

the wavenumber λ, for a given value of β: theoretically, it is possible to assess the most unstable mode and wavenumber. The characteristics of the reach can be summarized in the following way: the Shields number is θ_{max}=0.73, the particle Reynolds number R_p=7.4, the width B at NAP is in the range 400÷1300 m, corresponding to a range of values of the aspect ratio β in the range 40÷130. For this set of parameters, the model predicts the possibility that also higher transversal modes develop, whereas only alternate bars are present in that reach of the estuary. However, since the model is linear, the selected mode should be that with the large growth rate, which is the first mode in the considered range of values of the wavenumber.

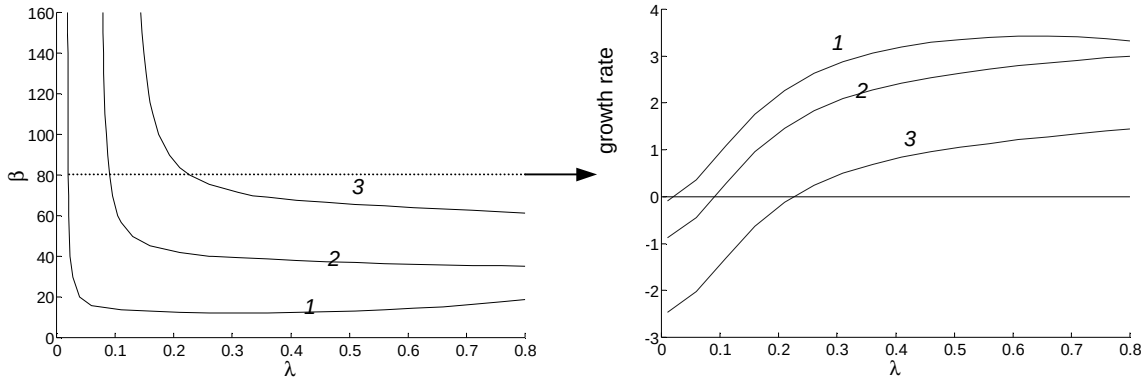

Figure 39. Belgian part of the estuary: marginal stability curves (left) and growth rate of free bars as a function of the wavenumber for β=80 (right), for the first three odd transversal modes (the first mode is related to the lower curve on the left and to the upper one on the right, respectively). The model is explained in Paragraph 7.3.1. [U_{max} = 0.9 m/s, D =10 m, d_s = 150 μm, n_{Manning} = 0.022 $m^{-1/3}s$]

There are still other reasons of discrepancy between the prediction and the reality: the limitations of the theoretical framework (e.g. the model does not take into account the influence of the tidal range), the non-linear interactions among different harmonics, the forcing effect of curvature.
Figure 40 shows the importance of a correct evaluation of the friction term: with the same parameters of the previous case, the Einstein's plane-bed (without dunes) relationship has been adopted to assess the value of the Chézy coefficient (C_h≅31) and hence of the Shields stress (θ_{max}=0.34). In this case, a reduction in friction reduces dramatically the number of transversal modes that are excited.
In the right sides of Figure 39 and Figure 40, the real part of the growth rate is plotted versus the wavenumber for the first three odd modes, for an assigned value of β=80. From the comparison, even if the first mode is always the most unstable in this linear framework, we can argue that in the situation of Figure 39 (stronger friction) the higher modes are supposed to play a relevant role in the non-linear competition for a significant range of values of the wavenumber (those for which the growth rate of the considered mode is positive).

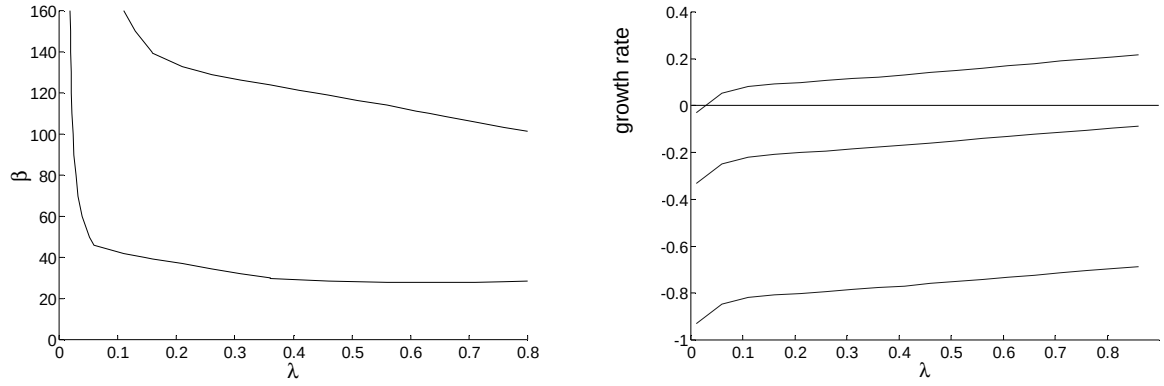

Figure 40. Belgian part of the estuary: marginal stability curves (left, first two odd modes) and growth rate of free bars as a function of the wavenumber for β=80 (right, first three odd transversal modes); the order of the modes in the two plots is the same as in previous figure. [U_{max} = 0.9 m/s, D =10 m, d_s = 150 μm, plane bed]

In order to apply the model to an estuarine section with complex geometry, we can try to define an equivalent rectangular cross section with the same area. In this way we investigate the formation of the present-day situation starting from small amplitude perturbations of the bottom and we can estimate the number of transversal modes to give a qualitative idea of the kind of morphological features (e.g. development of higher modes). Of course, since the analysis is linear, the final configuration could be significantly different, usually with the higher modes collapsing into the lower ones.
The assumption that the equivalent rectangular cross-sectional area is almost the same of the real cross section has already been discussed and can be justified if we adopt the working hypothesis that the system is in equilibrium at the mega-scale. As already noted, the cross-sectional area is related to the tidal prism; if the variation in the form of the section does not affect strongly the tidal volumes that flow through it, we expect that the system does not have to adapt the area to the new situation. Under these assumptions, the macro-scale evolution is mainly due to the internal redistribution of sediments.

If we try to apply the model to an equivalent section of the Western Scheldt in its *Dutch part*, using real data, we found that a very large number of transversal modes are excited in the actual range of variation of β (approximately 180÷400, for the width in the range 1800÷4000 m), as can be noted from Figure 41: the number of transversal modes that can grow (at least potentially: the ones above the marginal stability curve in the left plot, or the ones with positive growth rate in the right plot, for a given β) is very large, even if the most unstable mode is strictly the first one. Anyway, all the modes with a similar growth rate develop during the first stage of amplification of the small perturbations and give rise to a strong non-linear interaction in the following finite-amplitude development. The resulting cross section is likely to be "morphologically rich", even if the final configuration cannot be investigated using such a model.
However, these simple indications are not surprising: the typical cross sections observed in this part of the estuary are complex, with a lot of more or less pronounced channels and shoals.

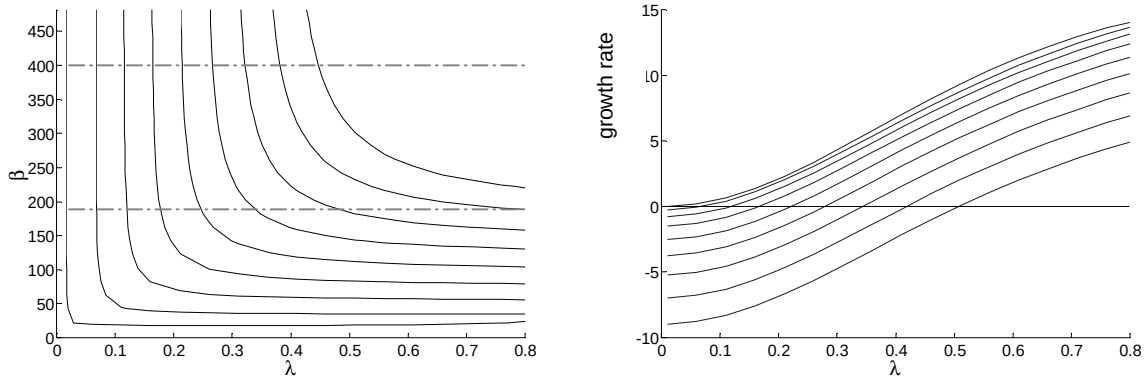

Figure 41. Example of application of the model to the Dutch part of the estuary: marginal stability curves (left) and growth rate as a function of the wavenumber for β=300 (right). The range of variation of β in the Western Scheldt is shown in the left plot.
[U_{max} = 1.0 m/s, D =10 m, d_s = 160 μm, n_{Manning} = 0.022 $m^{-1/3}s$]

8.3 Selected parameters

The results of the present analysis suggest that the most relevant factors affecting estuarine morphology are:

1) width to depth ratio (aspect ratio β) of the estuarine sections;
2) a parameter describing the frictional stress on the bottom, namely the Shields parameter or the bottom friction parameter (see Paragraph 6.1.5);
3) the sediment type and a reference grain size;
4) Chézy coefficient (if available, otherwise the dimensionless grain size may supply some information about it);
5) the tidal range, or the ratio between tidal range and average depth;
6) the tidal asymmetry;
7) the phase lag between discharge and water level.

Existing theoretical models can provide indications about the relevance of the first four parameters. In particular, the model developed by Schuttelaars et al. (2001) shows a relevant dependence by the parameter involving friction; the model by Seminara and Tubino (2001) confirms this kind of dependence, but suggests also the importance of the aspect ratio, which is confirmed by the analysis of the available data (see Paragraphs 6.1.2 and 8.1.2).
However, the relevance of the parameters arises from two different aspects: the sensitivity of the models to the chosen parameter and its range of variation along the estuary. The parameter is distinctive for the morphological characterisation only if it changes considerably in different estuarine sections and this variation reflects in different results of the models.
For example, the reference velocity does not seem to be strongly varying along the estuary and its importance in the models is not crucial in the range of typical values. More important for the friction is the Chézy coefficient, but its evaluation is not straightforward on the basis of field data, like the dimensionless grain size, if macro-roughness (like dunes) can form. An accurate estimation is possible only with a calibration of the model with a relevant number of data.
This uncertainty also affects the determination of the Shields parameter. However, its range of variation is not as large as the changes in the aspect ratio, and hence its relevance is less crucial than that of the latter parameter.
Schoor et al. (1999) found a similar behaviour determining the threshold lines in river morphology (see Figure 42): it appears clearly that a variation in the width to depth ratio produces a significant change in the morphological characterisation.

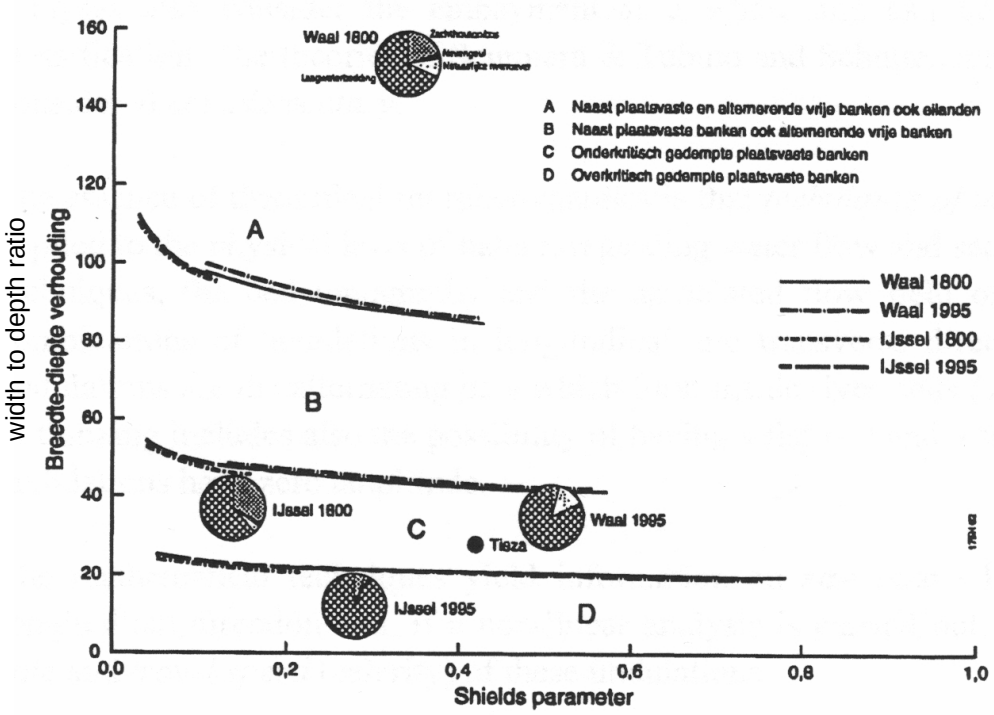

Figure 42. Morphological characterisation of the river Rhine in the Netherlands (Schoor et al., 1999): threshold lines divide the plane aspect ratio β – Shields parameter θ into different morphological types.

The tidal asymmetry and the phase lag between discharge and water level are relevant parameters, but existing models are not able to fully clarify their role on macro-scale morphology (they have been taken into account mainly regarding the mega-scale evolution).
The phase lag α (see Paragraph 6.1.3) can be important because it connects the bed-forming conditions, which occur when the velocity and the bottom shear stress are largest, and the aspect ratio β of the section, which depends on the free surface elevation and is assumed to be relevant for the bar formation (as explained in Paragraph 8.2.2). The two limit cases are:

- when the phase lag is $\pi/2$, the peak of ebb and flood discharge corresponds to the mean sea level (the Western Scheldt behaves approximately in this way, as shown in Figure 10);
- if the phase lag is 0 or π, the maximum of ebb and flood discharge occur at low or at high water level, when the aspect ratio β can be quite dissimilar if the section is not V-shaped (see Paragraphs 6.1.2 and 8.1.2).

In the latter case, a morphological asymmetry is introduced between the ebb and the flood phases.

However, this parameter seems no to be crucial in the Scheldt estuary: in its Belgian part the aspect ratio β is almost constant during the tidal cycle (see Figure 17); in its Dutch part, even if the sections are Y-shaped, the phase lag is approximately $\pi/2$.

The sediment type variation does not seem to be strongly correlated with the presence of intertidal areas and the sediment characteristics probably play only an indirect role on the morphological response. Besides, the available data on the grain size do not allow to deepen the analysis.
As pointed out in Chapter 6, several other parameters arise when considering the overall geometry of the estuary, but they concern the mega-scale characterisation. For this reason, we do not take them into account, even if they can play a role also in macro-scale morphology. Furthermore, since only one estuary has been analysed, it was not possible to recognize their importance.

9 CONCLUSIONS

The aim of the study, the morphological characterisation of the Scheldt estuary, has not been completely reached by the present analysis, due to the lack of both data and theories suitable to handle such a kind of complex environment. However, several indications have been found about the importance of different physical factors, which have been quantified using dimensionless parameters.
The selection of the most relevant parameters arises from the choice of the suitable variables to measure the physical characteristics of the morphological elements. The variables have been grouped into a restricted number of parameters, chosen among those used by available theoretical models. The parameters have been further selected on the basis of their role in the morphological evolution, their range of variation inside the estuary and the feasibility of their measurement (for the methodological approach, see Chapter 4).
In particular, ratios between geometrical variables (width, depth, tidal range etc.) have been considered for their significance and because they are easily evaluated using bathymetric data and other accessible information. The definitions proposed refer mainly to macro-scale averaged lengths, as explained in Paragraph 6.1.2. It is worthwhile to note that their definition is not univocal and depends on the scale and the phenomena that we are studying.

The analysis of the available data of the Scheldt estuary allows to recognize three morphological zones using (for the definitions of the parameters please refer to Chapter 6):

- the ratio between wetted planimetric surfaces at high and low water level during the tidal cycle,
- the ratio between the tidal range and the depth,
- the aspect ratio of the estuarine section (ratio between width and depth).

Three clusters of these parameters can be identified (see for instance Figure 28 and Figure 38), corresponding to a qualitative subdivision into multiple-channel, two-channel and single-channel systems. This subdivision had been proposed also independently.
The definition of the thresholds among these zones is not achievable by means of the analysis of data of a single estuary, because also several other factors are supposed to play a role, and their importance is assessable only when a comparison among different cases is made. Indeed, the number of degrees of freedom of the analysis cannot be much larger than the number of estuaries considered: if we want to investigate the role of several parameters, we must study a wider range of their variation.
Besides, also the mega-scale classification of the estuaries is crucial for the macro-scale characterisation. The mega-scale classification is based also on other parameters, those affecting the longer-time evolution, thus the results of the present analysis are valid only for a given type, namely the macro-tidal estuary.

Theoretical models are able to give some indications about the most important factors, even though they are quite simplified and cannot tackle the complexity of the real configurations.
As found in previous analogous analyses about river morphology (Schoor et al., 1999, and Middelkoop et al., 2001), the main controlling parameter seems to be the aspect ratio, which is related also with the number of channels in the cross section. Indeed, if we consider both the sensitivity of the models to the parameters and the range of their variation along the estuary, the macro-scale ratio between width and depth (aspect ratio) results to be the fundamental factor characterizing the morphology of the estuarine section.

Another relevant remark concerns the importance of a proper evaluation of the friction factor and hence of the bottom shear stress, especially in the dimensionless form of the Shields number. This parameter has been used also in the fluvial characterisation, for example by Schoor et al. (1999).
The most important new element, typical of tidal embayment, is the variation of the water level due to the propagation of the tidal wave. The ratio between tidal range and averaged depth seems to be meaningful with respect to the presence of intertidal areas, in combination with the number of channels of the estuarine section, which is probably related to the aspect ratio.
Besides, the phase lag between discharge and water level can introduce a morphological asymmetry during the tidal cycle, shifting the bed-forming conditions from the mean water level (and the corresponding aspect ratio) towards the ebb or flood phases, when the aspect ration can vary, as explained in Paragraph 8.3. The role of this parameter is currently investigated by the author.

The tidal asymmetry, which has been showed to control the mega-scale evolution (for a short discussion, refer to Paragraph 6.1.3), is not as crucial in the macro-scale characterisation as the previous parameters, at least in the

author's opinion. For a more sound evaluation, comparisons between estuaries with a different residual effect are necessary.
The sediment composition can be an important factor as well, but its variation inside the Scheldt estuary and the lack of models dealing with cohesive sediments does not allow to fully recognize its role.

9.1 Limitations of the analysis

As pointed out in the previous chapters, at present we do not have any theory able to predict the overall behaviour of tidal environments. The main limitations are:

- almost all the theoretical models are linear and can handle only a configuration of the bed that is slightly different from a schematic single channel;
- numerical models can be used to estimate the evolution of the system only for relatively short times, because several uncertainties arise when considering long simulations (tens or hundreds of years);
- suitable idealised models to describe tidal morphological cells are not available yet.

Furthermore, it is not always easy to separate the scales of the problems, i.e. to distinguish the macro-scale from the upper (mega-scale) and lower (meso-scale) scales. Tidal systems are typically different from rivers and concentrate a large variation of length scales in a limited space: lagoons are extreme examples of hydrographic networks concentrated in few tens of kilometres, with a fast transition between large channels and drainage gulleys. Even if the characteristic length of an estuary is larger, relevant feedback mechanisms occur between the mega- and the meso-scale evolution, on a time scale that is probably similar to the scale of evolution typical of the macro-scale morphological elements. In this way, separate macro-scale features are determinable with difficulty.

Finally, the role of vegetation on the morphological evolution of tidal environments is not clear yet. This topic should be investigated with the combined effort of morphologists, biologists and ecologists, since the feedback mechanisms between the biotic and abiotic components are supposed to be strong.

9.2 Suggestions for future research

The major suggestion for future research arises from the limitations encountered in the present analysis. Some of the improvements needed by the models will be reached in a short time, and have been discussed in the previous sections. In particular, in the author's opinion, the development of a model able to handle morphological cells with channels and shoals, and capable to assess the residual effects, is desirable and necessary.

A further suggestion which is not related to the theoretical aspects of the analysis, but to the practical management of the information, is to share the existing database of the Western Scheldt estuary, for example on a web site open to the public, and to try to merge it with the data of the Belgian part of the estuary. Many researches are working on this subject and the possibility to have access to such a tool would be broadly appreciated.

10 ACKNOWLEDGEMENTS

This project is part of the author's research within the framework of the PhD program "Ingegneria idraulica e modellistica dei sistemi ambientali", under the supervision of Prof. Marco Tubino (University of Trento, Italy).
This work has been jointly funded by the Delft University of Technology (the Netherlands), in the framework of the Delft Cluster project "Biogeomorphology of Estuaries" (Project Number 03.01.06), by WL|Delft Hydraulics (RUIMTECOL project) and by the University of Padova (Italy). Prof. Huib de Vriend and Prof. Andrea Rinaldo (coordinators) are gratefully acknowledged.
The author wishes to thank all participants to the project: Huib de Vriend, Mindert de Vries, Henk Schuttelaars, Z.B. Wang, Claire Jeuken, and especially Alessandra Crosato. The author is grateful also to Erik Mosselman, Anneke Hibma, Mathijs van Ledden and Marcel Stive for the interesting discussions and the data put at disposal.

11 REFERENCES

The references are subdivided in two groups, the usual printed publications and the web sites, which collect a lot of information. The latter source is relatively new, but it is potentially very useful, rich and easy to update.

11.1 Publications

E. Allersma, Studie inrichting Oostelijk deel Westerscheled. Analyse van het fysische system *(in Dutch)*, WL|Delft Hydraulics, report Z368, 1992

E. Allersma, Geulen in estuaria. 1D modellering van evenwijdige geulen *(in Dutch)*, WL|Delft Hydraulics, 1994

G.I. Barenblatt, *Dimensional analysis*, Gordon and Breach Science Publishers, 1987

J. van den Berg, C.J.L. Jeuken, A.J.F van der Spek, Hydraulic processes affecting the morphology and evolution of the Westerschelde estuary, in: Nordstrom and Roman (eds.), *Estuarine shores: evolution, environments and human alterations*, J. Wiley & Sons Ltd, cap.7, p.157-184, 1996

P. Blondeaux, G. Seminara, A unified bar-bend theory of river meanders, *J. Fluid Mech.*, vol. 157, pp. 449-470, 1985

G. Blöschl and D. Gutnecht, *Scale and scaling in hydrology*, Technische Universität Wien, Institut für Hydraulik, Gewässerkunde und Wasserwirtschaft, 1996

M. Bolla Pittaluga, N. Tambroni, C. Zucca, L. Solari, G. Seminara, Long term morphodynamic equilibrium of tidal channels: preliminary laboratory observations, *Proceedings of 2nd RCEM Symposium*, pp 423-432, Obihiro (Japan) 10-14 September 2001

M. Bolla Pittaluga, R. Repetto, M. Tubino, Channel bifurcation in braided rivers: equilibrium configuration and stability, *submittedt to Water Resources Research*, 2002

J. de Brouwer, A. Crosato, N. Dankers, W. van Duin, P.M.J. Herman, W. van Raaphorst, M.J.F. Stive, A.M. Talmon, H. Verbeek, M.B. de Vries, M. van der Wegen, J.C. Winterwerp, Eco-morphodynamic processes in the Rhine-Meuse-Scheldt delta and the Dutch Wadden Sea, March 2001

M. Colombini, G. Seminara, M. Tubino, Finite-amplitude alternate bars, *J. Fluid Mech*., vol. 181, pp 213-232, 1987

A. Crosato, M. de Vries, K. Kuyper, A tool for intertidal flat classification, Project Intrmud, report Z2037, WL|delft hydraulics, August 1999

A. Hibma, H.J. de Vriend and M.J.F. Stive, Channel and shoal formation in estuaries, *Proceedings of 2nd RCEM Symposium*, pp 463-471, Obihiro (Japan) 10-14 September 2001

G. Di Silvio, G. Barusolo and L. Sutto, Competing driving factors in estuarine landscape, *Proceedings of 2nd RCEM Symposium*, pp 453-462, Obihiro (Japan) 10-14 September 2001

A.R. van Dongeren and H.J. de Vriend, A model of morphological behaviour of tidal basins, *Coastal Engineering*, n. 22, pp. 287-310, 1994

J. Dronkers, Morphodynamics of the Dutch Delta, in: Dronkers & Scheffers (eds.), *Physics of Estuaries and Coastal Seas*, Balkema, Rotterdam, 1998

H.G. Enggrob, S. Tjerry, Simulation of morphological characteristics of a braided river, *Proceedings of 1st RCEM Symposium*, pp 585-594, Genova (Italy), September 1999

M. Falcon, Secondary flow in curved open channels, *Annual Review of Fluid Mechanics*, vol. 16, pp. 179-193, 1984

S. Fagherazzi, A. Bortoluzzi, W. E. Dietrich, A. Adami, S. Lanzoni, M. Marani, A. Rinaldo, Tidal Networks 1. Automatic network extraction and preliminary scaling features from digital terrain maps, *Water Resources Research*, vol. 35, n° 12, pp. 3891-3904, December 1999

J. Fredsøe, Meandering and braiding of rivers, *J. Fluid Mech.*, vol. 74, pp. 609624, 1978

J. Fredsøe, B.M. Sumer, K. Bundgaard, Scour at a riprap revetment in currents, *Proceedings of 2nd RCEM Symposium*, pp 245-254, Obihiro (Japan) 10-14 September 2001

C.T. Friedrichs, D.G. Aubrey, Tidal propagation in strongly convergent channels, *J. Geophys. R*es., vol. 99, pp. 3321-3336, 1994

C.T. Friedrichs, B.D. Armbrust, H.E. de Swart, Hydrodynamics and equilibrium sediment dynamics of shallow, funnel-shaped tidal estuaries, in: Dronkers & Scheffers (eds.), *Physics of Estuaries and Coastal Seas*, Balkema, Rotterdam, 1998

R.J. Fokkink, B. Karssen, Z.B. Wang, J.D.M. van Kerckhoven, A. Langerak, Morphological modelling of the Western Scheldt estuary, in: Dronkers & Scheffers (eds.), *Physics of Estuaries and Coastal Seas*, Balkema, Rotterdam, 1998

M. Garcìa, Y. Niño, Dynamics of sediment bars in straight and meandering channels: experiments on the resonance phenomenon*, J. Hydraulic Res*., vol. 31, n. 6, pp. 739-761, 1993

K. Gíslason, J. Fredsøe, Impact of riprap revetment on flow within a river bend and bend scour, *Proceedings of 2nd RCEM Symposium*, pp 645-651, Obihiro (Japan) 10-14 September 2001

S. Grass, Verloop van het getijverschil over het Schelde-estuarium (*in Dutch*), Afstudeerraport, TUDelft, Oktober 2001

G. Green, On the motion of waves in a variable canal of small depth width, *Trans. Cambridge Philos. Soc*., 6, 457-462, 1837

S. Ikeda, G. Parker, K. Sawai, Bend theory of river meanders. Part 1. Linear development, *J. Fluid Mech.*, vol. 112, pp. 363-377, 1981

D.A. Jay, Green's law revisited: tidal long-wave propagation in channels with strong topography, *J. Geophys. Res*., vol. 96, n. C11, pp. 20585-20598, 1991

M.C.J.L. Jeuken, On the morphologic behaviour of tidal channels in the Westerschelde estuary, PhD thesis, 2000

M.C.J.L. Jeuken, A. Crosato, M.B. de Vries, Ruimtecol-proces. Naar fysische graadmetes voor de zoute wateren vanuit ecologisch perspectief. Rapport 2 (*in Dutch*), WL|Delft Hydraulics, March 2001

H. de Jong, F. Gerritsen, Stability parameters of Western Sheldt estuary, in: B.L. Edge (ed.), *Proceedings of the 19th Coastal Engineering Conference*, ASCE, vol.3, p.3078-3093, 1984

K. de Jong, Tidally averaged transport models, PhD Thesis, Delft University, 1998

M.A.F. Knaapen, S.J.M.H. Hulscer, H.J. de Vriend, A. van Harten, Height and wavelength of alternate bars in rivers: modelling vs. laboratory experiments, *J. Hydraulic Res*., vol. 39, n. 2, pp. 147-153, 2001

J. van de Kreeke, Adaptation of the Frisian Inlet to a reduction in basin area with special reference to the cross-sectional area of the inlet channel, in: Dronkers & Scheffers (eds.), *Physics of Estuaries and Coastal Seas*, Balkema, Rotterdam, 1998

S. Lanzoni, Experiments on bar formation in a straight flume. 1. Uniform sediment, *Water Resources Research*, vol. 36, n. 11, pp. 3337-3349, November 2000

S. Lanzoni, G. Seminara, On tide propagation in convergent estuaries, *J. Geophys. Res.,* vol. 103, pp. 30.793-30.812, 1998

S. Lanzoni, G. Seminara, Long term evolution and morphodynamic equilibrium of tidal channels, *J. Geophys. Res.*, vol. 107, pp. 1-13, 2002

M. van Ledden, Sediment segregation in estuaries and tidal lagoons. A literature review, TUDelft, October 2000

M. van Ledden, Z.B. Wang, Sand-mud morphodynamics in an estuary, *Proceedings of 2nd RCEM Symposium*, pp 505-514, Obihiro (Japan) 10-14 September 2001

S.M. van Leeuwen, H.M. Schuttelaars and H.E. de Swart, Tidal and Morphologic Properties of Embayments: Effects of Sediment Deposition Processes and Length variation, *Phys. Chem. Earth* (B), Vol. 25, No. 4, pp 365-368, 2000

H. Middelkoop, Morfologische karakterisatie van het Nederlandse benedenrivierengebied. Verkenning van parameters (*in Dutch*), Centre for Geo-ecological Reasearch, August 2001

G. Mol, A.M. van Berchum, G.M. Krijger, (MOVE) Detoestand van de Westerschelde aan het begin van verdieping 48'/43'. Beschrijving van trends in de fysische, biologische en chemische toestand, Rapport 1, Rapport RIKZ-97.049, and Beschrijving van trends in de fysische toestand. Appendix met bijlagen, Rijksinstituut voor Kust en Zee, 1997

E. Mosselman, Prediction of number of channels in a braided system. Theoretical prediction, Contribution to FAP 21/22 Final Report of Planning study, Consulting Consortium FAP 21/22, Annex 1, pp 115-116, 1993

C.A.J. Neessen, Empirische relaties in de morfologie van het Westerschelde estuarium *(in Dutch)*, RIKZ Middelburg, August 2000

G. Parker, Self-formed straight rivers with equilibrium banks and mobile bed. Part 1. The sand-silt river, *J. Fluid Mech*., Vol. 89, part 1, pp. 109-125, 1978

A. Rinaldo, S. Fagherazzi, S. Lanzoni, M. Marani, W. E. Dietrich, Tidal Networks 2. Watershed delineation and comparative network morphology, *Water Resources Research*, vol. 35, n° 12, pp. 3905-3917, December 1999

A. Rinaldo, S. Fagherazzi, S. Lanzoni, M. Marani, W. E. Dietrich, Tidal Networks 3. Landscape-forming discharges and studies in empirical geomorphic relationships, *Water Resources Research*, vol. 35, n° 12, pp. 3891-3904, December 1999

M.M. Schoor, H.P. Wolfert, G.J. Maas, H. Middelkoop and J.P. Lambeek, Potential for floodplain rehabilitation based on historical maps and present-day processes along the River Rhine, The Netherlands, in: Marriot and Alexander (eds), *Floodplain: Interdisciplinary Approaches*, Geological Society, London, Special Publications, 163, 123-137, 1999

H.M. Schuttelaars, Evolution and stability analysis of bottom patterns in tidal embayments, PhD Thesis, Utrecht University, 1997

H.M. Schuttelaars and H.E. de Swart, Initial formation of channels and shoals in a short tidal embayment. *J. Fluid Mech., 386,* 15-42, 1999

H.M. Schuttelaars and H.E. de Swart, Multiple morphodynamic equilibria in tidal embayments. *J. Geophys. Res., 105,* 24105-24118, 2000

H.M. Schuttelaars and H.E. de Swart Morphodynamic equilibria in tidal embayments with decreasing cross-section: model results and field data, *submitted to JCR*, 2001

H.M. Schuttelaars, H.E. de Swart and G.P. Schramkowski, Initial formation of estuarine sections, *Proceedings of 2nd RCEM Symposium*, pp 443-452, Obihiro (Japan), 10-14 September 2001

G.P. Schramkowski, H.M. Schuttelaars and H.E. de Swart, The effect of geometry and bottom friction on local bed forms in a tidal embayment, *submitted to Continental Shelf Research,* 2001

G. Seminara, Stability and morphodynamics, *Meccanica*, vol. 33, pp. 59-99, Kluviert Academic Publishers, 1998

G. Seminara, M. Tubino, Alternate bars and meandering: free, forced and mixed interactions, in: S. Ikeda and G. Parker (eds.), *River Meandering*, AGU Water Resources Monography, 12, Washington D.C., pp. 267-320, 1989

G. Seminara, M. Tubino, Weakly non-linear theory of regular meanders, *J. Fluid Mech*., vol. 224, pp. 257-288, 1992

G. Seminara, M. Tubino, On the formation of estuarine free bars, in: Dronkers & Scheffers (eds.), *Physics of Estuaries and Coastal Seas*, Balkema, Rotterdam, 1998

G. Seminara, M. Tubino, Sand bars in tidal channels. Part 1. Free bars, *J. Fluid Mech*., vol. 440, pp 49-74, 2001

G. Seminara, S. Lanzoni, M. Bolla Pittaluga and L. Solari, Estuarine patterns: an introduction to their morphology and mechanics, *draft*, to appear in: *Fluid Mechanical Problems in Geomorphology*, Lecture Notes in Physics, Springer, December 2001

L. Solari, Topics in fluvial and lagoon morphodynamics, PhD thesis, Firenze University Press, 2001

L. Solari, G. Seminara, S. Lanzoni, M. Marani and A. Rinaldo, Sand bars in tidal channels. Part 2. Tidal meanders, *J. Fluid. Mech*., vol. 451, pp. 203-238, 2002

L. Solari, M. Toffolon, Equilibrium bottom topography in tidal meandering channels: preliminary results, *Proceedings of 2nd RCEM Symposium*, pp 81-89, Obihiro (Japan) 10-14 September 2001

A.J.F. van der Spek, Large-scale evolution of Holocene tidal basins in the Netherlands, PhD Thesis, Utrecht University, 1994

M. Toffolon, G. Vignoli, M. Tubino, Sull'amplificazione dell'onda di marea in canali convergenti (On the amplification of tidal wave in convergent channels, *in Italian*), *Proceedings, XXVIII Convegno di Idraulica e Costruzioni Idrauliche*, Potenza, 16-19 September 2002 (*in press*)

M. Tubino, R. Repetto, G. Zolezzi, Free bars in rivers, *J. Hydraulic Res*., vol. 37, n. 6, pp. 759-776, 1999

H.J. de Vriend, Large-scale coastal morphological predictions: a matter of upscaling?, Third Conference on Hydroscience and Engineering (ICHE98), 1998

H.J. de Vriend, J. Dronkers, M.J.F. Stive, A. Van Dongeren, Z.B. Wang, Coastal inlets and tidal basins *(partly in Dutch)*, TU Delft, January 2000

M.B. de Vries, A. Crosato, M.C.J.L. Jeuken, S. Tatman, M.J. Baptist, Ruimtecol-proces. Naar fysische graadmetes voor de zoute wateren vanuit ecologisch perspectief. Rapport 1 *(partly in Dutch)*, Report Z2941, WL|Delft Hydraulics, 2001

J. van Veen, Eb- en Vloedschaar Systemen in de Nederlandse Getijwateren *(in Dutch)*, Journal of the Royal Dutch Geographical Society, vol. 67, 303-325, 1950
Now translated into English with annotations*: Ebb and Flood Channel Systems in the Netherlands Tidal Waters*, Delft, November 2001 (http://www.hydraulicengineering.tudelft.nl/research/Van_Veen.pdf)

H. Verbeek, F.T.G. Tank, M.D. Groenewoud, Drumpels in de Westerschelde, natuur en mens samen ann het werk *(in Dutch)*, Rapport RIKZ-98.011, April 1998

J. Vroon, C. Storm and J. Coossen, Westerschelde, stram of struits? Eindrapport van het project Oostwest, een studie naar de beinvloeding van fysische en verwante biologische patronen in een estuarium *(in Dutch)*, Rijkswaterstaat, Rapport RIKZ-97.023, 1997

Z.B. Wang, Mathematical modelling of morphological processes in estuaries, *Communications on hydraulic and geotechnical engineering*, TU Delft, March 1989

Z.B. Wang, J.C. Winterwerp, Impact of dredging and dumping on the stability of ebb-flood channel systems, *Proceedings of 2nd RCEM Symposium*, pp 515-524, Obihiro (Japan) 10-14 September 2001

Z.B. Wang, R.J. Fokkink, M. De Vries, A. Langerak, Stability of river bifurcations in 1D morphological models, *Journal of Hydraulic Research*, vol. 33, n. 6, pp. 739-750, 1995

Z.B. Wang, B. Karssen, R.J. Fokkink, A. Langerak, A dynamic-empirical model for estuarine morphology, in: Dronkers & Scheffers (eds.), *Physics of Estuaries and Coastal Seas*, pp 279-286, Balkema, Rotterdam, 1998

J.C. Winterwerp, Z.B. Wang, M.J.F. Stive, A. Arends, C. Jeuken, C. Kuijper, P.M.C. Thoolen, A new morphological schematization of the Western Scheldt estuary, The Netherlands, *Proceedings of 2nd RCEM Symposium*, pp 525-533, Obihiro (Japan) 10-14 September 2001

11.2 Web sites

The following web sites are only the first indications for a deeper research, since the offer of information is changing and growing very rapidly. At present, some of these sites are available only in Dutch.

Schelde Informatie Centrum: http://www.scheldenet.nl

Waterland: http://www.waterland.net

Port of Antwerp: http://www.portofantwerp.be

Rijkswaterstaat: http://www.rijkswaterstaat.com

Rijksinstituut voor Kunst en Zee: http://www.rikz.nl

The Tide: http://www.getij.nl

Deflt Cluster: http://www.delftcluster.nl